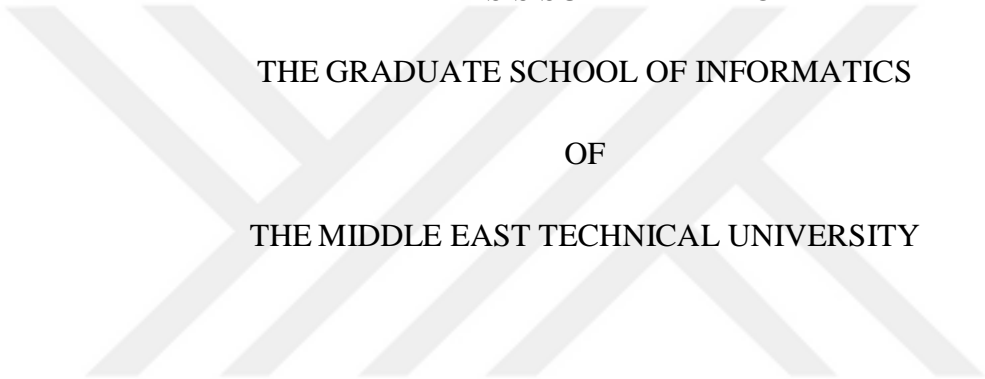


A COMPREHENSIVE SIMULATION OF FACTORS THAT AFFECT
PERFORMANCE OF ARRAY BASED ACOUSTIC GUNSHOT LOCALIZATION
ON HELICOPTERS



A THESIS SUBMITTED TO
THE GRADUATE SCHOOL OF INFORMATICS
OF
THE MIDDLE EAST TECHNICAL UNIVERSITY

BY
MURAT YILMAZ

IN PARTIAL FULFILLMENT OF THE REQUIREMENTS
FOR
THE DEGREE OF MASTER OF SCIENCE
IN
INFORMATION SYSTEMS

FEBRUARY 2016

**A COMPREHENSIVE SIMULATION OF FACTORS THAT AFFECT
PERFORMANCE OF ARRAY BASED ACOUSTIC GUNSHOT
LOCALIZATION ON HELICOPTERS**

Submitted by **Murat Yılmaz** in partial fulfillment of the requirements for the degree of **Master of Science in Information Systems, Middle East Technical University** by,

Prof. Dr. Nazife Baykal
Director, Informatics Institute

Prof. Dr. Yasemin Yardımcı Çetin
Head of Department, Information Systems

Assoc. Prof. Dr. Banu Günel Kılıç
Supervisor, Information Systems, METU

Examining Committee Members

Assoc. Prof. Dr. Altan Koçyiğit
Information Systems, METU

Assoc. Prof. Dr. Banu Günel Kılıç
Information Systems, METU

Assoc. Prof. Dr. Hüseyin Hacıhabiboğlu
Modeling and Simulation, METU

Assoc. Prof. Dr. Ali Cafer Gürbüz,
Electrical and Electronic Engineering, TOBB
University of Economics and Technology

Prof. Dr. Adnan Yazıcı,
Computer Engineering, METU

Date:

02.02.2016



I hereby declare that all information in this document has been obtained and presented in accordance with academic rules and ethical conduct. I also declare that, as required by these rules and conduct, I have fully cited and referenced all material and results that are not original to this work.

Name, Last name: Murat Yılmaz

Signature:

ABSTRACT

A COMPREHENSIVE SIMULATION OF FACTORS THAT AFFECT PERFORMANCE OF ARRAY BASED ACOUSTIC GUNSHOT LOCALIZATION ON HELICOPTERS

Yılmaz, Murat

Department of Information Systems

Supervisor: Assoc. Prof. Dr. Banu Günel Kılıç

February 2016, 105 Pages

Self-defense solutions on current aircraft usually handle advanced weapons while most helicopters down or damaged are known to be attacked from ground using rifles or Rocket-Propelled Grenades (RPG). Although there are ground based localization solutions for Small Arms Fire (SAF) attacks, there are only a few implementations of onboard applications. A simple Acoustic Source Localization (ASL) application employs a microphone array for collecting audio signals, so as to locate sound sources using the measurements from the sound field. The aim of this study is to investigate the possibility of Acoustic Gunshot Localization on a helicopter so as to detect and localize SAF attacks, by simulating the effects of both wave propagation and signal processing parameters for different localization algorithms. Pre-processing and post-processing for each individual algorithm were also proposed considering domain specific issues, such as the effects of helicopter noise, environmental factors (temperature and humidity), gunshot signal characteristics and real life mission requirements.

Keywords: Acoustic gunshot localization, Helicopter acoustics, Acoustic simulation, Atmospheric sound attenuation

ÖZ

HELİKOPTER ÜZERİNDE MİKROFON DİZİSİ TABANLI ATEŞLİ SİLAH ATIŞ YÖNÜ TESPİTİNİ ETKİLEYEN ETMENLERİN SİMÜLE EDİLMESİ

Yılmaz, Murat

Bilişim Sistemleri Bölümü

Tez Yöneticisi: Doc. Dr. Banu Günel Kılıç

Şubat 2016, 105 Sayfa

Hava araçlarında kullanılmakta olan kendini koruma sistemlerinin büyük çoğunluğu, gelişmiş silah ve tehditlere karşı savunma sağlamaktadır. Halbuki, düşürülen ya da yara alan helikopterlerin genellikle tüfek ya da yerden atılan roketler tarafından vurulduğu bilinmektedir. Bu tarz silahların konumunu belirlemek için yerde kurulu sistemler bulunmakla birlikte, hava araçlarına entegre konum belirleme uygulamaları yok denecek kadar azdır. Basit bir Ses Kaynağı Belirleme uygulaması bir mikrofon dizisini algılayıcı olarak kullanarak, belirli bir menzil içerisinde bulunan ses kaynaklarının konumunu belirleyebilir. Bu çalışmada helikopter üzerinde silah ses kaynağını belirlemenin mümkün olup olmadığını anlamak amacıyla, hem sesin yayılımı ile ilgili etmenler hem de sinyal işleme parametrelerinin farklı ses kaynağı belirleme algoritmaları için simüle edilmesi amaçlanmaktadır. Ayrıca, helikopter gürültüsü, çevresel faktörler (sıcaklık, nem gibi), silah sesi özellikleri, görev gereksinimleri gibi sisteme özgü konular göz önünde bulundurularak her bir algoritma için sinyal işleme teknikleri önerilmiştir.

Anahtar Kelimeler: Silah sesi kaynağı belirleme, Helikopter akustiği, Akustik simülasyon, Atmosferde ses yayılımı

ACKNOWLEDGEMENTS

I would like to express my deepest gratitude to Assoc. Prof. Dr. Banu Günel Kılıç for her guidance, advice, understanding and supervision throughout the development of this thesis study.

I appreciate Halit Sefa Eman, Arda Yücekayalı and Yüksel Ortakaya for sharing of valuable experiences during the development of this thesis study.

I owe Burcu Kılıç a dept of gratitude for her love, support and understanding not only throughout this study but also all my life.

Last but not the least; I would like to express my special thanks to my friends Gizem Sezen, Siner Gökhan Yılmaz and Elif İrem Şenyurt for their valuable friendship and every kind of support.

TABLE OF CONTENTS

ABSTRACT.....	iv
ÖZ	v
ACKNOWLEDGEMENTS	vi
TABLE OF CONTENTS	vii
LIST OF TABLES	ix
LIST OF FIGURES	x
LIST OF ABBREVIATIONS	xiv
CHAPTER 1 INTRODUCTION	1
1.1 Aims and Objectives	1
1.2 Real-life Requirements and Scenarios	2
1.3 Implementation Challenges	4
1.4 Scope of the Study	5
1.5 Outline of the Thesis	6
CHAPTER 2 PROBLEM TOP-DOWN ANALYSIS	7
2.1 Domain Specific Spectrotemporal Characteristics	8
2.1.1 Helicopter Sound Characteristics	8
2.1.2 Onboard Sound Sources	11
2.1.3 Gunshot Sound Characteristics	13
2.2 Wave Propagation Characteristics.....	16
2.3 Acoustic Source Localization Theory and Implementation	19
2.3.1 Acoustic Source Localization Theory: Basics of Operation	20
2.3.2 Acoustic Source Localization Implementation: Microphones and Microphone Arrays.....	22
2.3.2.1 Microphones: Basic Operation and Types	22
2.3.2.2 Microphone Arrays.....	23
2.3.3 Acoustic Source Localization Algorithms	25
2.4 Acoustical Simulation	26
2.4.1 Straight Line Propagation	27

2.4.2	Curved Path Simulation	28
2.5	Solution Methodology: Simulation of Factors That Affect Array Based Acoustic Gunshot Localization on Helicopters	29
CHAPTER 3 PROPOSED METHODS FOR GUNSHOT LOCALIZATION ON HELICOPTERS		33
3.1	Algorithms Selection	33
3.2	Domain Specific SNR Examination	35
3.3	Beamforming	39
3.3.1	Theory of Operation	39
3.3.2	Pre-processing and Post-Processing	40
3.4	Generalized Cross Correlation	44
3.4.1	Theory of Operation	44
3.4.2	Pre-processing and Post-Processing	45
3.5	Multiple Signal Classification	50
3.5.1	Theory of Operation	50
3.5.2	Pre-processing and Post-Processing	51
CHAPTER 4 SIMULATION OF FACTORS THAT AFFECT LOCALIZATION ON HELICOPTERS		59
4.1	Microphone Spacing	60
4.2	Number of Microphones	67
4.3	Source to Microphone Array Distance	73
4.4	Angle of Incidence	79
4.5	STFT Size	82
4.6	Discussion of Results	84
CHAPTER 5 CONCLUSIONS		85

LIST OF TABLES

Table 1 Factors that affect acoustic source localization outdoors.....	29
Table 2 Domain-specific factors that affect gunshot localization on helicopters	30
Table 3. Helicopter SPL estimation using previous studies in the literature	36
Table 4 Gunshot SPL estimation using inverse-square law	37
Table 5. Theoretical illustration of sound field distances and travel times.....	54
Table 6 SNR levels corresponding to different source to microphone array distances	73

LIST OF FIGURES

Figure 1 Breakdown of the factors associated with acoustic gunshot localization on helicopters	8
Figure 2 Spectrogram of an example helicopter sound signal windowed with a 1024-sample Hamming window and FFT size:1024. Both periodic blade passage and low frequency dominance are easily observable. Distortion above 20 kHz results from Nuyquist frequency and can be discarded	12
Figure 3 Spectrogram of an example gunshot sound signal windowed with a 1024-sample Hamming window and FFT size:1024. Gunshot occurs at 0.1 sec.....	16
Figure 4 Simple sound field geometry	20
Figure 5 Simple sound field geometry with plane wave assumption.....	22
Figure 6 Gunshot localization parameters and simulations coverage	31
Figure 7 Block Diagram of the simulation framework developed using MATLAB in the scope of this study	32
Figure 8 Beamformer output for a source at $\theta=45^\circ$ with microphone spacing, $S = 0.1$ m, number of microphones = 4, sampling frequency, $F_s = 44100$ Hz when no pre-processing is applied.	41
Figure 9 DOA estimation of Beamformer for a source at 45° with pre-filtering of frequencies below 700 Hz, where helicopter noise components are dominant, and above 1750 Hz, where spatial aliasing is observed. Microphone spacing, $S = 0.1$ m, number of microphones = 4, sampling frequency, $F_s = 44100$ Hz.	42
Figure 10 Beamformer for a source at 45° with both pre-filtering (700-1800 Hz) and Spectral Subtraction applied as pre-processing. Parameters of Spectral Subtraction are assumed to be known since localization stage is assumed to follow a detection stage in a typical localization implementation. Target angle is 45° with microphone spacing, $S = 0.1$ m, number of microphones = 4, sampling frequency, $F_s = 44100$ Hz.	43
Figure 11 Combined DOA output of the whole microphone array with GCC. Target angle is 45° with microphone spacing = 0.1 m, number of microphones = 4, sampling frequency $F_s = 44100$ Hz. No pre-processing is applied.....	46
Figure 12 Combined DOA output of the whole microphone array with GCC. Target angle is 45° with microphone spacing = 0.1 m, number of microphones = 4, sampling frequency $F_s = 44100$ Hz. Spectral Subtraction applied as pre-processing.....	47

Figure 13 Combined DOA output of the whole microphone array with PHAT-weighted GCC. Target angle is 45° with microphone spacing = 0.1 m, number of microphones = 4, sampling frequency $F_s = 44100$ Hz. No Spectral Subtraction is applied.....	49
Figure 14 Combined DOA output of the whole microphone array for GCC. Target angle is 45° with microphone spacing = 0.1 m, number of microphones = 4, sampling frequency $F_s = 44100$ Hz. Both Spectral Subtraction and PHAT-weighting applied as pre-processing.	50
Figure 15. Gunshot sound field geometry illustration	53
Figure 16 MUSIC with no additional post-processing. Target angle is 45° with microphone spacing = 0.1 m, number of microphones = 4. STFT size is 1024, all 512 frequency bins are used.....	55
Figure 17 Spatial aliasing observed at the output of MUSIC algorithm for a source at 45° . Spatial aliasing was observed for all SNR values in the range of $[-34,-4]$ dB with microphone spacing, $S = 0.1$ m sampling frequency, $F_s = 44100$, Target angle = 45° , number of microphones = 4, STFT size = 1024.	56
Figure 18 Spatial aliasing at different frequency bins of MUSIC output for a source at 45° . The high-limit on the frequency so as not to have spatial aliasing is 1750 Hz for microphone spacing. Microphone spacing, $S = 0.1$ m, number of microphones, $M = 4$, STFT size = 1024.....	57
Figure 19 Output of MUSIC with post-processing for a source at 45° . Frequency bins below 400 Hz are omitted because of dominant helicopter noise components. Frequencies above 1750 Hz are omitted because of spatial aliasing limitation. STFT size = 1024 microphone spacing, $S = 0.1$ m, number of microphones, $M = 4$	58
Figure 20 Parameters simulated for their effects on gunshot localization.....	59
Figure 21 Beamforming with no Spectral Subtraction applied. Effects of microphone spacing with and without including air absorption. $\theta=45^\circ$, $D=200$ m, $F_s=44100$, $M=4$	61
Figure 22 Beamforming with Spectral Subtraction. Effects of microphone spacing with and without including air absorption. $\theta=45^\circ$, $D=200$ m, $F_s=44100$, $M=4$	62
Figure 23 GCC without PHAT-weighting. Effects of microphone spacing with $\theta=45^\circ$, $D=200$ m, $F_s=44100$, $M=4$	63
Figure 24 GCC with PHAT-weighting. Effects of microphone spacing with and without including air absorption. $\theta=45^\circ$, $D=200$ m, $F_s=44100$, $M=4$	64
Figure 25 GCC with both PHAT-weighting and Spectral Subtraction. Effects of microphone spacing with and without including air absorption. $\theta=45^\circ$, $D=200$ m, $F_s=44100$, $M=4$	65

Figure 26 MUSIC with post-processing that selects frequency bins of interest. Effects of microphone spacing with and without including air absorption. $\theta=45^\circ$, $D=200\text{m}$, $F_s=44100$, $M=4$, FFT size=1024	66
Figure 27 MUSIC with no post-processing. Effects of microphone spacing with and without including air absorption. $\theta=45^\circ$, $D=200\text{m}$, $F_s=44100$, $M=4$, STFT size=1024	67
Figure 28 Beamforming with suggested pre-processing. Effects of number of microphones with and without including air absorption. $\theta=45^\circ$, $D=400\text{m}$, $F_s=44100$, $S=0.15\text{m}$	68
Figure 29 Beamforming without suggested pre-processing. Effects of number of microphones with and without including air absorption. $\theta=45^\circ$, $D=400\text{m}$, $F_s=44100$, $S=0.15\text{m}$	68
Figure 30 Beamformer with and without suggested pre-processing comparison for a larger source to microphone array distance, $\theta=45^\circ$, $D=800\text{m}$, $F_s=44100$, $S=0.15\text{m}$	69
Figure 31 GCC with only PHAT-weighting. Effects of number of microphones with and without including air absorption. $\theta=45^\circ$, $D=400\text{m}$, $F_s=44100$, $S=0.15\text{m}$	70
Figure 32 GCC with only PHAT-weighting with two different microphone spacing values, $\theta=45^\circ$, $D=400\text{m}$, $F_s=44100$	70
Figure 33 GCC with PHAT-weighting. Effects of number of microphones with and without including air absorption. $\theta=45^\circ$, $D=800\text{m}$, $F_s=44100$, $S=0.15\text{m}$	71
Figure 34 MUSIC with post-processing that selects output frequency bins. Effects of number of microphones with and without including air absorption. $\theta=45^\circ$, $D=300\text{m}$, $F_s=44100$, $M=4$, STFT size=4096, $S=0.15$	72
Figure 35 MUSIC, effect of proposed post-processing that selects frequency bins of interest, $\theta=45^\circ$, $D=300\text{m}$, $F_s=44100$, $M=4$, FFT size=4096	72
Figure 36 Effects of proposed pre-processing for Beamforming, $\theta=45^\circ$, $F_s=44100$, $M=4$, $S=0.15\text{m}$	74
Figure 37 Beamforming with proposed pre-filtering. Effects of source to microphone array distance with and without including air absorption. $\theta=45^\circ$, $F_s=44100$, $M=4$, $S=0.15\text{m}$	75
Figure 38 Beamforming with both spectral subtraction and pre-filtering applied. For both cases, effects of source to microphone array distance with and without air absorption are illustrated with $\theta=45^\circ$, $F_s=44100$, $M=4$, $S=0.15\text{m}$	75
Figure 39 PHAT-GCC without spectral subtraction. Effects of source to microphone array distance with and without including air absorption. $\theta=45^\circ$, $F_s=44100$, $M=4$, $S=0.2\text{m}$	76
Figure 40 PHAT-GCC without spectral subtraction for an increased number of microphones. Effects of source to microphone array distance with and without including air absorption. $\theta=45^\circ$, $F_s=44100$, $M=8$, $S=0.2\text{m}$	77

Figure 41 PHAT-GCC with spectral subtraction with an increased number of microphones. Effects of source to microphone array distance with and without including air absorption. $\theta=45^\circ$, $F_s=44100$, $M=8$, $S=0.2$ m	78
Figure 42 MUSIC with proposed post-processing. Effects of source to microphone array distance with and without including air absorption. $\theta=45^\circ$, $F_s=44100$, $M=4$, $S=0.2$ m, STFT size=4096.....	79
Figure 43 Beamforming with and without spectral subtraction, performance with respect to source angle. $F_s=44100$, $M=4$, $S=0.2$ m, $D=300$ m. Proposed pre-filters are applied.....	80
Figure 44 PHAT-GCC with and without spectral subtraction, performance with respect to source angle. $F_s=44100$, $M=4$, $S=0.2$ m, $D=300$ m.....	80
Figure 45 MUSIC with post-processing that selects frequency bins of interest, performance with respect to source angle. $F_s=44100$, $S=0.2$ m, $D=300$ m, $M=4$, STFT size = 4096.....	81
Figure 46 MUSIC with post-processing that selects frequency bins of interest for an increased number of microphones, performance with respect to source angle. $F_s=44100$, $S=0.2$ m, $D=300$ m, STFT size = 4096.....	82
Figure 47 MUSIC with post-processing that selects frequency bins of interest. Change in DOA estimation output for different STFT sizes. $\theta=45^\circ$, $D=200$ m, $F_s=44100$, $M=4$	83
Figure 48 MUSIC with post-processing that selects frequency bins of interest. Change in DOA estimation output for different STFT sizes. $S=0.15$ m, $\theta=45^\circ$, $D=200$ m, $F_s=44100$, $M=4$	83

LIST OF ABBREVIATIONS

ASL	Acoustic Source Localization
BPF	Blade Passage Frequency
BVI	Blade Vortex Interaction
dB	Decibel
DOA	Direction of Arrival
EPNL	Effective Perceived Noise Level
STFT	Short-time Fourier Transform
GCC	Generalized Cross Correlation
IR	Infra-red
MUSIC	Multiple Signal Classification
NUSLA	Non-Uniformly Spaced Linear Arrays
PHAT	Phase Transform
RPG	Rocket Propelled Grenade
RPM	Revolution per Minute
SAF	Small Arms Fire
SNR	Signal to Noise Ratio
SPL	Sound Pressure Level
SPL (A)	A-weighted Sound Pressure Level
SRP	Steered Response Power
TDOA	Time Delay of Arrival
USLA	Uniformly Spaced Linear Array

CHAPTER 1

INTRODUCTION

Self-defense solutions on current aircraft usually handle advanced weapons while most helicopters down or damaged are known to be attacked from ground using low technology, hand-carried weapons, such as rifles or Rocket-Propelled Grenades (RPG). This situation arises from the characteristic mission conditions of helicopters. By its nature, missions including helicopters cover the cases where both altitude and speed (relative to ground) are low. Moreover, during the take-off and landing parts of the flight, helicopter pilots are confronted with great risks of ground-based attacks. However, due to the extreme environmental conditions and excessive cockpit noise levels, estimating the direction of an attack is very difficult for a pilot, especially when it is not directed from angles visible to the crew. Indeed, even the detection of the gunshot sound signature may not be possible until bullets pass close to the aircraft or in some cases, after multiple shots have been fired (Fertig, Young, and Nance, 2012).

Considering the serious risk of bodily injury or damage to the aircraft together with crew's difficulty in hearing the acoustic signature of a weapon shot, detection and localization of gunshots on helicopters is a great necessity for better situational awareness (Fertig et al., 2012).

1.1 Aims and Objectives

In the light of onboard localization problem mentioned above, the idea behind this work is that Acoustic Source Localization (ASL) algorithms can solve the problem once the detection has been successfully achieved and the effects of aircraft noise and environmental factors have been handled accordingly. However, despite there being several implementations of ground based gunshot localization for SAF and snipers in the literature, such as the works of (Bandi, Rizkalla, and Salama, 2012), (Freire and Apolinario, 2011) and (Sallai, Volgyesi, Pence, and Ledeczi, 2013), there are only a few studies of onboard applications for helicopters or other aircraft.

Common to all these studies, microphone arrays are used as the sensory equipment to collect data from the sound field. Then, the contributions of the muzzle blast and the shock wave (or a combination of them) are used so as to detect the gunshot and localize its position. Localization on a helicopter is a much more challenging acoustic implementation, considering both extreme environmental conditions and helicopter's self-noise. Signal to Noise Ratio (SNR) range of interest for ground based gunshot localization implementations is relatively high since gunshots are considered easily detectable in a normal environment, considering their impulsive nature and high intensity (Gerosa, Valenzise, Tagliasacchi, Antonacci, and Sarti, 2007). (Valenzise, Gerosa, Tagliasacchi, Antonacci, and Sarti, 2007) also reported in another publication that localization performance is greatly reduced for SNRs below -10 dB. An onboard-helicopter application, however, is expected to tolerate lower

SNR ranges, considering that Sound Pressure Level (SPL) outside helicopters is in excess of 100-110 dB (True and Rickley, 1977).

Due to the reasons stated above, this thesis study primarily aims to investigate the applicability of ASL algorithms and related signal processing methods in the extreme conditions of the problem domain. The major, and the minimal, question to be answered by this study is whether it is possible to achieve microphone array based gunshot localization on helicopters during a flight or some parts of the flight, and if so, what the expected localization performance is as a factor of array and algorithm parameters and environmental factors.

In order to achieve this major aim, the main objectives throughout this study were designated as follows:

- Determining domain specific signal to noise ratio (SNR) requirements and traditional ASL algorithms' ability to handle these SNR levels
- Proposing pre/post processing for different localization algorithms, in the light of domain specific sound field characteristics and examining performance of the proposed methods
- Determining and simulating algorithm and array parameters with their effects on localization performance
- Determining and simulating outdoor wave propagation parameters with their effects on localization performance

So as to achieve these objectives, development of a simulation environment appeared to be mandatory since available sound field simulation tools address issues such as aircraft noise monitoring or community noise limitation. These tools offer practical determination of sound pressure levels as well as other parameters of interest, but only for a predetermined set of scenarios specific to their domain. That is why this study included development of a simulation environment addressing

- algorithm and array parameters
- outdoor wave propagation characteristics

specific to their effects on gunshot localization on helicopters.

1.2 Real-life Requirements and Scenarios

Military helicopters are attacked from ground using low technology weapons such as SAF or RPG, since their operational usage covers low altitude and low speed missions. Due to extreme aircraft noise conditions and excessive cockpit SPL levels, estimating the direction of incoming attacks is very difficult for a pilot. Moreover, the crew may not be able to even realize that there is ongoing gunshot fire, until bullets pass close to the aircraft. Therefore, gunshot localization on helicopters is a real-life mission problem, which makes it possible that mission and hazard conditions can be defined as real-life scenarios so as to determine requirements expected from such a system. Although not all these scenarios are covered in the scope of this work, they are given below so that the directions taken can be better supported.

- Rotary-winged aircraft operates in lower velocities and performs missions at lower altitudes as compared to fixed-wing aircraft, making it more open to ground attacks with SAF and RPGs.
- Excessive noise levels of not only external building blocks (motor, exhaust etc.) but also avionics equipment inside the cockpit makes hard, if not impossible, for flight personal to localize SAF attacks aimed at aircraft (Eman, H.S., personal communication, May, 2015).
- In some cases, the crew cannot even realize that there is ongoing SAF fire, until bullets pass close to the aircraft (Eman, H.S., personal communication, May, 2015).
- There are current procedures for minimizing threats of ground-based attacks, such as using an escort helicopter or ground troops' securing the landing area. Neither of these procedures can always be provided.
- Research (Lago, L., Sven, and P.-a., 1997) has shown that SPL level inside helicopter cockpit is in the range of 80-90 dB. Moreover, communication system headsets add up to this sound level making the total SPL at pilot's ear in the range of 90-100 dB.
- A high-pitch short-duration pressure can be sensed by pilots in case of ultra-sonic bullets; however, localization requires angle-of-sight and/or the flash of explosion caused by muzzle blast which is visible only at night (Eman, H.S., personal communication, May, 2015).
- Cruising portion of flight (where aircraft is at high altitudes and high speeds) is when it is least open to ground attacks. The most critical portions on the other hand are hover (where it is stationary), take-off and landing (where it is closest to threats) and sweep flights (where it follows a route from a hilltop to another, momentarily close to ground surface). All these scenarios make attacks both from above and below possible (Eman, H.S., personal communication, May, 2015).
- SAF attacks against helicopters are not dared to if the helicopter has onboard weapons and is not close at hand. Although effective ranges of small arms weapons are much greater, most assaults are performed from distances of 200 meters or less, except for long distance sniper attacks (Eman, H.S., personal communication, May, 2015).
- When the helicopter is on ground just before or after flight, sniper attacks mostly target the pilot rather than the aircraft itself and can be effective for ranges up to 1500-2000 meters.
- Ultra-sonic projectile speeds cause extraordinary sound wave characteristics that depend on weapon characteristics and varies even among specific bullets, requiring specific consideration.
- Although there are real-life examples of single shot cases such as sniper or RPG attacks, low altitude mission conditions require that an onboard helicopter application has to consider conventional battle situations, too, where lots of gunshots are incident from different directions, simultaneous to human perception.
- Since gunshot is a highly impulsive sound, multiple reflections represent a serious problem. Even on ground, military personal has difficulty distinguishing the real source of the gunshot. Infrared (IR) vision devices, apart from seeing during night, are used in such situations, scanning possible directions to determine the actual sound source. Still, it is possible to mislead IR vision devices in specific

environmental conditions and, in some cases, localization with IR has not been possible.

- A realistic target range should include SAFs weapons such as rifles, handguns and snipers as well as RPGs.
- A realistic application should cover as much of the weather conditions where the aircraft is operational as possible.
- A realistic system should be reliable such that it has to either output results within an acceptable error range or notify if it cannot. This requires the capability of assessing its own error range and/or deciding whether current conditions are operational.

1.3 Implementation Challenges

Gunshot localization on a helicopter is a challenging problem. Although there is plenty of research and implementation in the literature concerning Acoustic Source Localization (ASL) or Gunshot Source Localization (GSL), extreme conditions of our problem add up onto the problem of basic ASL.

Firstly, ambient noise is significantly higher than a regular ASL implementation should be confronted. Sound level of the host vehicle is so strong that, in most cases, crew inside the cockpit cannot be aware of the gunshot, let alone localize the position of it (Fertig et al., 2012). This sound level is not caused only by the rotating blades of the helicopter. Although sound produced by main and tail rotors are what human ear perceives from a distance, an onboard application should consider various more noise components such as engine, transmission, exhaust, cooling system, avionics equipment and so on (Robinson, 1973).

In order to localize gunshot sound on helicopters, characteristics of gunshot sound should also be considered. Although SPL levels of weapons are considerably high, even up to 160 dB in some cases (R. C. Maher, 2006), a significant amount of signal energy is lost due to gunshot distance, as explained in detail in the following chapters of this study. Apart from considering simply the wideband SPL, one should notice that important clues regarding signature of the gunshot are in higher bands of the audible frequency spectrum (Bronuzzia, Monaib, and Patruccob, 2012). However, attenuation of higher frequency components due to atmospheric absorption is known to be higher (Harris, 1966). In that case, specific band signal information that would otherwise be useful is expected to be lost.

Another aspect that adds up onto the basic ASL problem is outdoor wave propagation characteristics. Attenuation of sound in air is dependent on temperature, relative humidity and atmospheric pressure and the relations vary with varying frequency, building the necessity of narrowband calculations (Harris, 1966). Moreover, the speed of sound in air itself is known to change with temperature. Although these effects can be accounted for using well-established formulas in literature and standards (International Organization for Standardization, 2007), there are less predictable effects, considering extreme conditions of a helicopter's mission environment (Eunkuk, Seungmin, and Soogab, 2010). (Arntzen, Rizzi, Visser, and Simons, 2012) listed some of these major factors as effects of wind, air moisture, soil characteristics, weather conditions such as rain or snow and gradients of temperature

and wind in atmosphere. These sound propagation characteristics pose significant challenges that should be resolved for a realistic implementation.

Unlike a regular ASL solution where sensory array is stationary, localization on a helicopter has an additional challenge concerning host vehicle's movement. First of all, both amplitude and directivity of sound generated by a helicopter may change between steady and turning maneuvers (Schmitz et al., 2007). Besides, (Robinson, 1973) reported that parameters such as rotation per minute (rpm), load and torque of mechanical parts of engine and rotors are dependent on dynamic behavior of the vehicle and they affect the characteristics of sound generated. For the purposes of this study, the dynamic behavior implies that what is considered as noise in the acoustic recordings varies with time and is related to maneuvers and aircraft dynamics.

In case these challenges are successfully handled and the signals of interest are successfully discriminated, there are still factors that could misguide localization algorithms. Reflections, shockwave of supersonic projectiles and simultaneous gunshots are the most critical of these factors as depicted in previous researches (Robinson, 1973) and (R. C. Maher and Shaw, 2008). Characteristics of these disturbances were investigated and solution suggestions were introduced in this study.

1.4 Scope of the Study

Gunshot audio surveillance applications may aim detection, localization and classification of events. This study investigates the factors related to the localization of ground based gunshots attacks on helicopters. In this regard, the simulations of this study assume that the existence of the transient gunshot event was detected by a preceding detection phase. Yet, comments were included concerning the effects of the sound field geometry and the environmental factors on the possibility of successful detection.

As explained by Section 1.3 Implementation Challenges, as compared to a basic acoustic source localization problem, following real-life considerations add up onto the problem:

- Outdoor wave propagation characteristics
- Aircraft sound characteristics
- Gunshot sound characteristics
- Domain-specific problem scenario and geometry consideration
- Effects of aircraft dynamics
- Meteorological conditions

The scope of this study was restricted to the steady or low speed helicopter movements considering both alterations of the sound field and the coupling between helicopter dynamics and sound characteristics. Moreover, although the effects of temperature, humidity and air pressure were accounted for, the atmospheric gradients and meteorological events, such as rain or snow, were not included.

Lastly, a complete localization application should yield both horizontal and vertical axes Direction of Arrivals (DOA). However, it should be noted that once the DOA estimation on one axis is shown to be achievable, the same procedures can be repeated for the remaining axis. Therefore, the scope of this study includes only the horizontal DOA estimation, as an initial attempt.

1.5 Outline of the Thesis

This thesis was organized in a manner that first defines the breakdown of the problem of array based gunshot localization on helicopters. In this regard, Chapter 2 gives the background information regarding each specific problem, presenting previous studies in the literature, followed by a brief explanation of and coverage of our simulation approach. The major outcome of Chapter 2 is the list of parameters that should be examined in the scope of gunshot localization on helicopters.

Chapter 3 proposes three different methods with pre-processing and post-processing suggestions that address domain specific requirements and real-life scenarios. Both theoretical and implementation issues are explained for the three widely known acoustic source localization algorithms commenting on their applicability to the problem domain. The major outcome of Chapter 3 is the domain specific SNR expectancy from these methods as well as suggestions in the processing domain so as to meet this expectancy.

Having determined the SNR range expectancy and required pre-processing or post-processing, Chapter 4 manipulates both algorithm related parameters and outdoor wave propagation related parameters in a selective manner. Therefore, Chapter 4 addresses the effects of both algorithm-related and outdoor wave propagation related factors, as well as the proposed processing methods' ability to enhance the localization performance.

Finally, Chapter 5 concludes the thesis together with suggestions on future work.

CHAPTER 2

PROBLEM TOP-DOWN ANALYSIS

A simple Acoustic Source Localization (ASL) application locates a sound source by applying acoustic localization algorithms on signals collected from the sound field (Chacón-Rodríguez, Julián, Castro, Alvarado, and Hernández, 2011). There are effective methods and algorithms in the literature that can locate sound sources given that input signals are not severely distorted. Some of these algorithms can be grouped under Steered Response Power (SRP) localizers, High Resolution Spectral Estimation based localizers (Schmidt, 1986), Time Delay of Arrival (TDOA) based localizers, intensity vector direction based localization techniques and biologically inspired methods (Günel and Hacıhabiboğlu, 2011).

However, evident from the “Implementation Challenges” section above, acoustical source localization is only the core part of the problem since signals of interest will be severely distorted due to extreme conditions caused by the helicopter noise, outdoor weather conditions, supersonic projectile characteristics and real-life mission scenarios. Although the amount of this distortion and decrease in localization performance is algorithm-dependent, these conditions make sure that additional signal processing, other than ASL algorithms, needs to be applied referring to real-life challenges and domain-specific characteristics of the problem space.

Host vehicle’s own sound appears to be the most significant problem. Serious SPL levels of helicopters make it suspicious whether gunshot signals can be distinguished. A rough comparison of previously reported SPL levels of helicopter by (Wagner, n.d.) and (True and Rickley, 1977) with results of studies (R. C. Maher and Shaw, 2008) and (Beck, Nakasone, and Marr, 2011) on characteristics of gunshots reveals that both excessive power and impulsive nature of the gunshot sound are expected to be detected. However, environmental factors and operational gunshot distances add up onto the problem, extending the task beyond simply comparing amplitude or frequency characteristics. Moreover, even the simplest ASL algorithms require careful selection of parameters, related to both signal processing calculations and data acquisition (Freire and Apolinario, 2011).

Figure 1 illustrates the breakdown of above mentioned major problems that add up onto the basic localization problem together with its origin from problem domain. This view not only defines the problems that should be resolved, but also supports designation and structure of the simulations developed throughout this study, which are explained in more detail in 2.1, 2.2 and 2.3.

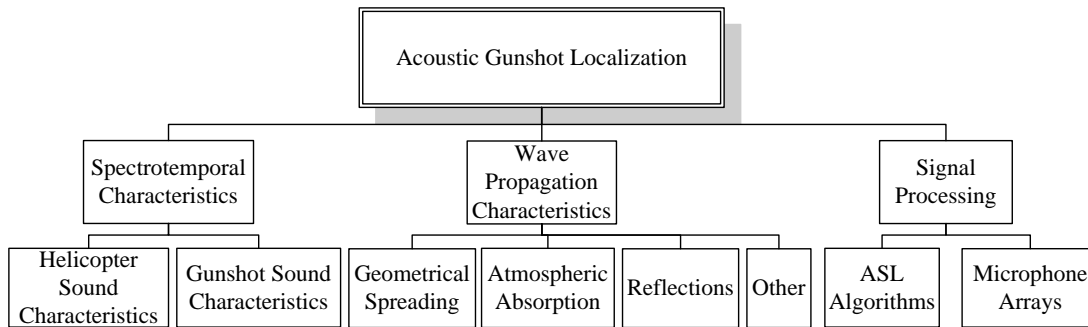


Figure 1 Breakdown of the factors associated with acoustic gunshot localization on helicopters

2.1 Domain Specific Spectrotemporal Characteristics

Using signals from sound field in the presence of such a noisy vehicle as a helicopter is a challenging problem. (Ahmed, Uppal, and Muhammad, 2013) stated that a realistic gunshot detection system addressing battlefield applications has to consider several performance goals such as rate of detection, minimization of false alarms or processing time. These issues concerning event detection are not in the scope of this study. Still, so as to localize the gunshot, we have to at least investigate robustness of the system to background noise and decide whether it would be possible to distinguish the gunshot sound despite helicopter noise and other environmental inferences.

2.1.1 Helicopter Sound Characteristics

As (Gerosa et al., 2007) stated, the Signal to Noise Ratio (SNR) range of interest for ground based gunshot localization implementations is relatively high since gunshots are considered easily detectable in a normal environment. Another research (Sadler, Sadler, and Pham, 1997) has shown that usage of invertible linear transforms can be successfully used for robust detection of gunshot components for moderate to high (over 10 dB) SNR range. More similar to our problem, (Ramos, Holm, Gudvangen, and Otterlei, 2013) included effects of a host vehicle during gunshot detection by using sound of a steel tracked military truck running on asphalt such that input SNR was set to about 0 dB. Successful results were obtained using de-noising methods; however, we have to investigate sound characteristics of helicopters to assess applicability of such methods and SNR ranges to our problem.

Aiming onboard sound localization, it is crucial to have prior knowledge of helicopter sound characteristics. Several sound sources on a helicopter add up to form the total sound produced by the helicopter, which is the major noise component for the purposes of this study. Previous researches can be examined so as to obtain an understanding of resultant amplitude and frequency characteristics of helicopter noise.

(True and Rickley, 1977) investigated sound characteristics of eight helicopters, namely, Hughes 300C, Hughes 500C, Bell 47G, Bell 206L, Bell 212, Sikorsky S-61,

Sikorsky S-64, and Boeing Vertol CH-47C using microphone recordings of level flyovers at 500 feet (150 meters) at several airspeeds as well as hover (steady) recordings with 500 and 250 feet altitude. That way, helicopters of small to large scale were included and different maneuver cases were covered. (True and Rickley, 1977) presented the results as 1/3 octave band spectra and time histories of both Effective Perceived Noise Level (EPNL) and peak A-weighted noise levels. Among these two alternatives, A-weighted sound levels of the study of (True and Rickley, 1977) were used as reference. As explained in Section 3.2, so as to account for human perception related A-weighting, an extra error interval was considered while examining SNR range of problem domain since we are interested in actual signal and noise levels rather than human perception of them. (True and Rickley, 1977) measured peak A-weighted SPLs between 75 dB and 95 dB for different models from 500 feet (150 meters) below. Researcher concluded that SPL levels were directly and logarithmically proportional to gross-weight of the helicopters. Examining effect of airspeed on induced SPL levels, moderate speeds caused the lowest sound amplitude for all helicopters. That is 70-100 knot range can be taken as minimum SPL region for all models. Moreover the difference between the tests with airspeed yielding lowest SPL and the highest SPL were examined for all helicopter models. The results revealed that there was a maximum of 2 dB to 10 dB SPL difference for the helicopter models, as helicopter velocities changed.

Results in frequency domain are also of specific interest. For all eight models and for different airspeeds, Blade Passage Frequencies (BPF) were easily observable at low frequencies. BPF range of helicopters (considering both main rotors and tail rotors) was 11Hz to 104Hz. More critical for the purposes of this study, components outside the frequency region of BPFs and their harmonics were significantly recessive. Except for Sikorsky S-61 helicopter, results reveal a 10 to 20 dB decrease at frequency bands above 500 Hertz.

The study (True and Rickley, 1977) also examined SPL differences between microphones positioned 500 feet below the helicopters and at 8 different angle positions so as to reveal directivity effects. Although effects of noise directivity were successfully obtained for all eight models, there was not a strict commonality among different models.

Much relevant to the purposes of our study, two of the helicopters generated impulsive type components, Bell 212 and CH-47C, namely. Author concluded that impulsive sounds corresponded to the passage of each main rotor blade. Moreover, in case helicopter approaches to receivers, a more complex but lower level impulsive signature was observed caused by phenomena called Blade Vortex Interaction. Blade Vortex Interaction (BVI) occurs when, in certain maneuvers, rotating blades encounter the vortices of air stream caused by preceding blades (Thom and Duraisamy, 2010). These certain maneuvers, however, cover only a very small portion of a typical flight profile as reported by (JanakiRam, Sim, Kitaplioglu, and Straub, 2009).

Another study (Robinson, 1973) aimed isolating and evaluating individual noise sources of a light observation helicopter, namely OH-6A, so as to comment on different mechanical design parameters and their effects on helicopter noise. The SPL was recorded at a point 200 feet below the helicopter in an open area, during the

middle of the night with no significant wind present. The A-weighted SPL for free hover from below 200 feet was measured to be 87 dB, which lies in the range indicated by (True and Rickley, 1977) for eight different helicopter models.

Although both SPL levels and 1/3 octave band spectra revealed different sound characteristics for individual designs, it was observed that small frequency components were dominant. Different from the work of (True and Rickley, 1977), 1/3 octave band spectra of OH-6 helicopter contain significant components around 1000 Hz too, still not as strong as those under 500 Hz.

While these two studies give sound characteristics information for a wide variety of helicopters, distance between microphones and helicopters is so large that they should be compared with measurements with smaller helicopter-to-microphone distance so as to be basis for more confident conclusions. Another study (Aravindakshan, Aravind, and Vyawahare, 2002) measured on-ground and in-flight sound levels of two helicopters, Chetak (Allouette HI) and Pratap (Mi-8), namely. Sound data was collected at eight positions at angular separation of 45° at a radius of 10 meters from the axis of the main rotor. The maximum SPL values averaged over eight angular positions were 113.9 dB and 108.9 dB for Chetak and Pratap, respectively. Maximum values of A-weighted peaks, on the other hand, were 129.4 dB(A) and 124.7 dB(A). Comparison of individual angular positions, however, did not yield any generic conclusions since variation of SPL with angular directivity was not common for the two helicopters. That is, SPL of Chetak was minimal at 0° and 180°, while all eight positions yielded quite similar values for Pratap helicopter. This result is similar with that of (True and Rickley, 1977) where no commonality among directivity characteristics was observed across different helicopters.

Another interesting result of the study was that the A-weighted sound levels at pilot's ear position during flight were in the excess of 99.3 and 94.4 dB(A) inside Chetak and Pratap cockpits for one-third of the sortie duration and in the excess of 97.6 and 93.2 dB(A) for two-thirds of the sortie duration. Although in-cockpit measurements can not to be taken as reference for our study, where microphones are to be placed outside the helicopter, it is evident from in-cockpit measurements why flight crew cannot mostly hear acoustic signature of gunshot events during flight.

Being interested in sound field around a helicopter still closer than 10 meters of (Aravindakshan et al., 2002), one can examine intensity measurements around helicopter fuselage. Previous measurement of helicopter sound intensity was carried out at a distance of 10 meters around the helicopter, when it was on ground with engine running at maximum rpm and main rotor fully engaged (Sujatha, 2010). SPLs were recorded in the 1/3 octave bands ranging from 50 Hz to 10 kHz. An example intensity level corresponding to front side of the helicopter had similar SPL and frequency characteristics with (Aravindakshan et al., 2002) and (True and Rickley, 1977) while another measurement was taken from advancing side of helicopter and included significant high-frequency components, too. This difference in spectra was reported to be caused by main gearbox noise component.

The change in characteristics with closer-to-helicopter recordings reveals that, as microphones get closer to the aircraft, dominance of main and tail rotor BPFs and their harmonics are lessened so that other onboard sound sources, too, has to be taken into consideration, details of which are given in 2.1.2 Onboard Sound Sources.

2.1.2 Onboard Sound Sources

By their nature, helicopters are constituted of several sub-systems and have a complex sound field of excessive power. Therefore it is crucial to investigate sound sources on a helicopter, individually, considering both frequency and SPL characteristics.

Considering their excessive signal amplitudes, the major contributors to helicopter sound are the two rotors (True and Rickley, 1977). A typical helicopter has two rotors of varying sizes, weights and blade numbers which are main rotor and tail rotor, namely. These rotors rotate with predetermined frequencies supplying the aircraft with required lift force. By their nature, periodic characteristics of their movement cause strong signal components at passage frequencies of each blade, namely Blade Passage Frequency (BPF) and their harmonics (Wagner, n.d.). (Lago et al., 1997) stated that these components, corresponding to main rotor, tail rotor and their harmonics, are easily observable in signal spectra and the actual BPFs can be calculated using Equation (1).

$$\text{BPF} = \frac{\text{rpm}}{60} * N_b \quad (1)$$

where N_b is the number of blades, rpm is revolution per minute for the rotor and BPF is the blade passage frequency given in Hz.

For example, BPF for main rotor of the AS332 “Super Puma” helicopter is 17.6 Hz and up to 6th harmonics of main rotor were observed at sound measurements (Lago et al., 1997). The same study also shows that BPF of the tail rotor is 107 Hz with a higher amplitude than that of main rotor.

(True and Rickley, 1977) also investigated BPF sound characteristics of eight helicopters with measurements from 500 feet (150 meters) below and concluded that tail rotor components dominated frequency spectra of helicopters, where tail rotor BPFs ranged from a low of 55 Hz for Bell 212 to a high of 103 Hz for Hughes 300c and Hughes 500c. Moreover, the study reported that rotor BPFs and their harmonics constitute the low frequency region (50-400 Hz) of the spectra.

For both illustration and verification purposes, *Figure 2* reveals a spectrogram of one of the helicopter sound signals used as noise component in the scope of this study. Both FFT size and window size of the Hamming window are 1024. These values were chosen such that both time and frequency characteristics of the helicopter is well-observed. In particular, time resolution (vertical axis) increases with decreasing window size, while frequency resolution increases with increasing FFT size. By careful selection of these values, periodic passage of helicopter blades is easily seen on *Figure 2*. Moreover, as previous studies in the literature stated, low frequency components (below 700 Hz for this specific example) are dominant. Finally, components in the range of [1500, 2000] Hz, which are not caused by main or tail rotor are of considerable interest since they correspond to various other sound-emitting components on the helicopter. That, too, is expected because, although sound produced by main and tail rotors are what human ear perceives from a distance, since the sensory equipment is to be placed on the helicopter, we should

also consider various other noise components that are to be heard close to vehicle fuselage such as the noise of the engine, transmission, exhaust, cooling system, avionics equipment and so on (Yücekayalı, A., Aerodynamics and Performance Technical Specialist, personal communication, May, 2015)

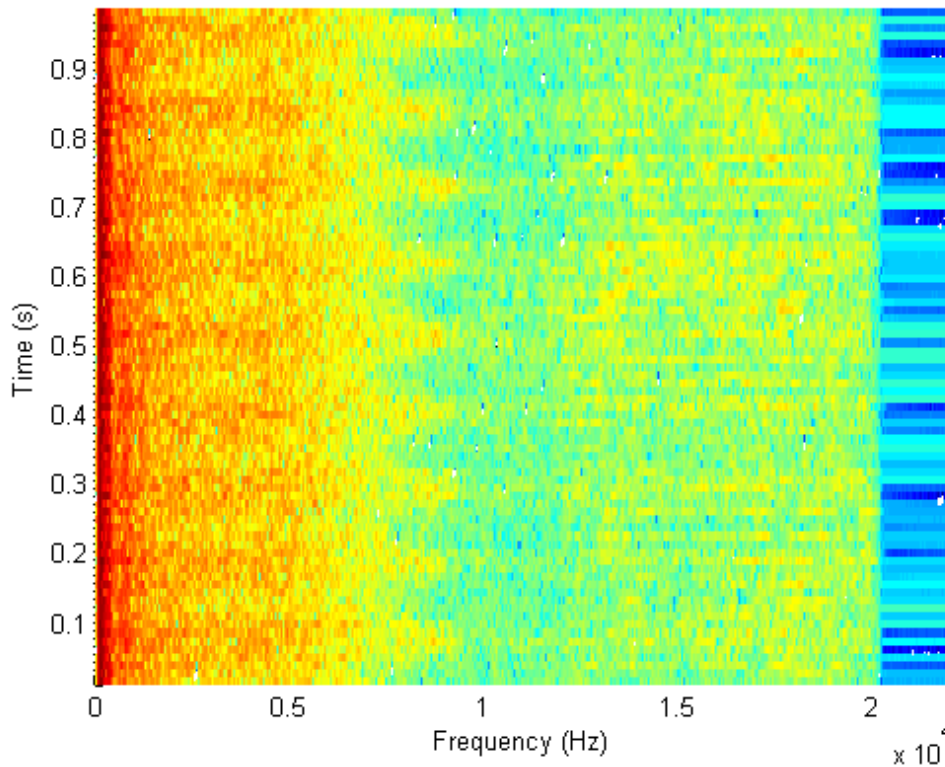


Figure 2 Spectrogram of an example helicopter sound signal windowed with a 1024-sample Hamming window and FFT size:1024. Both periodic blade passage and low frequency dominance are easily observable. Distortion above 20 kHz results from Nuyquist frequency and can be discarded

(Robinson, 1973) investigated such additional noise components that constitute the sound produced by a helicopter together with design parameters such as weight, number of blades and blade tip speed. Results revealed that onboard systems such as power plant and dyno cooler system have noticeable contribution, as well as engine air inlet and exhaust outlet, when measured from a closer distance (200 feet) to the helicopter as compared to the measurement distances of 500 feet by (True and Rickley, 1977). According to another study (Lago et al., 1997), turbines, oil pump and tail drive shaft were also observed to have components of significant power at higher frequencies.

Apart from the major contributors mentioned above, we should also consider sound produced by the avionics equipment and other mission specific equipment such as onboard weapons (Ortakaya, Y., Aerodynamics and Performance Senior Technical Specialist, personal communication, May, 2015). Although not present on all helicopters, some of these may have considerable effect on the measured noise and

require specific consideration especially while deciding sensor locations. However, examination of specific effects of such systems is not in the scope of this study.

2.1.3 Gunshot Sound Characteristics

Being a subject of increasing concern, there is plenty of work on acoustical solutions for gunshot detection, classification and localization. Signal data from audio recordings can provide information about the existence (Sallai et al., 2013), distance and angle of incidence of the gunshot as well as the speed and trajectory of the projectile (Duckworth, Gilbert, and Barger, 1996). Even the weapon type can be determined (Khan, Divakaran, and Sawhney, 2009). Previous studies in the literature aimed at one or more of the detection, classification and localization issues related to gunshots, using different characteristics captured from the sound field. Apart from academic research or prototype studies, there are some commercially available systems, too, for localization and identification of sniper shots (Duckworth et al., 1996). Although not all these issues are in the scope of this study, accurate and through understanding of gunshot signal characteristics is crucial.

A successfully recorded gunshot sound can contain information corresponding to three major components of a typical gunshot sound, which are the muzzle blast, the shock wave component if the projectile is moving at supersonic speeds and firearm's mechanical action (R. C. Maher and Shaw, 2008). As compared to the first two, mechanical action of the firearm has the lowest amplitude and is not expected to be observable for the purposes of this study, considering excessive noise levels of helicopter and the firearm-to-helicopter distance. The other two, however, being significantly distinct from each other, are to be examined for both their SPL and frequency characteristics.

(R. Maher, 2007) has examined characteristics of gunshot, giving not only these three major sound components but also effects of geometrical and environmental surroundings on them. In another study (R. C. Maher and Shaw, 2008), gunshot characteristics were examined separately for positions close to the firearm and the target. (Sallai et al., 2013) carried out a more integrated addressing of muzzle blast and shock wave components so as to take advantage of sensor fusion techniques with the aim of using detectable characteristics of both these components.

The primarily addressed signal component for the purposes of this study is the sound generated by the muzzle blast. A firearm, a rifle, a sniper or an RPG, uses explosive charge inside the gun barrel so that the bullet is thrown out with a very high velocity (R. Maher, 2007). This explosive action, together with the sound generated by it, is called the muzzle blast and spreads out of the barrel at all directions. Still, another study by the same author (R. C. Maher, 2006) measured that pressure levels caused by this explosion varies as much as 20 dB with direction and is at its highest at the direction pointed by the firearm. Other indications of the study were that, signature of a typical muzzle blast lasts for approximately 3 milliseconds and propagates through the air at speed of sound.

(R. Maher, 2007) also stated that, for sound field measurements close to the gunshot, muzzle blast is considered the major sound source and is very useful for purposes of both detection and localization of the acoustical event. However, for gunshot

distances of several hundred meters, the gunshot sound is reduced, as any other sound would be, by factors such as spherical spreading and air absorption (Harris, 1966). Besides, as stated by (Satué-villar and Fernández-rubio, 2005), received signal is expected to be weaker in amplitude, distorted by reflection, reverberation and obstacles in the sound field, as explained in more detail Section 2.2 of this study.

Prior to any deeper investigation of gunshot characteristics at large distances from the firearm, it is necessary to explain the other major sound component of a typical gunshot, the shockwave. For projectiles with higher velocity than the speed of sound, an acoustic shockwave is produced as the bullet travels faster than speed of sound. This cone-shaped shockwave expands behind the bullet and the speed of expansion is the same as speed of sound, therefore reaching the microphones before the muzzle blast (Bandi et al., 2012). The inner angle of the cone is the Mach Angle and given by

$$\theta_M = \sin^{-1}\left(\frac{1}{M}\right) \quad (2)$$

where M is defined as Mach number and given by

$$M = \frac{V}{c} \quad (3)$$

where V is the bullet's speed and c is the speed of sound.

Using these equations, direction of arrival for the shockwave can be calculated, once projectile speed is known. It is also observable that as the bullet slows down during its travel in the air, the Mach angle widens.

Both (Bandi et al., 2012) and (R. C. Maher, 2006) reported that the shockwave of a typical gunshot appears in sound recordings as a 200-microsecond N-shaped signal. That way, it can be discriminated from the succeeding muzzle blast and used for both positioning and identification of firearms. However, as (R. C. Maher and Shaw, 2008) states, complete calculation of bullet's trajectory, miss distance or firearm characteristics requires prior knowledge of bullet speed and caliber, which is, most of the time, hard to know beforehand. Still, there are gunshot identification and classification studies that are based on searching for similarities between the detected gunshot signal and characteristics of a set pre-recorded known gunshot signals. For example, (Gerosa et al., 2007) employed two parallel GMM classifiers, training with a set of 47 audio features, obtaining a false rejection rate of %8.

Having examined the major components contributing to a typical gunshot sound with physical phenomena behind it, it is now useful to list the amplitude and frequency characteristics of typical firearms. A comprehensive list of gunshots was given by (Beck et al., 2011), containing five revolvers, six pistols and three rifles. The weapon range covered barrel lengths of 6.4 cm to 56.4 cm and barrel-leaving speeds of 250.2 m/s to 889.1 m/s for five different bullet types. SPL levels varied between 151.4 dB and 160.8 dB, where all of the three rifles had larger SPL (around 160 dB) than other two gunshot types. It is also notable that all three rifles had supersonic bullets. The SPL measurements were taken at 2 meters from the barrels. Authors concluded that high frequency losses of the muzzle blast component were significant at long ranges

and both muzzle blast and shockwave components were highly affected by shooting direction.

(R. C. Maher and Shaw, 2008) recorded gunshot signals with supersonic projectiles for different target distances and obtained the time difference between shockwave and muzzle blast components. That way, acoustic characteristics of .308 caliber Winchester cartridges were compared for microphones located near the gunshot and the target. The particular bullet speed was 831.5 m/s yielding a Mach Number, M , of 2.54 and a Mach Angle, θ_M , of 23.2°. Results revealed a shockwave-to-muzzle blast time difference around 100 ms for a 91 meters downrange gunshot recording, while the two components were in the same time window of 10 ms for an 8 meter distance. A most critical observation from the measurements is that, although the muzzle blast component dramatically loses its amplitude above a distance of 300 meters, the shockwave component is not significantly reduced and still easily observable, so long as the miss distance is kept constant.

Examining frequency characteristics of gunshot signals, all (Ramos et al., 2013), (Bronuzia et al., 2012) and (Chacón-Rodríguez et al., 2011) could observe the expected impulsive behavior in gunshot recordings. That is frequency spectra of all four studies revealed wideband characteristics at the time window of gunshot occurrence. The details of spectra, however, varied considerably among different gunshot models. Calculating 1/3 octave band spectra of 4-inch barrel DWM pistol with a 7.65 Luger P LNR cartridge, (Bronuzia et al., 2012) have reported a 10 dB to 25 dB increase in SPL levels for frequencies above 1 kHz. (Chacón-Rodríguez et al., 2011) observed similar frequency spectra with a .22 Carbine ; however, the dominant frequencies were below 500 Hz for a .12 shotgun and below 1500 Hz for a 9mm Pistol, all recorded at 30 meters from the firearm.

Spectrograms of example gunshot signals were examined for their frequency characteristics with purposes of both illustration and checking compatibility of gunshot signals used in this study. Figure 3 reveals one such spectrogram example with gunshot occurring at 0.1 sec. Both impulsive nature and wideband characteristics are clearly observable and the result is in conformance with previous studies in literature.

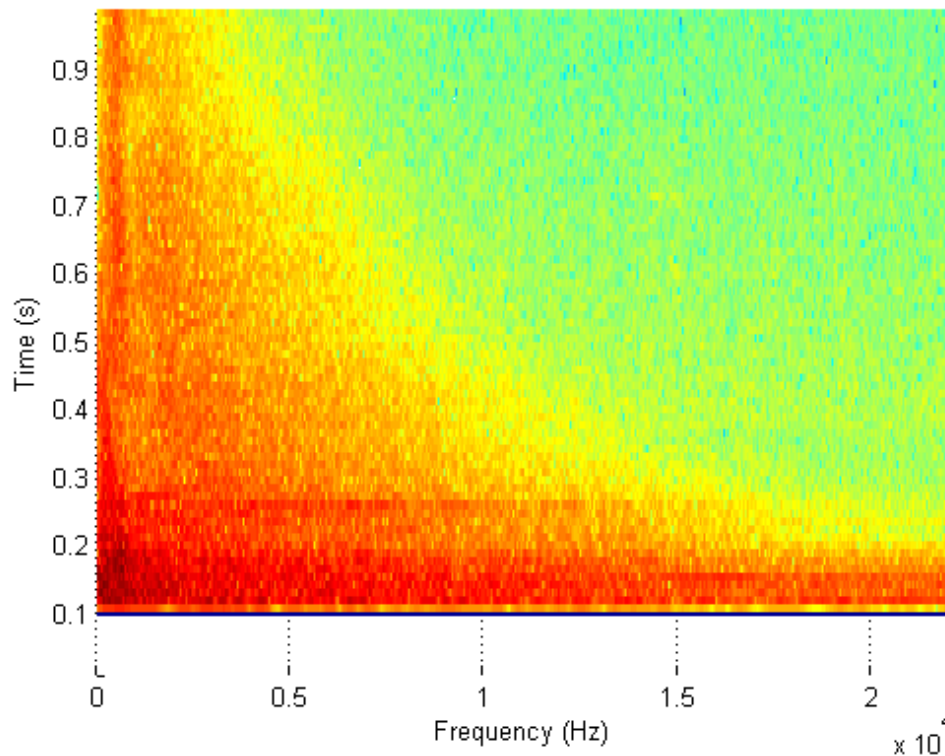


Figure 3 Spectrogram of an example gunshot sound signal windowed with a 1024-sample Hamming window and FFT size:1024. Gunshot occurs at 0.1 sec

To conclude, previous work in the literature explain the physical phenomena and geometry of gunshot sound characteristics and give a consistent idea of SPL levels of different gunshots at different distances and directivities. However, spectral characteristics of weapons and bullets, as explained above, are not consistent for different firearms and bullets.

2.2 Wave Propagation Characteristics

As stated in Section 1.3 Implementation Challenges, one of the major problems that add up onto a regular ASL implementation is the environmental challenges. As expected from an outdoor solution, effects of environmental factors on the sound field should be examined. Moreover, operational scenarios have to be investigated with their connections to environmental factors so as to determine operational limits for these factors.

The ISO 1996 standards aim standardization of procedures while describing noise outdoors for community noise studies. ISO9613 (International Organization for Standardization, 2007) in particular enables prediction of noise levels from noises of known emission and can be applied to the examination of a wide variety of noise sources. ISO9613 standard defines the octave-band attenuation, in decibels, between the source and the receiver, A , as

$$A = A_{\text{div}} + A_{\text{atm}} + A_{\text{gr}} + A_{\text{bar}} + A_{\text{misc}} \quad (4)$$

where

A_{div} is the attenuation due to geometrical divergence,

A_{atm} is the attenuation due to atmospheric absorption,

A_{gr} is the attenuation due to ground effect,

A_{bar} is the attenuation due to a barrier and

A_{misc} is the attenuation due to miscellaneous other effects.

Similarly, (Piercy, Embleton, and Sutherland, 1986), in the scope of studies on noise propagation in the atmosphere related to the control of community noise, listed the phenomena related to outdoor sound propagation as geometrical spreading, atmospheric absorption, ground effect, refraction, the effect of atmospheric turbulence and the effect of topography. These factors come together to form the outdoor attenuation effects on sound signals and can be individually investigated.

The geometrical spreading of sound from a coherent source brings signal power decrease with increasing source-to-target distances. This phenomenon is evident from conservation of signal power such that, as the sound waves propagate, the total signal power on any bound surface is equal for different travel distances. As a result, theoretical approach to geometrical spreading can be explained as follows: an attenuation of 6 dB per doubling of distance for spherical expansion from a point source, 3 dB per doubling of distance for cylindrical expansion from an infinite line source and parallel loss-free propagation from an infinite area source. In practical uses of these relations with finite sound sources, either a near field where these relations are approximately true or a far field where spherical spreading applies can be assumed and used (Piercy et al., 1986). In our case of gunshot localization on helicopters, spherical spreading and far field assumptions are valid, considering that a gunshot is effectively a point source and that there is a significant distance between the firearm and the helicopters as compared to microphone spacing.

ISO9613 (International Organization for Standardization, 2007) representation of the 6 dB per doubling of distance approach is given as

$$A_{\text{div}} = \left[20 * \log \left(\frac{d}{d_0} \right) + 11 \right] \quad (5)$$

in decibels, where the constant related the sound power level to the sound pressure level at the reference distance of 1 m from a point sound source, d is the distance from the source to receiver in meters and d_0 is the reference distance equal to 1 meter.

Another phenomenon to consider is the absorption of sound in air which is strongly dependent on the temperature and humidity but only weakly on the ambient pressure. Corresponding to the atmospheric absorption term in Equation (4), A_{atm} is defined as

$$A_{\text{atm}} = \frac{\alpha_b}{1000} \quad (6)$$

where α_b is the atmospheric attenuation coefficient, in decibels per kilometer, for each octave band at the mid-band frequency, samples of which are tabulated for practical usage in the ISO standard. The standard also formulates α_b so that, if a more detailed representation is required, values corresponding to all temperature, humidity and pressure values of interest can be calculated. An important characteristic of the formulation of ISO standard is that the value of atmospheric attenuation coefficient varies among frequency bands. Therefore, narrowband handling of atmospheric absorption calculations is necessary. Still, although the exact values for attenuation coefficient require these calculations, (Harris, 1966) presented in his study that, in general, lower values of percentile humidity resulted in more air absorption, while particular maximum-absorption points are encountered with respect to temperature for different frequency bands. Moreover, attenuation of higher frequency bands were higher, causing a 3 dB difference at 100 meters between 2 KHz and 12.5 kHz bands for 20°C.

The A_{gr} term in ISO equation corresponds to ground effects and is mainly due to sound reflected from ground surface interfering with the direct sound propagation from the source to the receiver. The ISO standard (International Organization for Standardization, 2007) categorizes ground types as hard ground, porous ground and mixed ground and puts emphasis on source and receiver locations rather than the ground characteristics in the middle region. Resultant ground attenuation coefficient depends also on the receiver height from the ground level, which would be the helicopter altitude in our case. However, the standard also states that its proposed method for calculating the ground attenuation is applicable only for flat surfaces, which is not a realistic assumption for our case, considering incompatible geographical characteristics. Moreover, because of the impulsive short duration nature of gunshot signals, ground reflections of an individual gunshot would not be overlapping with the primary sound signal once the processing window of interest is selected small enough so as not to include reflective components. Therefore ground reflections, as well as ground attenuation, were not taken into consideration for the calculations of this study. It should still be noted for possible future work that, for a real-life conventional battlefield scenario with multiple simultaneous gunshots, a primary gunshot signal of interest might be overlapped with reflections of another individual gunshot, resulting in reflective distortions in spite of small processing windows. Although not in the scope of this study, it is deemed that discrimination of the primary and reverberant signals in such a scenario could be handled in the signal processing domain by additional methods concerning battlefield event classification.

Another environmental effect applies directly on the speed of sound in air. As the temperature range of a helicopter implementation is expected to be wide and time-delay of arrival based calculations extensively use speed of sound, it is crucial to account for the environmental effects that change the sound speed. Equation (7) gives the formula that defines the variation of speed of sound with temperature as

$$c = c_0 * \sqrt{1 + \frac{T}{T_0}} \quad (7)$$

where c_0 is the speed of sound at 0°C equal to 331.3 m/s, T_0 is 273.15 K corresponding to 0°C and T is the ambient temperature.

Another environmental factor that affects sound propagation is wind since sound waves propagate as vibrations of molecules in the air and wind alters the mechanics of air itself. Moreover, as (Walker and Hedlin, 2009) states wind noise induced in microphones results also from turbulence–sensor, turbulence–turbulence, and turbulence–mean shear interactions. For a helicopter in motion, the major wind contribution comes from the fact that the vehicle, and so the microphones, are moving inside air and thus yielding a much higher turbulence-sensor interaction level than that of regular atmospheric wind. (Walker and Hedlin, 2009) listed some of the available techniques that might be deployed so as to cope with wind noise as Daniels filter, Rosette Pipe filter, Porous media filters, wind barriers and distributed sensors. Of these alternatives, distributed sensors, which applies adaptive processing on inputs from a densely spaced array, seems suitable with the purposes of array based acoustic source localization.

However, recall from Section 1.2 Real-life Requirements and Scenarios that the most critical sections of the flight, in terms of ground based firearms threat, are take-off, landing and hover maneuvers. As a precaution against the effects of atmospheric wind noise with speed below 5 m/sec, the usage of windscreens on each microphone yields significant reduction in wind noise levels. (R. G. Zhang and Kanapathipillai, 2008) stated that the usage of a 90 mm windscreen has reduced the wind noise SPL by 3 to 6 dB covering wind speeds in the range of 2.5 m/sec to 5 m/sec. This wind speed range is suitable as only the regular atmospheric wind is concerned with steady maneuvers of the helicopter. Moreover, non-stationary portions of the flight, i.e. forward flight at cruising speed, can be addressed since the wind would have a known direction in that case, that is the opposite of helicopter motion. This knowledge, together with information on aerodynamics specific to the helicopter model, can be used to build additional precautions that physically address the direction of strongest wind components. Therefore, effects of wind noise were not simulated in the scope of this study.

Although the effects of distance, temperature, humidity and pressure can be calculated using well-established formulas in literature (Harris, 1966) and standards (International Organization for Standardization, 2007), there are less predictable effects, considering extreme conditions of a helicopter's mission environment. Effects of wind (Eunkuk et al., 2010), air moisture, soil characteristics (Piercy et al., 1986), weather conditions such as rain or snow and gradients of temperature and wind in atmosphere (Arntzen et al., 2012) may pose additional challenges for a realistic implementation, although they are not simulated in the scope of this study.

2.3 Acoustic Source Localization Theory and Implementation

Although there are additive issues and additional challenges on top of ASL, as given in the earlier sections of this study, gunshot localization on Helicopters is primarily an Acoustic Source Localization problem. Therefore, factors that are known to affect a simple Acoustic Source Localization application are of interest for the purposes of

this study, too. In this regard, common characteristics of ASL algorithms and means for their realization are examined in this section.

2.3.1 Acoustic Source Localization Theory: Basics of Operation

A simple Acoustic Source Localization (ASL) application locates a sound source by applying acoustic localization algorithms on signals collected from the sound field. As (Günel and Hacıhabiboğlu, 2011) states, these algorithms use time and/or level differences between the signals captured by more than one microphone so as to calculate the information of interest regarding the position of the sound source. This position information may be only the direction of the source, in which case it is called direction-of-arrival (DOA), or may include distance between the source and the microphones, too, so as to determine coordinates of the source.

So as to give a simple description of the ASL problem, consider a simple sound field with a source and two receivers, MIC₁ and MIC₂, with receiver separation of S . Sound signals travel along the paths from the source to MIC₁ and MIC₂, with distances D_1 and D_2 as illustrated by *Figure 4*.

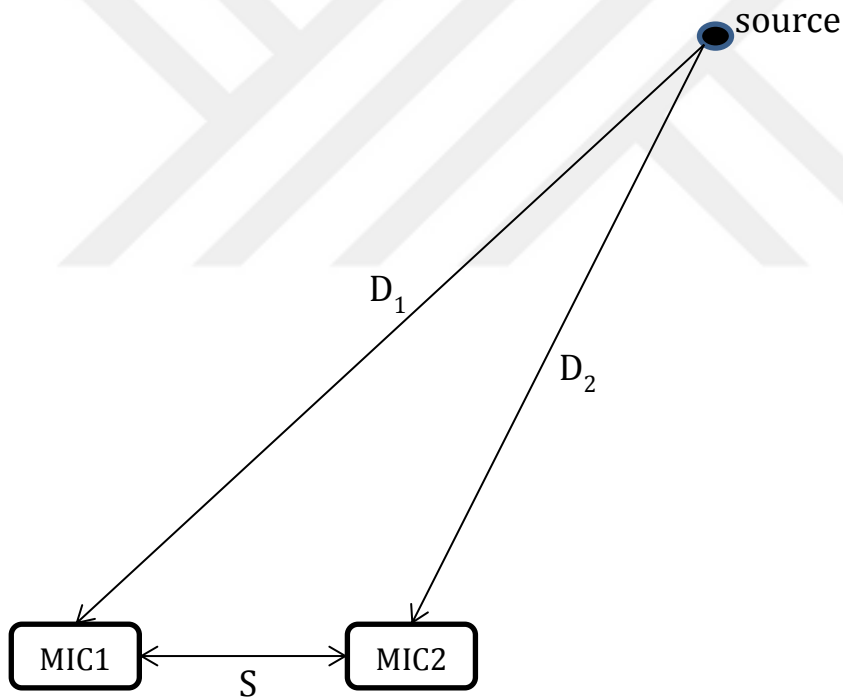


Figure 4 Simple sound field geometry

Corresponding travel times for the two signals, T_1 and T_2 can be simply calculated using Equation (8) as

$$T_1 = D_1/c \quad (8)$$

$$T_2 = D_2/c$$

where c is the speed of sound in air.

Due to this time difference between T_1 and T_2 resulting sound signals receiver positions can be modeled by Equation (9) as

$$\begin{aligned} \text{MIC}_1(t) &= s(t) + n_1(t) \\ \text{MIC}_2(t) &= \alpha * s(t + \tau) + n_2(t) \end{aligned} \tag{9}$$

where

$s(t)$ is the acoustic signal due to source at MIC_1 , $n_1(t)$ is the noise component at MIC_1 , $n_2(t)$ is the noise component at MIC_2 , τ is the time difference, $T_2 - T_1$, between arrivals of acoustic wavefronts and α is the attenuation (or amplification) factor due to the difference in source-to-receiver distances.

For the purposes of this illustration, let noise components at the two receiver positions be uncorrelated and let $\alpha = 1$, such that attenuation (or amplification) among the two receiver positions is neglected.

According to the acoustical far field assumption, if the receivers are positioned sufficiently far from the sound source, wave front appear as plane waves and the closest paths from the source to the two receivers are parallel lines. The geometry of the problem with acoustical far field assumption is given in *Figure 5*.

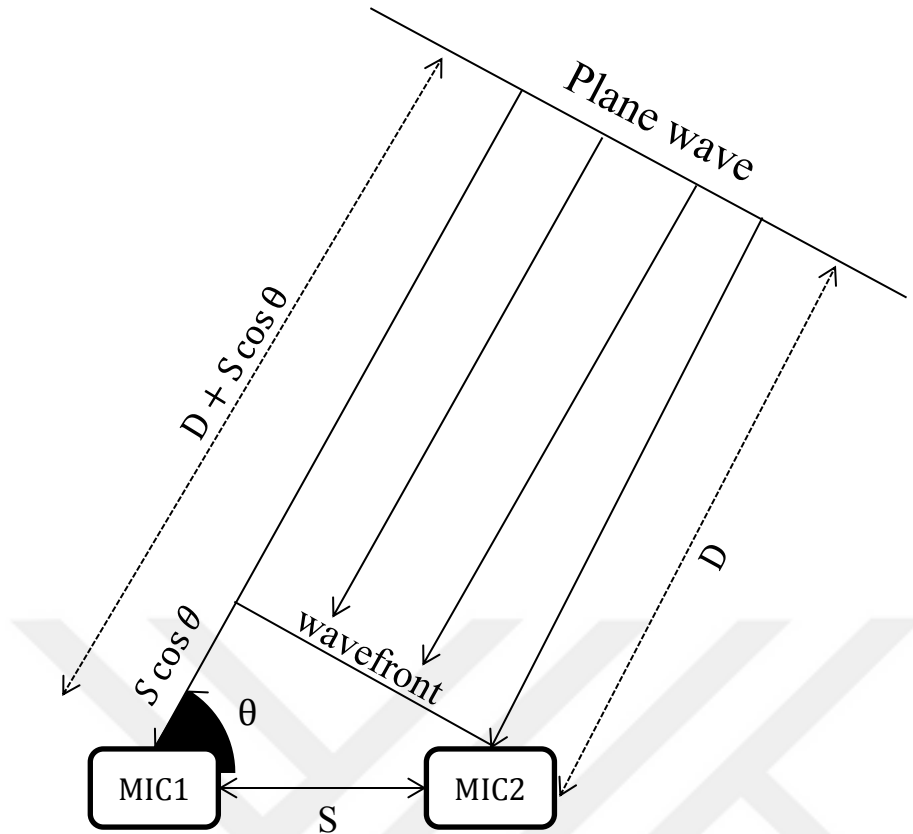


Figure 5 Simple sound field geometry with plane wave assumption

Using this simpler form of the sound field geometry, direction-of-arrival (DOA) algorithms convert the time difference between the two signals, τ , into angle of arrival, θ , information. The methods for obtaining τ and extraction of angle of arrival, θ , using that information varies among different DOA algorithms, some of which are to be given in the following sections of this study. In any case, DOA determination can be seen as the initial step of acoustical source localization and specific implementations may combine knowledge of microphone array geometry and amplitude differences at separate receiver signals together with this DOA information so as to determine optimal source location (Günel and Hacıhabiboğlu, 2011).

2.3.2 Acoustic Source Localization Implementation: Microphones and Microphone Arrays

2.3.2.1 Microphones: Basic Operation and Types

Microphones are the sensory equipment deployed in audio applications. Although there are various types with different characteristics and different working principles, the basic idea behind them all is to convert physical signals from the sound field into electrical signals so that they can be transmitted processed or converted.

A major classification of microphones, which is also important for purposes of gunshot localization on helicopters, divides them into two categories both with their own advantages and disadvantages depending on the application (Chung, 2012). The first class of microphones, which is known as omnidirectional microphones, converts air pressure into electrical signals, thus giving the same output for wave-fronts arriving from different directions. Directional microphones on the other hand are based on the pressure gradients caused by sound signals in the air and thus their response changes with changing input signal directions. There are various types of directional microphones with different directional characteristics, such as bidirectional, cardioid or hypercardioid, making it possible to select according to the problem's physical requirements.

More specific to the purposes of this study, analyzing on ground and in flight sound levels of two helicopter models, (Aravindakshan et al., 2002) have successfully used omnidirectional condenser microphones of $\frac{1}{2}$ inch diameter having a flat frequency response between 4 Hz to 21 kHz. That way, effects of outdoor environment and wide-band nature of helicopter sound was accounted for. Another study (Schmitz et al., 2007), again used omnidirectional microphones fitted with nose cones, in the form of a microphone boom placed underneath a helicopter in order to record and analyze steady-state and maneuvering sound characteristics.

Further classification of a wide range of microphones is possible with respect to their sources of energy, transducer principle and implementation technology and materials (Boré and Peus, 1999). The list may include, but not limited to, dynamic microphones, magnetic microphones, AF condenser microphones, crystal microphones, RF condenser microphones, carbon microphones and micro electromechanical systems (MEMS) microphones. For the purposes of an outdoor localization application, free field, omnidirectional microphones with a flat frequency response, similar to those used by (Aravindakshan et al., 2002) and (Schmitz et al., 2007), should be considered.

Another consideration regarding possible real-life implementation is the dynamic range of microphones. As given in Section 2.1.3 Gunshot Sound Characteristics, gunshot acoustics related studies in the literature reported both muzzle blast and shockwave components with SPL levels as high as 160 dB which, in most cases, results in signal clipping at microphone outputs. However, considering that the gunshot sound is to be significantly attenuated due to the source to microphone distance and environmental effects as described in Section 2.2 Wave Propagation Characteristics, high SPL limit of most typical microphones (140 dB to 160) was deemed sufficient for an onboard gunshot localization application.

2.3.2.2 *Microphone Arrays*

A microphone array is the sensory part of an ASL implementation, which consists of a set of microphones located in a way that sound signals from different locations of interest are captured (Benesty, Chen, and Huang, 2008). (Rabinkin, 1997) and (Benesty et al., 2008) mention a list of studies in the literature that deploy microphone arrays as speech enhancement, teleconferencing, talker tracking, vehicle detection and tracking, gunshot localization as well as other surveillance applications.

Geometry of this sensory array can be adjusted in accordance with the requirements of the problem domain such that valuable information is captured concerning the amplitude and frequency characteristics of signal and noise components. Moreover, (Rabinkin, 1997) states that the locations of the microphones must be determined during systems' design phases so as to obtain the desired performance. The primary consideration concerning the microphone array geometry is the physical spacing between adjacent microphones. One of the most commonly used geometry for microphone array applications is known as Uniformly Spaced Linear Arrays (USLA), and is formed by linearly placing microphones with an equal microphone spacing distance (Ward, Kennedy, and Williamson, 2001). Although details of specific systems and problems may pose different limitations on microphone spacing, a primary concern is known as the spatial aliasing, which arises from the fact that in order to avoid signal aliasing, the phase difference between a pair of microphones should be less than π . As (Ward et al., 2001) explain, this makes sure that the phase difference between the signals received by the two microphones is certainly smaller than the signal period and signals are reconstructable according to the Sampling Theorem. This puts a high-limit on the frequency of operation for a pair of microphones which can be given as

$$2 \pi f_{\max} \tau \leq \pi \quad (10)$$

where f_{\max} is the maximum allowable frequency and τ is the time difference of arrival between the pair of microphones. Substituting

$$\tau = d/c \quad (11)$$

where d is the physical spacing between the pair of microphones and c is the speed of sound, for the case with maximum value of τ when the sound source is in line with the microphone pair, we get the frequency limitation for a given microphone spacing as

$$f_{\max} < \frac{c}{2 * d} \quad (12)$$

Apart from the spacing of the microphones, physical arrangement of the array plays an important role in achieving expected characteristics. There are studies in the literature proposing different array geometries in order to achieve different performance goals and it has been shown for a fixed number of microphones, that the array geometry has a critical role in enhancing processing algorithms' performance. Although a linear sequencing of microphones with equal microphone spacing, USLA, appears to be the most common and simple design, (Ward et al., 2001) stated that performance requirements such as frequency range may impose modifications as in the case of constant directivity beamforming, where a linear array of varying microphone spacing was found useful. This type of array geometry is referred to as NUSLA, Non-Uniformly Spaced Linear Array, and has found wide usage in the literature with the purpose of meeting beam-width, side-lobe and directivity characteristics of arrays (Oraizi and Fallahpour, 2008) (Shanan and Pomalaza-Raez, 1989). Another example from literature is the use of spherically symmetric microphone arrays on the vertices of regular convex polyhedral, which was found to be helpful on canceling the direction dependent errors caused by the spatial sampling on a three-dimensional array (Günel and Hacıhabiboğlu, 2011).

Another important parameter regarding microphone arrays is the number of microphones. Obviously, having a larger number of microphones in an array mostly brings algorithm-wise advantages, or in any case, does not bring algorithm performance penalties, since in such a case, the application could always use a reduced number of input channels. Indeed, by the application of Nyquist Theorem on a uniformly spaced linear array, it can be concluded that there is a lower-limit for the number of elements in a microphone array such that

$$M > \frac{2 \lambda_{\max}}{w_{\text{desired}} \lambda_{\min}} \quad (13)$$

where M is the number of elements in the microphone array, λ_{\min} is the smallest wavelength of interest, λ_{\max} is the largest wavelength of interest and w_{desired} is the desired width of the main lobe of localization estimation output.

However, as (Gazer and Grenier, 1995) stated, concerns such as the array size, computational complexity or cost of the system may induce limitations on the number of microphones in an array. This may result in a tradeoff where an optimal number of elements should be determined for meeting implementation specific goals on both size and accuracy.

2.3.3 Acoustic Source Localization Algorithms

Acoustic Source Localization algorithms perform on multi-channel signals captured by a microphone array in order to estimate the parameters regarding the direction, position or frequency contents of a sound source, or multiple sound sources. The traditional ASL approaches in the literature can be divided into three subcategories which are Steered Response Power (SRP) localizers (Ward et al., 2001), Time Delay of Arrival (TDOA) based localizers (Bandi et al., 2012) (Hero and Schwartz, 1984) and High Resolution Spectral Estimation (Schmidt, 1986) based localizers.

SRP techniques can localize multiple sources simultaneously and possess the simplest calculations; however, despite its low complexity, the algorithm may take a long processing time since it is based on repeatedly forming beams for all directions.

TDOA is known to have good directional localization accuracy and is also robust with white noise since it applies cross-correlation on input signals. However, reflections in the sound field are historically known to cause problems since the method provides no suppressing for such components (Pourmohammad and Ahadi, 2012) (Benesty, 2001).

High Resolution Spectral Estimation technique is good for its multiple simultaneous source localization and noise suppression (Schmidt, 1986). However, it requires narrowband operation which may result in increased processing time and memory requirements depending on application requirements.

In addition to above-given traditional approaches of Time Delay of Arrival (TDOA), High Resolution Spectral Estimation and Steered Response Power (SRP) localizers, (Günel and Hacıhabiboğlu, 2011) have listed more recent approaches in the literature, some of which are intensity vector based localization techniques and biologically inspired methods. Biologically inspired methods are based on

localization capabilities of biological hearing mechanism and cognitive aspects of hearing. Localization capability of human hearing mechanisms can be compared to a movable dual-microphone array while cognitive aspects include effects of sound field familiarity and applicability of artificial intelligence concepts. Intensity vector based localization techniques on the other hand, of the two describing components of sound field, which are scalar value (sound pressure) and vector value (acoustic particle velocity), uses the latter.

This study investigates the factors affecting Gunshot Source Localization on helicopters, deploying three ASL algorithms with pre-processing and post-processing suggestions, namely;

- Beamforming
- Generalized Cross Correlation (GCC)
- Multiple Signal Classification (MUSIC)

Beamforming can be listed under the SRP class of traditional ASL algorithms while GCC is the most widely used example of TDOA-based localization. Finally, MUSIC algorithm implements High Resolution Spectral Estimation approach. In this way, widely used examples of all three classes of conventional ASL algorithms are covered. More details on these three algorithms will be given in Chapter 3 Proposed Methods for Gunshot Localization on Helicopters, together with pre-processing and post-processing proposed for an onboard helicopter application.

2.4 Acoustical Simulation

Considering that there are several factors concerning sound propagation and domain specific spectrotemporal characteristics as well as algorithm-wise signal processing parameters, this study aims the development of a simulation environment such that the effects of different parameters of the problem domain can be investigated in a selective manner. In this regard, some of the previous work in the literature concerning simulations of both aircraft and gunshot sound are given below.

The primary source of information regarding sound simulation is the ISO9613 standard (International Organization for Standardization, 2007) which analyses the attenuation of sound during propagation outdoors and gives the formulation that can be used for wide-band signals. Both geometrical spreading and effects of environmental factors such as temperature or humidity are considered which are used in this work, while simulating propagation of sound signals of interest, i.e. gunshot and helicopter noise.

There is plenty of work in the literature concerning the simulation of aircraft noise since the subject is closely related with the popular issues of community noise and airport noise examinations. NASA Langley Research Center has been developing systems for this purpose, including not only simulation (Stephen A. Rizzi and Sullivan, 2003) but also rendering of the sound field for predicting aircraft-induced noise (Stephen A. Rizzi, Sullivan, and Aumann, 2008).

More generic studies on the sound field simulation also are available defining and simulating factors that affect the sound field for outdoor or room environments.

(Satué-villar and Fernández-rubio, 2005) have listed the phenomena that can alter a sound wave in its way as reflection, refraction and diffraction. The study used the widely known image method (Allen and Berkley, 1979) to simulate results of reflecting waves from the walls of a room environment.

2.4.1 Straight Line Propagation

Considering outdoor simulation case instead of room acoustics, as it is with the problem of gunshot localization on helicopters, (Stephan A Rizzi and Sullivan, 1996) have synthesized propagation in open-air environment, again in the scope of NASA's aircraft noise impact studies. A standard environment model was described where time delay, gain and filter operations were applied on the source signal, corresponding to the absolute delay, spreading loss and atmospheric absorption, respectively. Together with a uniform atmosphere absorption model, the propagation is said to depend on, and so can be calculated using, constant atmospheric conditions (pressure, temperature and relative humidity), the frequency of interest and the straight-line path length between source and observer. Another comparable model for atmospheric absorption calculation is the ANSI S1.26-1995 standard (American Institute of Physics, 1995) on the subject. (Stephan A Rizzi and Sullivan, 1996) have compared their calculations deploying the aforementioned filters with ANSI standard atmospheric absorption and found similar results except the fact that straight line propagation with uniform atmosphere model of the study revealed more pessimistic results (more attenuation) in the range of 3-5 dB for 50, 121.9 and 200 meter ranges, as compared to ANSI standard.

Another study (Piercy et al., 1986) has listed a more extensive list of phenomena that should be considered while simulating noise propagation in the atmosphere as geometric spreading, atmospheric absorption, reflection, refraction, turbulence, ground impedance and obstructions. This study, too, included a comparison of simulations and actual measurement on 1/3 octave band spectra, presenting the results of comparison by dividing the 50-3200 Hz range into three sub-bands. In the low frequency band (50-200 Hz) for both 110 meters and 615 meters, the calculated attenuation was slightly smaller than that of measurements. In the middle frequency region (200-1500 Hz); however, simulations resulted up to 10 dB larger attenuation levels than measurement. For the high frequency region (1500-3200 Hz), close similarity was observed among simulations and measurements.

Still more specific to our problem, another sound field simulation study (R. C. Maher, 2006) simulated the sound field caused by a gunshot in open air and compared the results with actual gunshot recordings. The method and calculations basically depended on geometrical examination of the surrounding, taking into consideration both the muzzle blast and the shockwave components, together with ground reflections. The results revealed good agreement with the actual recordings. Therefore, a similar approach was carried out in this study while simulating the propagation of the gunshot signal and determining signal processing parameters such as the window size. Further details of this geometrical examination are given in Chapter 3 of this study.

2.4.2 Curved Path Simulation

Either for the simulation of room acoustics (Lentz, Schröder, Vorländer, and Assenmacher, 2007) or for the simulation of sound propagation outdoors with non-uniform atmospheric effects (Arntzen et al., 2012), there is previous work in the literature applying curved path simulations. In curved path simulation sound rays are launched from the source position at many initial angles, as would be with a realistic point sound source and only the rays that reach the receiver positions are further processed since they contain the information regarding the paths the synthesized sound would follow while traveling from the source to the listener. As this is an iterative process, temporal and angular refinements can be applied to obtain the desired resolution and accuracy.

As (Arntzen et al., 2012) states, effects of an inhomogeneous atmosphere where wind and/or temperature gradients cause refraction, adds the requirement to include an arbitrary atmosphere by determining the curved path(s) as a function of time and to compute and apply the integrated absorption, time delay and spreading loss along each path. The propagation characteristics, e.g., travel time, spreading losses and absorption, are calculated with the help of ray tracing where, along each path, the atmospheric absorption is accumulated as the sum of piecewise frequency dependent absorptions per length.

Although the attenuation is applied by delay, filtering and gain operations similar to the straight line path approach given in 2.4.1, the curved-path approach is more complex since similar calculations are applied for a large number of pre-determined curved paths of sound propagation. For the straight-line propagation case with a stationary receiver, the calculations are carried out once as a function of a single range from the source to the receiver, which is readily calculated from problem geometry. However, (Arntzen et al., 2012) observed small differences, under 1 dB, between A-weighted maximum SPL levels of straight-path and curved path approaches. This close proximity was due to the fact that a maximum-SPL-path would correspond to a smallest-range path which is the most similar case to a straight line between source and receiver. Researcher concluded that weather dependent effects would be more significantly reflected with curved path simulations, in case of prominent directional sources that also emit a lot of low frequency components, as with helicopters. In this regard, it can be concluded that an implementation that aims helicopter near field sound simulation should consider multipath effects and curved path simulation.

The suggestion of (Arntzen et al., 2012) is for directional sources with prominent low frequency components. In our case gunshot signals have wideband characteristics. Moreover, there is adequate level of similarities between the straight line simulations and actual measurements or standards, given by (Piercy et al., 1986) and (Stephan A Rizzi and Sullivan, 1996) respectively. Moreover, straight line propagation approach involves simpler calculations. Due to these reasons, for this work, the straight line propagation approach was found useful. Further details regarding outdoor wave propagation factors that affect the sound propagation and gunshot localization are given in Chapter 4 Simulation of Factors that Affect Localization on Helicopters.

2.5 Solution Methodology: Simulation of Factors That Affect Array Based Acoustic Gunshot Localization on Helicopters

As given in the previous sections of this chapter, microphone based acoustical localization of gunshots on helicopters is a challenging problem with many factors and parameters in place. These factors can be listed under the three categories; wave propagation characteristics, signal processing parameters and domain-specific spectrotemporal characteristics. The first two categories of factors apply to outdoor acoustic source localization applications in general and are given in more detail in *Table 1*. The third group, on the other hand, is specific to the problem of gunshot localization on helicopters as given in *Table 2*. These two tables present a more detailed breakdown of the factors affecting localization and better illustrate the dimensionality of parameters for such a system.

Table 1 Factors that affect acoustic source localization outdoors

Factors that Affect Wave Propagation		Factors that Affect Signal Processing	
Geometrical Spreading Factors	Atmospheric Absorption Factors	ASL Algorithms Parameters	Microphone Array Parameters
<ul style="list-style-type: none"> - Distance - Angle of Incidence - Reflections - Weather Gradients - Soil Characteristics - Wind - Meteorological Events 	<ul style="list-style-type: none"> - Temperature - Humidity - Pressure 	<ul style="list-style-type: none"> - Window Size - Sampling Frequency - Simultaneous Sources 	<ul style="list-style-type: none"> - Number of Microphones - Microphone Spacing - Array Geometry

Table 2 Domain-specific factors that affect gunshot localization on helicopters

Spectrotemporal Sound Characteristics	
Helicopter Sound Characteristics	Gunshot Sound Characteristics
<ul style="list-style-type: none"> - Sound Pressure Level - Helicopter Gross Weight - Blade Passage Frequencies - Blade Tip Speed - Blade Vortex Interaction - Airspeed - Maneuvers - Mission-Specific Equipment 	<ul style="list-style-type: none"> - Sound Pressure Level - Firearm Type - Barrel Dimensions - Explosive Type - Projectile Speed - Miss Distance - Bullet Caliber - Direction of Trajectory

As explained in this chapter, all these factors are presumed to affect gunshot localization on helicopters, as supported not only by previous studies in the literature but also by opinions of military personnel and engineers from the related domain. However, the extent to which these factors are effective and which factors are dominant over others are not easily predictable. Moreover, although there are several studies concerning the effects of these three categories of factors separately on localization and detection performance, to the knowledge of the author, only limited information is available that comprehensively addresses all these aspects; namely, helicopter and gunshot sound characteristics, wave propagation in open-air environment as well as algorithm and array parameters.

Apart from above given reasons, considering the excessive dimensionality of the problem, it is very difficult to test for all these parameters in a controlled manner such that the effects of individual factors on localization are revealed. Indeed, such an approach would require a large number of costly flight tests with strict safety measures. Therefore it was deemed that a feasibility study should simulate array based acoustic gunshot localization on helicopters, including as much of the above mentioned factors as possible in the form of input parameters. The addressing of the factors from problem domain by the simulations of this study is given in *Figure 6* where factors marked as blue are covered in the scope of simulations.

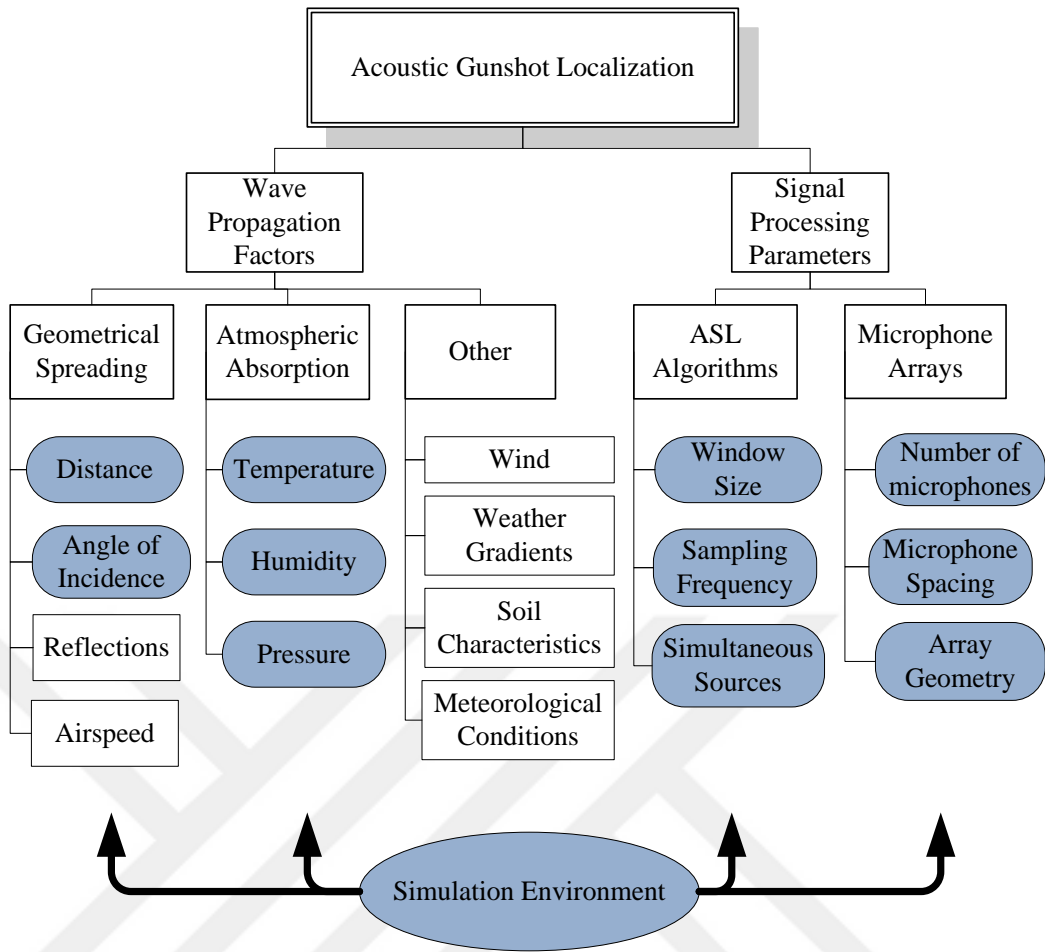


Figure 6 Gunshot localization parameters and simulations coverage

Figure 7 gives the block diagram of simulation the framework developed in MATLAB that has two major stages: simulation and localization. The simulation stage is capable of either simulating an environmental and geometrical gunshot sound field scenario so as to obtain resulting signal amplitude and frequency characteristics, or adjusting the gunshot and helicopter sound levels so that the SNR value of interest is obtained. Then, the localization stage applies ASL algorithms with or without proposed pre/post processing operations so as to yield localization performances. It should be noted that operation and outputs of the simulation environment were not formally validated in the scope of this study; however, the simulation infrastructure deploys widely used signal processing methods such as Spectral Subtraction (Boll, 1979) or well-known formulas such as inverse square formula which are already known to be valid. Moreover, considering possible implementation faults and coding errors, simulation outputs were continuously compared with theoretical expectations throughout the study and reported together with results in Chapter 3 and Chapter 4.

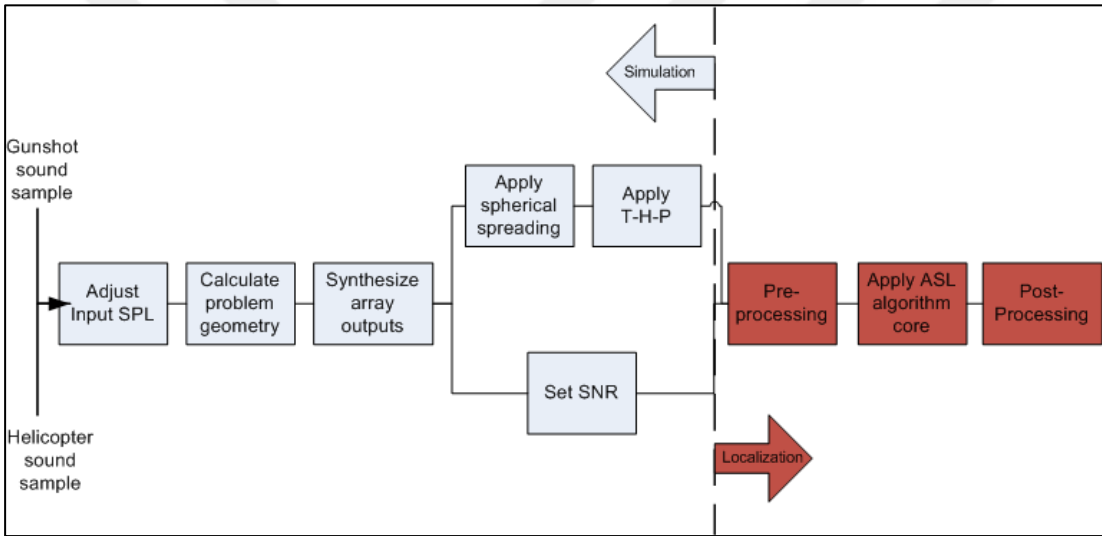


Figure 7 Block Diagram of the simulation framework developed using MATLAB in the scope of this study

In the light of these factors as given by Table 1 and Table 2 and using the simulation framework of Figure 6 and Figure 7, this study first compares the localization performances of the three ASL methods; Beamforming, GCC and MUSIC, with pre-processing and post-processing suggestions that address domain specific sound field characteristics. Then signal processing parameters concerning both individual ASL algorithms and microphone arrays are simulated so as to illustrate their effects on the localization performance. Finally, parameters of outdoor sound propagation are simulated such that the effects and limitations of environmental operating conditions on source localization are revealed.

CHAPTER 3

PROPOSED METHODS FOR GUNSHOT LOCALIZATION ON HELICOPTERS

3.1 Algorithms Selection

As given in Section 2.3.3 Acoustic Source Localization Algorithms, ASL approaches in the literature can be divided into three subcategories, namely Steered Response Power (SRP) localizers, Time Delay of Arrival (TDOA) based localizers and High Resolution Spectral Estimation based localizers. This study investigates factors affecting Gunshot Source Localization on helicopters, by proposing pre-processing and post-processing methods specifically for the following three ASL algorithms:

- Beamforming
- Generalized Cross Correlation (GCC)
- Multiple Signal Classification (MUSIC)

Beamforming can be listed under SRP class of traditional ASL algorithms while GCC is the most widely used example of TDOA. Finally, MUSIC algorithm implements High Resolution Spectral Estimation approach. That way, widely used examples of all three classes of conventional ASL algorithms are covered.

While selecting the three algorithms of this study, major classification of ASL algorithms were considered. One popular example of each sub-class of algorithms, namely Steered Response Power (SRP) localizers, Time Delay of Arrival (TDOA) based localizers and High Resolution Spectral Estimation based localization, were selected depending on both theoretical characteristics and suggestions of previous measurement and simulations in the literature.

In a historical perspective, beamformers were the first examples of attempts to determine the direction of arrival information. Apart from localization the beamforming concept offers directional enhancements of signal components over noise which is promising for such a noisy environment as with the problem of gunshot localization on helicopters. Despite its simple and calculations, the operation principle depends on searching for angle of incidence which may impose limitations on real time behavior. However, the same operation principle also makes it possible to selectively determine the angular range of interest which may not only reduce the number of calculations but also gives the chance of neglecting the predicted directions of helicopter noise. Moreover, direction-selective characteristics of beamformers can also help with handling of reflections which result from multiple attenuated and delayed replicas of the source signal due to boundaries and objects in mission environment's geometry (Chen, Benesty, and Huang, 2006). Another issue with Beamforming is the narrowband limitation since usage of uniformly spaced linear arrays is predicted (Ward et al., 2001). That is, the phase difference between a pair of microphones should be less than π for the signal to be reconstructable according to the Sampling Theorem. This implies a frequency limitation that depends on microphone spacing according to Equation (12). Therefore, since the gunshot is a

wideband signal, filtering of the receiver inputs is required so as to apply narrowband operations.

Despite its narrowband limitations, beamforming algorithm may provide advantages concerning robustness to noise by taking advantage of the number of microphones in the array. That is, as opposed to pair-wise processing of TDOA algorithms, beamforming works on the whole channels of the microphone array, offering the possibility of narrowing down the output beamwidth (Oraizi and Fallahpour, 2008). That way, as (Ramos, Holm, Gudvangen, and Otterlei, 2011) state, the gain of the array is increased by $10 \log \frac{M}{2}$, where M is the number of microphones in the array, which means a theoretical SNR enhancement of 6 dB by doubling the number of microphones in the array. Considering the problem of gunshot localization on helicopters, this would presume a theoretical doubling of detection range. Considering these advantages as well as limitations, a simple Delay-and-Sum Beamformer was selected and performance improvement by pre-processing and post-processing was suggested.

Generalized Cross Correlation (GCC) algorithm was selected as the second algorithm considering its robustness with noise, calculation efficiency and previously reported successful implementations with gunshot specific localization applications. Firstly, the method applies cross correlation to the input channels which improves probability of both detection and localization, making it a convenient approach for noisy environments. Secondly, simple calculations of the algorithm require low processing requirements, and offers good real-time performance. Finally, variants of GCC algorithm were reported to operate successfully under outdoor conditions for the localization of wideband impulsive signals of scream, gunshot (Valenzise et al., 2007) despite the effects of excessive noise levels and low sampling rate (Freire and Apolinario, 2011).

On the other hand, there are limitations related to GCC usage. Firstly, despite being able to eliminate noise and offering sharpened signal component, GCC output suffers from what is known as the threshold effect below a certain implementation-defined SNR (Valenzise et al., 2007). Determination of this threshold for an onboard gunshot localization application is crucial and pre-processing methods are to be suggested for widening the SNR range of GCC in accordance with the limits of problem domain.

Secondly, GCC requires prior knowledge of signal characteristics (Knapp and Carter, 1976) which is very hard to predict considering the wide variety of firearm types as well as outdoor environment conditions' unpredictable alterations on them. However, there are variants of GCC approach that offer pre-processing methods so as to remove this dependency on source signal characteristics. Despite depending on an uncorrelated noise components assumption, the localization independent from the input signal characteristics is deemed very promising and cannot be offered by the other two algorithms.

Considering its extensive usage of matrix operations together with a final search for determining the optimal angle of arrival, the MUSIC algorithm's calculation complexity is higher than that of TDOA techniques. Another constraint is that this method is suitable for narrowband signals. Although it is possible to divide broadband signals into narrowband segments, this certainly adds up onto the above-

mentioned calculation complexity. However, a simpler implementation of the algorithm is available, namely root-MUSIC algorithm proposed by (Barabell, 1983), that can reduce this calculation complexity for practical purposes, once the approach is found useful for the goal of gunshot localization on helicopters. Moreover, there are also variants of MUSIC, namely Estimation of Signal Parameters using Rotational Invariance Technique (ESPRIT) proposed by (Roy and Kailath, 1989), that overcomes the uniformly spaced linear array (ULA) restriction that applies for both TDOA and Steered Response Power (SRP) techniques. This advantage arises from the fact that the MUSIC algorithm makes no assumptions about the array geometry. Moreover, (Schmidt, 1986) states that the receivers are permitted to have different amplitude/phase characteristics in terms of directionality. Finally, by its definition, MUSIC algorithm can be employed for multiple simultaneous signals without loss of performance which is important for a gunshot localization implementation, considering real life challenges of conventional battle requirements as given in Section 1.2 Real-life Requirements and Scenarios.

3.2 Domain Specific SNR Examination

Considering the extreme sound levels of the host vehicle together with alterations caused by the outdoor environment and real life mission cases, gunshot localization on helicopters is expected to suffer much from noise issues. Therefore, the ability to perform under noisy conditions was an important criterion of choice for all the ASL algorithms in the scope of this study. Although it is evident that each algorithm is expected to have a considerable level of robustness to noise, the exact SNR range for successful localization has to be determined for each specific algorithm so as to be able to conclude on their applicability to onboard gunshot localization. Moreover, despite being easily anticipated to be very low, the effective SNR values to be encountered are unknown. It should also be noted that a comprehensive estimation would require the usage of domain-specific signal and noise components while concluding on the required robustness to noise.

Therefore, before examining the performances of different ASL algorithms, a domain-specific investigation of signal and noise levels was performed, taking into account the helicopter and gunshot sound characteristics as well as real-life mission scenarios and problem geometry. That way an SNR range of interest was determined so that the following questions can be answered for each specific ASL algorithm.

- What is the SNR-range expectancy from the algorithm?
- Is the algorithm applicable for such SNR levels?
- Does the algorithm require SNR-enhancing pre-processing methods?
- Which frequency components (of the host vehicle, especially) should be filtered?
- Can any conclusions be made on the algorithm's reliability depending on the SNR level?

The sound pressure level of the host vehicle was reported to be ranging from 80 dB (A) to 110 dB(A) by different studies (True and Rickley, 1977) (Aravindakshan et al., 2002), for different helicopter models and different sensor arrangements as given in Section 2.1.1 Helicopter Sound Characteristics. Generally speaking one can

conclude that the sound levels of helicopters increase with increasing gross weight and no exact correlation can be assumed between the SPL and airspeeds. A more predictable effect of the airspeed, however, is related to microphones' motion in air that affects the measured helicopter hover noise levels above 5-10 knots.

An important inference, examining the measurements by (Eunkuk et al., 2010), (True and Rickley, 1977) and (Aravindakshan et al., 2002) reveals the practical values for the attenuation of helicopter noise for outdoor conditions. Apparently, a 7-8 dB decrease in helicopter SPL by doubling of distance is a good approximation, which can be interpreted as a 1-2 dB increased version of the theoretically defined 6 dB loss due to spherical spreading. This increase could be related to atmospheric absorption. Although a more deterministic estimate would require calculations related to temperature, humidity and atmospheric pressure, an approximation of 7.5 dB per doubling of distance can be taken as an adequate reference while determining only a range of SNR values.

Table 3 lists the SPL values of previous measurements from literature with helicopter to microphone distances of 400 feet, 200 feet, 100 feet and 10 meters.

Table 3. Helicopter SPL estimation using previous studies in the literature

Reference	Distance	SPL (mean)
(True and Rickley, 1977)	400 feet (121 meters)	74-80 dB(A)
(Robinson, 1973)	200 feet (60.5 meters)	87 dB (A)
(True and Rickley, 1977)	100 feet (30.25 meters)	94-98 dB(A)
(Aravindakshan et al., 2002)	10 meters	103-108 dB (A)
Estimation	5 meters	110-116 dB

These values were used so as to obtain an estimation value for helicopter sound SPL at a position below the helicopter. Positioning of the microphone array below the helicopter is expected to bring noise level advantages by the screening effect of helicopter fuselage. Precise calculation of the noise SPL value however would require consideration of wave-front scattering which is not in the scope of this study. Instead, estimation procedure of Table 3 was applied by taking a mean value of 5 meters for the level difference between the main rotor and microphone positions, which is a good approximation for many helicopters. The calculation was carried out using the widely known inverse-square law which is

$$SPL_{A-B} = 10 * \log_{10} \left(\left(\frac{D_B}{D_A} \right)^2 \right) \quad (14)$$

where D_A and D_B source-to-microphone distances for sound source positions, A and B, and SPL_{A-B} is the SPL level difference between A and B in decibels.

Once the SPL of the major noise contributor is accounted for, it is crucial to decide on a valid range of gunshot SPLs together with the effect of firearm to microphone distance. Considering real-life scenarios explained in Section 1.2 Real-life Requirements and Scenarios, the primary limitation on the source to microphone distance was set as 256 meters for the purpose of SNR range determination, although larger distances were also simulated in the scope of this study, as given in Section 4.3. Then, an approximation procedure similar to that of helicopter SPL was followed for gunshot SPL estimation, too. As given in 2.1.3. Gunshot Sound Characteristics, typical gunshot SPL for various firearms is around 160 dB, measured from 2 meters from the barrel (Beck et al., 2011) (R. Maher, 2007). Simply applying the inverse-square calculation of Equation (14) yields the approximations given in Table 4.

Table 4 Gunshot SPL estimation using inverse-square law

Distance	SPL
2 meters	150-160 dB
4 meters	144-154 dB
8 meters	138-148 dB
16 meters	132-142 dB
32 meters	126-136 dB
64 meters	118-128 dB
128 meters	112-122 dB
256 meters	106-116 dB

Moreover a quick lookup of the atmospheric absorption coefficient table of ISO:9613 (International Organization for Standardization, 2007) yields a less than 4 dB decrease in SPL for most of the signal spectrum which is to be subtracted from the SPL values of Table 4.

Comparing the estimated gunshot SPL of 102 dB to 112 dB at 256 meters distance from the sound source with helicopter noise SPL of 110 dB to 116 dB, an SNR range of -14 dB to 2 dB is estimated. However, as prediction of this range takes into account the effect of only spherical attenuation and atmospheric absorption, the effects of other predicted challenges, such as noise directivity, temperature and wind gradients should also be considered.

Additional SNR Considerations

Apart from the SPL levels, another issue on SNR examination concerns the helicopter's noise directivity. Although no common directional characteristics for different helicopters at steady flight was observed among various studies, it was reported by both (Eunkuk et al., 2010) and (Aravindakshan et al., 2002) that, during

forward flight, noise directivity was such that the highest SPL region is below the main rotor tip and at advancing blade side. Comparison of SPLs at different locations reveals that careful selection of microphone positions around the fuselage could bring a 4-5 dB SPL advantage.

Another point of considerable interest is directional characteristics of helicopter sound sources. As given in Section 2.1.2 Onboard Sound Sources, the dominant noise sources on helicopters are main rotor and tail rotor components, which produce both audible and inaudible components in the low frequency region of the spectrum. Therefore, these major noise sources and their harmonics could be filtered out; however other onboard sound sources require specific consideration. Engine, transmission, exhaust outlet as well as other avionics and mission specific equipment are all sources of anisotropic noise which means that, if not handled correctly, would be present at the localization output.

Since the measurements from previous studies were used as reference, the A-weighting applied at SPL measurements should be noted here. That is, the major noise contributor of main rotor blade passage frequency is below the limit of hearing for most helicopters. Direct usage of dB(A) results of previous studies does not take into account these inaudible frequencies although an array based signal processing application would suffer from these components as they are handled no different than other frequencies. Therefore, though slightly, a negative shift in the SNR range should be predicted taking into account the inaudible helicopter noise components.

Finally, as (R. Maher, 2007) states, the effects of atmospheric gradients may cause differences of up to 20 dB for distances over a few hundred meters between predicted and measured SPL of gunshots. In light of these additional challenges the worst case SNR limit was reduced by 20 dB and the best case SNR was reduced by 6 dB, updating the SNR range of -14 dB to +2 dB, as -34 dB to -4 dB.

Once is domain specific SNR requirement was determined, applicability of different ASL algorithms to such SNR levels, as well as to outdoor sound propagation effects were simulated. A custom simulating environment was developed using MATLAB since available sound field simulation tools are not applicable to this study's domain, as explained in 1.1 Aims and Objectives. Test cases and scenarios were inputted from MATLAB command window, instead of usage of a graphical user interface considering automatization of multiple consecutive test scenarios, such that parameters can be manipulated in a continuous manner.

For all simulations of this study, a single gunshot sound recording was used as input signal component so that comparing outputs of different methods and test cases could be valid. Similarly, the noise components at each microphone were extracted from a single helicopter sound recording, although different portions of helicopter sound were applied at different microphones. These portions were checked to be uncorrelated by examining pairwise cross-correlations. Both gunshot and helicopter sound signals were normalized so that their initial SPL was set as 136 dB and 95 dB respectively. These values are in the typical range of previous measurements in the literature, as summarized in Section 2.1.3 Gunshot Sound Characteristics and Section 2.1.1 Helicopter Sound Characteristics. Then signal and noise levels were adjusted so as to obtain SNR values which is defined as ratio of gunshot signal power to helicopter sound power, both with a duration of 0.25 seconds. No band selection,

pre-filtering or other pre/post processing was applied while calculating the SNR values so that the performances of all three methods as well as proposed pre/post processing could be compared with the same metric, that is raw input SNR.

For the test scenarios of this chapter, a constant set of parameters, other than SNR, was determined and fixed so that proposed methods' performances with respect to SNR level could be observed. After numerous tests and consideration of real-life requirements and problem geometry, parameter values that yield a good illustration of effects of SNR were selected and fixed for simulations of this chapter as

- Number of microphones: M: 4
- Microphones spacing: S: 0.1 m
- Sampling frequency F_s : 44100 Hz
- Window size L: 1024
- Target angle: θ : 45°

3.3 Beamforming

3.3.1 Theory of Operation

The basic idea behind the beamforming concept is to use a set of spatially separated microphones with the aim of selecting a direction from which to accept the signals. Implementation of this basic idea can be viewed in two steps. The first is to synchronize the signals such that the time delay resulted from microphones' spatial difference is cancelled. Then, the second step applies weighting and combination of the signals so as to form an enhanced signal in terms of SNR or other attributes of interest. Delay-and-Sum Beamformer is the simplest case, where the synchronization step is achieved by delaying the array input signals and the resulting signals are summed as the second step.

For the purposes of localization using beamforming concept, the amount of delays are selected for different look directions and the operation can be applied as many times as required by the requirements concerning localization resolution. That way signals corresponding to all directions are obtained among which the direction which yields the largest power can be selected. The maximum acoustic signal power is incident to the microphone array from this direction and, in case signal and noise components were carefully handled, direction of arrival for the signal of interest is estimated.

The handling of the signal and noise components is related to the frequency domain characteristics of beamformers. Although both narrowband and wideband implementation of beamforming are applicable, most of the DOA estimation algorithms deploy narrowband beamforming techniques. (Ward et al., 2001) explain that most beamforming applications depend on the narrowband assumption which implies that the signal arriving at the microphone array is narrowband, while signals such as speech and gunshot sound do not comply with this assumption. In that sense, handling of wideband signals requires additional processing for beamforming to be effective.

In order to explain the application of beamforming for localization, let $\mathbf{X}(t)$ represent the set of time domain signals received by $N+1$ microphones of a microphone array, which can be modeled as

$$\mathbf{X}(t) = [x_0(t) \ x_1(t) \ \dots \ x_N(t)] \quad (15)$$

Taking the first array microphone, M_{x_0} , as the reference, Equation (15) can be rewritten as

$$\mathbf{X}(t) = [a_0 x_0(t) \ a_1 x_0(t - \tau_1) \ \dots \ a_N x_0(t - \tau_N)] \quad (16)$$

where τ_i and a_i are the delay and gain of the i^{th} microphone.

Neglecting the pressure gains associated with microphones and taking the Fourier transform so as to obtain the frequency domain representation, $\mathbf{X}(\omega)$, can be written as

$$\mathbf{X}(\omega) = x_0(\omega)\mathbf{B}(\omega) + \mathbf{N}(\omega) \quad (17)$$

where $x_0(\omega)$ is the frequency domain representation of the reference microphone signal, $\mathbf{N}(\omega)$ is the noise component at each specific microphone and $\mathbf{B}(\omega)$ beamformer's steering vector, which is given as

$$\mathbf{B}(\omega) = [1 \ e^{-i\omega\tau_1} \ \dots \ e^{-i\omega\tau_N}] \quad (18)$$

Note that, using the prior knowledge of array geometry, τ_i can be calculated as

$$\tau_i = \frac{S_i \cos \theta}{c} \quad (19)$$

where S_i is distance of the specific microphone to the reference microphone and c is the speed of sound. Therefore, assuming uncorrelated noise at each microphone, one can determine the beamformer steering vector, $\mathbf{B}(\omega)$, of Equation(18) by selecting the angle of incidence, θ , and calculating the corresponding phase change using Equation(19) so as to form the beam at that angle.

In the scope of this study, beamforming was applied in frequency domain by applying delays corresponding to look directions in the range of 0° to 180° . The resolution for the set of directions was variable and implemented as an input for the simulations. The power levels corresponding to directions in the range of $[0^\circ, 180^\circ]$ were output of the beamformer so that an estimate of the direction of arrival for the gunshot signal was obtained.

3.3.2 Pre-processing and Post-Processing

As (Ward et al., 2001) states ASL with beamforming is mostly used with a narrowband approach and as (Chen et al., 2006) states applications on wideband signals such as speech or gunshots are also possible if the frequency characteristics of signal and noise components are handled correctly. In this regard, *Figure 8* gives the DOA estimation of the Beamformer algorithm without any pre-processing.

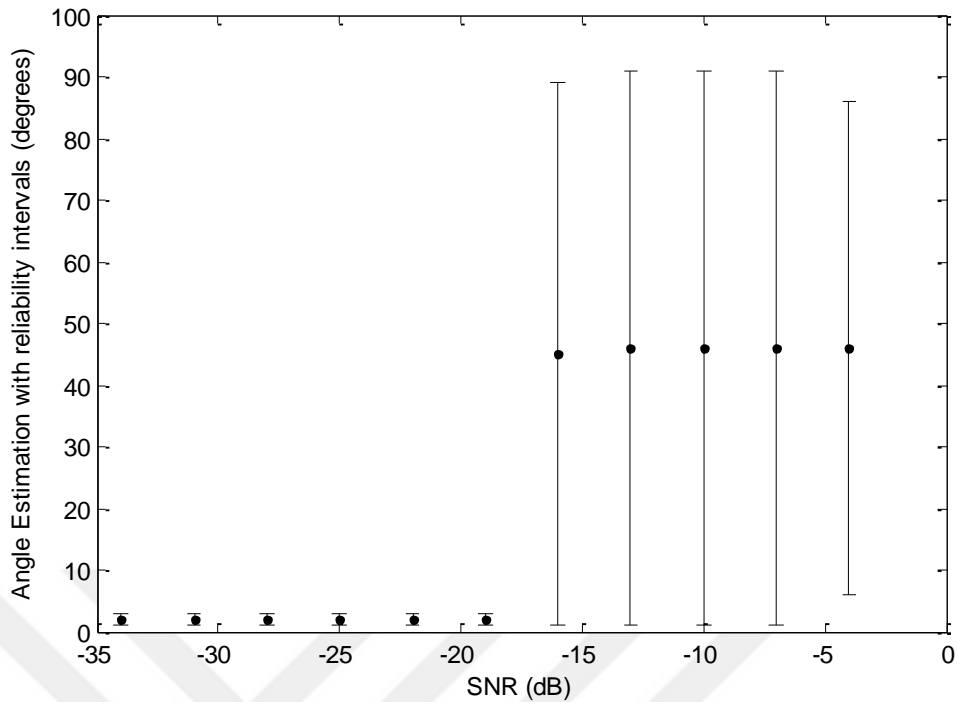


Figure 8 Beamformer output for a source at $\theta=45^\circ$ with microphone spacing, $S = 0.1$ m, number of microphones = 4, sampling frequency, $F_s = 44100$ Hz when no pre-processing is applied.

As Figure 8 reveals, the Beamformer algorithm could not estimate the expected DOA of 45° below -16 dB SNR. Moreover, the reliability intervals, defined as 3 dB decrease around DOA estimation peak, are quite wide even for the highest SNR values of interest. Therefore the frequency spectrum of both helicopter and gunshot sounds should be examined. As given in Section 2.1.3 Gunshot Sound Characteristics, many researches have reported a wideband spectrum for gunshot signals when measured at a position close to the firearm. This conclusion agrees with what would be expected from an impulse-like sound. However, different from an ideal impulse, low frequency portion of the spectrum appears to be relatively recessive, considering especially frequencies below 1 kHz (Bronuzzia et al., 2012). Although high frequencies are known to suffer more from air absorption (International Organization for Standardization, 2007), significant components above 1 kHz can still be expected since the air absorption is a small contributor to signal energy loss, as compared to spherical attenuation losses, as explained in Section 3.2 Domain Specific SNR Examination.

As opposed to the gunshot sound, numerous researches on helicopter sound have reported frequency spectrum with dominant low frequency components as given in 2.1.1 Helicopter Sound Characteristics. This is primarily due to the fact that major noise contributors of main rotor and tail rotor blade passing frequencies (BPF) and harmonics are in the 0-400 Hz range (Lago et al., 1997). Examining the helicopter sound spectrogram given in 2.1.1 Helicopter Sound Characteristics, noise dominant low frequency range for this specific example was selected as [0,700] Hz and, it was

deemed useful high pass filtering the microphone signals with a cut-off frequency of 700 Hz, so that the helicopter noise components are significantly reduced.

Having determined the low-frequency limit on the signal spectra, the high-frequency limit can also be deduced by microphone array considerations as explained in Section 2.3.2 Acoustic Source Localization Implementation: Microphones and Microphone Arrays. In order to avoid spatial aliasing, microphone array inputs should be filtered to avoid high frequencies, the cut-off frequency of which is dependent on the microphone spacing. Using Equation (12), the high-frequency limit for microphone spacing, S , of 0.1 m can easily be calculated as 1750 Hz.

Figure 9 reveals the increase in localization performance by application of such filtering. Although the SNR range of successful DOA estimation was extended for only 3 dB (that is -16 dB to -19 dB), reliability intervals (-3dB beamwidth) were significantly narrower as compared to Figure 8 where no pre-filtering was applied.

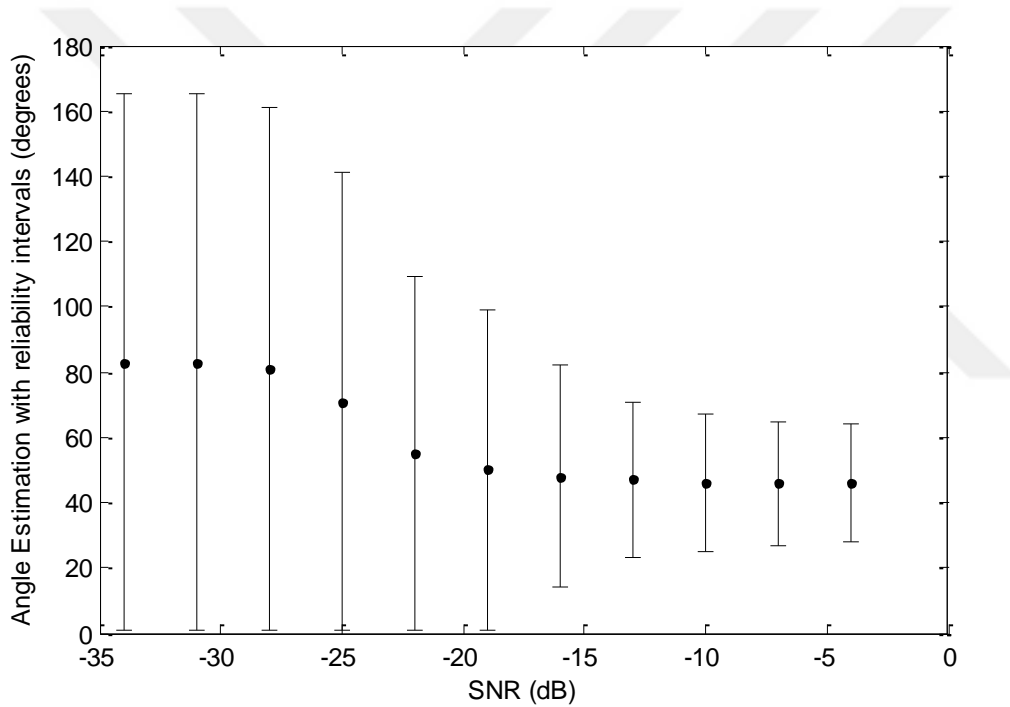


Figure 9 DOA estimation of Beamformer for a source at 45° with pre-filtering of frequencies below 700 Hz, where helicopter noise components are dominant, and above 1750 Hz, where spatial aliasing is observed. Microphone spacing, $S = 0.1$ m, number of microphones = 4, sampling frequency, $F_s = 44100$ Hz.

Although microphone array inputs can be filtered in accordance with the problem specific low and high cut-off frequencies, it should still be noted that, since there are various noise sources on a helicopter, noise components should be expected at frequencies in between, too. However, these frequencies cannot simply be filtered so as not to lose the gunshot components of interest. So as to handle excessive noise levels, application of Spectral Subtraction algorithm was considered. (Ramos et al., 2013) stated that field tests have proved that real life situations create challenging

problems for direction of arrival estimation of gunshot signals and suggested spectral subtraction as a means of noise reduction. Presented by (Boll, S.F., 1979), spectral subtraction is a noise suppression algorithm which is based on the principle of subtracting the relatively stationary noise from input sound recordings. The method calculates the spectral noise bias during intervals where signal of interest is not present (noise only). Recalling from Section 2.1.3 Gunshot Sound Characteristics that both muzzle blast and shockwave are impulsive signals with a typical duration of 3 to 6 milliseconds, characteristics of helicopter noise can be considered to be stationary as compared to gunshot signal of interest. Therefore, it is possible to calculate the noise (helicopter sound) bias for long time intervals with no gunshot. Moreover, appropriate updating of this noise bias may offer robustness with slowly changing sound characteristics due to helicopter maneuvers in a possible real-life implementation. Finally, implementation at the pre-processing phase was suggested since the spectral subtraction at post-processing would require a priori knowledge of the direction of arrival of the muzzle blast and the shockwave.

Therefore, spectral subtraction as presented by (Boll, 1979) was applied to the microphone array signals before beamforming. As Figure 10 illustrates, a significant enhancement was obtained on SNR range of successful DOA estimation, by the application of Spectral Subtraction at the pre-processing phase. That is, Beamformer preceded by spectral subtraction could estimate the DOA of 45° with a reasonable directional error for SNR values as low as -25 dB, which was not possible below -16 dB without pre-processing.

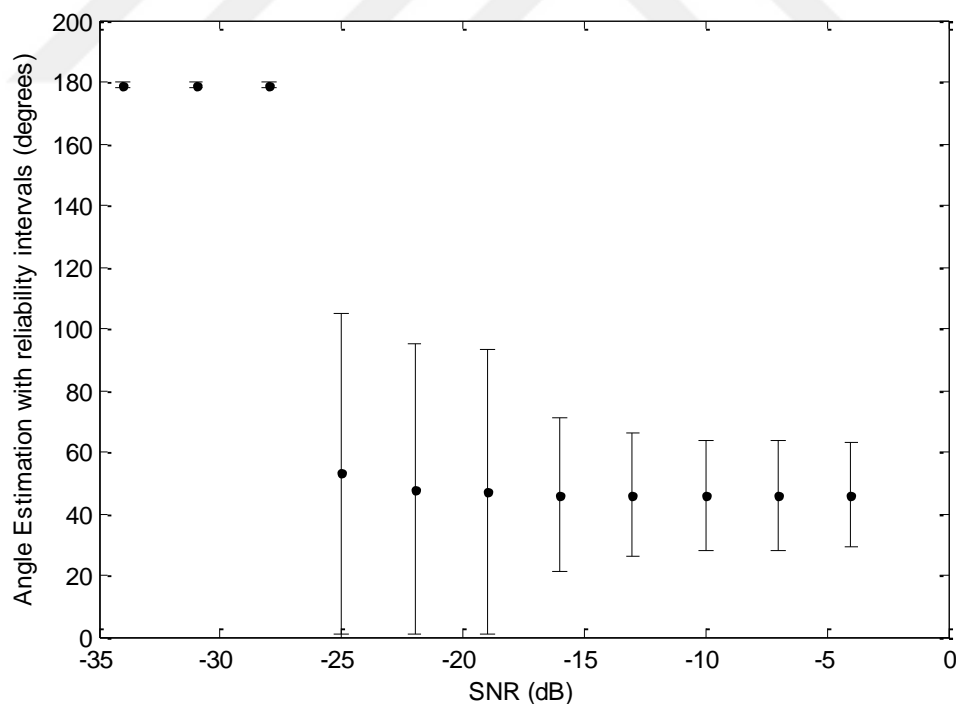


Figure 10 Beamformer for a source at 45° with both pre-filtering (700-1800 Hz) and Spectral Subtraction applied as pre-processing. Parameters of Spectral Subtraction are assumed to be known since localization stage is assumed to follow a detection stage in a typical localization implementation. Target angle is 45° with microphone

spacing, $S = 0.1$ m, number of microphones = 4, sampling frequency, $F_S = 44100$ Hz.

It should be noted that although the peak of localization estimation was greatly enhanced to cover SNR values as low as -25 dB, the -3 dB beamwidth was still large below -19 dB SNR, as observed in Figure 10. However, beamwidth concerns can be seen secondary as compared to DOA estimation angle (the peak) since beamwidth performance can be enhanced by increasing number of microphones as well as additional preprocessing techniques, if required.

Another processing consideration concerns the calculation burden of ASL using beamforming. Although calculation for forming a beam at a specific direction is trivial, ASL using beamforming requires these calculations to be exhaustively applied for all directions of interest. Therefore, a trade-off between directional resolution and processing time is necessary. For the purposes of gunshot localization on helicopters, an angular resolution of 1° is not strictly required as explained in 1.2 Real-life Requirements and Scenarios. Therefore, different step sizes in the $[0^\circ, 180^\circ]$ interval were simulated so as to observe if the calculation burden, and so the processing time could be reduced without a significant reduction of localization performance. Results revealed that step size of 2 degrees did not cause a significant degradation in proposed method's performance so that processing time could be decreased by a half.

3.4 Generalized Cross Correlation

3.4.1 Theory of Operation

The basic idea behind cross correlation techniques is that, in order to estimate the time delay between a pair of spatially separated microphone signals, cross correlation of the two signals can be used. Since the signals are shifted versions of each other, the cross correlation function will have peaks at points corresponding to the time delay in between, therefore the lag time that maximizes the cross correlation of the two signals will yield the true time delay.

Let $x_1(t)$ and $x_2(t)$ model the two signals received at two spatially separated microphones in the presence of noise as

$$\begin{aligned} x_1(t) &= s_1(t) + n_1(t) \\ x_2(t) &= a_1 s_1(t + \tau) + n_2(t) \end{aligned} \quad (20)$$

where $s_1(t)$ is the signal component at the first microphone, a_1 is the gain factor between the two microphones and noise components, $n_1(t)$ and $n_2(t)$ are uncorrelated with $s_1(t)$.

The simplest form of TDOA techniques, namely cross correlation (CC), is based only on estimating the maximum of cross correlation of $s_1(t)$ and $s_2(t)$, which is

$$R_{x_1 x_2}(\tau) = E[x_1(t)x_2(t - \tau)] \quad (21)$$

where $E[\dots]$ denotes expectation. Since the observation time is finite, only an estimate of this cross correlation is available by

$$\hat{R}_{x_1x_2}(\tau) = \frac{1}{T-\tau} \int_{\tau}^T x_1(t)x_2(t-\tau)dt \quad (22)$$

where T represents the observation interval.

However, considering the signals at the two microphones are not simple a delayed version of each other in real life environments, the basic cross correlation technique needs improvement of accuracy. (Knapp and Carter, 1976) offered the widely known method of Generalized Cross Correlation (GCC) that applies pre-filters, $H_1(f)$ and $H_2(f)$, to the signals $x_1(t)$ and $x_2(t)$ respectively.

Considering the relation between cross the correlation of $x_1(t)$ and $x_2(t)$, and cross power spectral density function by using Fourier transform

$$R_{x_1x_2}(\tau) = \int_{-\infty}^{\infty} G_{x_1x_2}(f)e^{-i2\pi f\tau}df \quad (23)$$

and applying the filters $H_1(f)$ and $H_2(f)$, the GCC between filter outputs $y_1(t)$ and $y_2(t)$ is given by

$$R_{y_1y_2}(\tau) = \int_{-\infty}^{\infty} \psi_g(f)G_{x_1x_2}(f)e^{-i2\pi f\tau}df \quad (24)$$

where $\psi_g(f)$ is the general frequency weighting of GCC, implemented with the pre-filters, $H_1(f)$ and $H_2(f)$, and is given by

$$\psi_g(f) = H_1(f)H_2^*(f). \quad (25)$$

Substituting $H_1(f) = H_2(f) = 1$ in Equation (25), Equation (24) becomes the same as Equation (23) thus resulting in simple CC. With proper selection of $H_1(f)$ and $H_2(f)$, however, (Knapp and Carter, 1976) state that precise estimation of delay even in the presence of noise can be achieved, yielding the GCC algorithm.

Despite its simple implementation and enhancement concerning the effects of noise, GCC has known limitations. Firstly, selection of the pre-filters requires prior knowledge of the signal characteristics (Knapp and Carter, 1976). Secondly, by its nature, GCC may enhance noise components, too, because of the cross correlation it applies to the input signals. Moreover previous research has shown that there is an implementation-defined SNR threshold, below which the localization based on GCC does not converge (Valenzise et al., 2007).

3.4.2 Pre-processing and Post-Processing

Application of GCC yields DOA information is related to a pair of microphones. A microphone array of M microphones; however, contains $\frac{M(M-1)}{2}$ such pairs. In other words, the output of GCC is not, as was with Beamforming and MUSIC, the direct DOA output of the whole array. Outputs of different microphone pairs should be combined appropriately so as to obtain the best estimate of DOA. (Pertilä, Tuomo W Pirinena, and Korhonen, 2003) compared post-processing methods for GCC outputs and stated that taking the average of these DOA outputs is the simplest option.

However the average of DOAs is easily corrupted by outliers. Another method was reported as “m out of k” selection that votes between microphone pairs which is reported by (Pertilä et al., 2003) to suffer significantly from loss of data. Considering extremely low SNR conditions of an onboard application as given in 3.2 Domain Specific SNR Examination, both outliers and loss of data are expected to occur. Therefore, both of these two simple post-processing techniques was deemed as unsuitable.

In this regard, a more robust post-processing technique was implemented in this study similar to work of (Freire and Apolinario, 2011) which calculates a cost function depending on square-errors for all possible incidence angles such that the angle that minimizes this cost function is the DOA output of the whole microphone array.

To give an illustration of calculation of cost function for different pairs, consider a microphone array of M microphones with DOA outputs $\theta_{12}, \theta_{13} \dots, \theta_{(N-1)N}$ where θ_{ik} represents the DOA calculated using the delay between i^{th} and k^{th} microphones. For all search angles, θ_s , in the range $0 < \theta_s < 180$, the cost function, $C(s)$, is calculated as

$$C(s) = \frac{1}{\sum(\theta_{ik} - \theta_s)^2} \quad (26)$$

Finally, θ_s that maximizes this cost function yields the combined DOA output of the whole microphones array. *Figure 11* illustrates this combined output of GCC with proposed post-processing and no pre-processing applied.

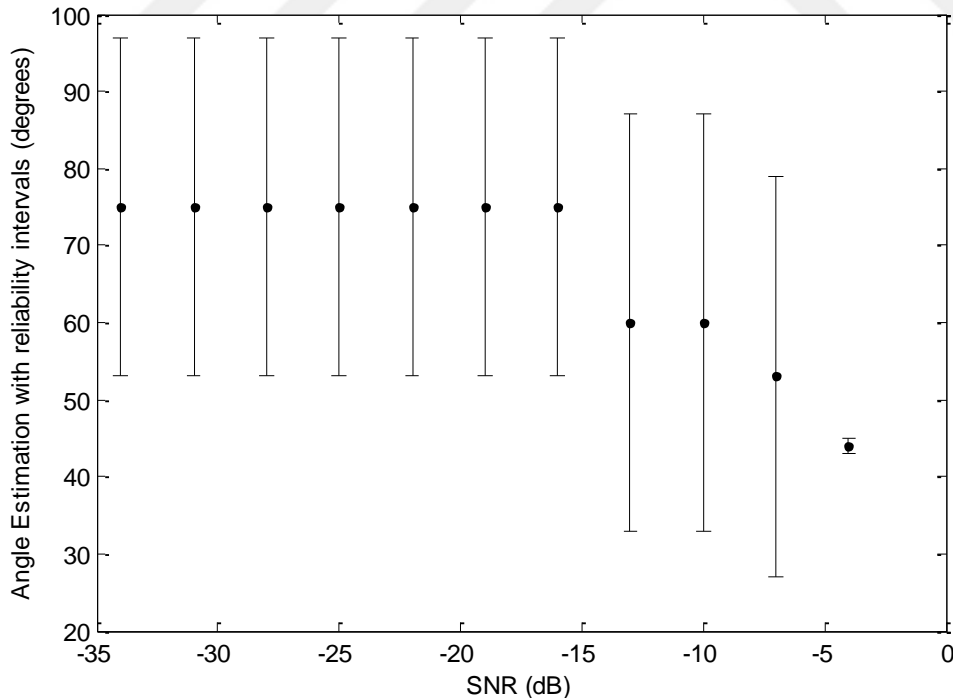


Figure 11 Combined DOA output of the whole microphone array with GCC. Target angle is 45° with microphone spacing = 0.1 m, number of microphones = 4, sampling frequency $F_s = 44100$ Hz. No pre-processing is applied.

It is obvious from *Figure 11* that DOA calculation of GCC with no pre-processing could calculate the target DOA of 45° only for SNR = -4 dB, while lower SNR values suffered greatly. This result is in accordance with findings of (Valenzise et al., 2007) who stated that performance of GCC techniques would be greatly degraded below -10 dB SNR. Indeed, *Figure 11* is a good illustration of the much mentioned threshold effect as explained in 3.4.1 Theory of Operation. In this regard, as with Beamformer algorithm, application of Spectral Subtraction was deemed useful so as to reduce effects of very low SNR. *Figure 12* reveals that the SNR range was extended down by as much as 20 dB with application of Spectral Subtraction.

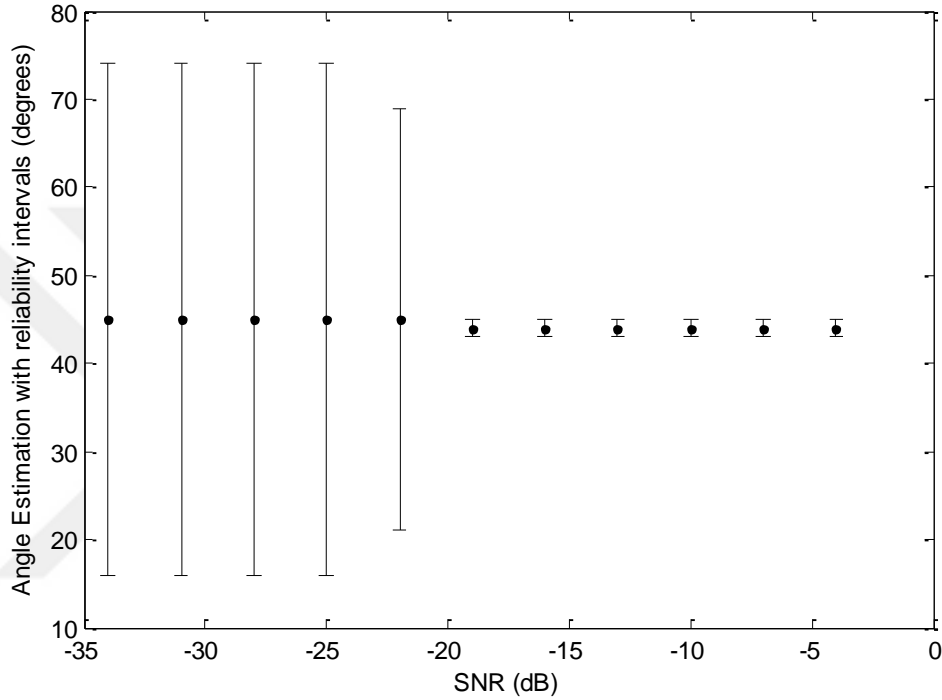


Figure 12 Combined DOA output of the whole microphone array with GCC. Target angle is 45° with microphone spacing = 0.1 m, number of microphones = 4, sampling frequency $F_s = 44100$ Hz. Spectral Subtraction applied as pre-processing.

In order to overcome the limitations of GCC regarding the noise and reverberation (Knapp and Carter, 1976), previous studies in the literature proposed various pre-processing methods, including noise reduction, how the estimate of signals is updated and how the signal propagation and reverberation are modeled (Chen et al., 2006). These methods differ in their selection of the general frequency weighting, $\psi_g(f)$.

(Chen et al., 2006) list the commonly used weighting functions as constant weighting, the smoothed coherence transform (SCOT), the Roth processor, the Echart filter, the maximum-likelihood (ML) estimation and the phase transform (PHAT). In this study, considering the extreme noise conditions because of both the helicopter and the outdoor conditions, the robustness with respect to low SNR levels was considered of specific importance. Examining in more detail, usage of PHAT

weighting prior to GCC algorithm has advantages concerning noise, reverberations and unknown signal characteristics.

Firstly, as it is known to sharpen the peaks at GCC output (Y. Zhang and Abdulla, 2005), PHAT pre-filtering was deemed useful. Another study (Bandi et al., 2012) reported that applying PHAT weighting prior to the GCC algorithm yielded results robust with both high noise levels and reverberations. (Pourmohammad and Ahadi, 2012), too, listed advantages of PHAT weighting as good performance in noisy environments, robustness with reverberations, accuracy in case of wideband signals and a sharper and more easily observable spectrum. This sharpness at the output is was reported by (Freire and Apolinario, 2011) to be helpful on distinguishing the closely-placed muzzle blast and shockwave components as compared to both the standard GCC with no pre-weighting and GCC with Maximum Likelihood pre-weighting.

Secondly, considering effects of different types of firearms and variations due to variable outdoor conditions and recalling that GCC algorithm requires prior knowledge of signal characteristics, preprocessing methods that tune the GCC algorithm for a specific firearm type would degrade the localization performance for other firearms types. Moreover, because of the outdoor conditions and impulsive nature of the gunshot signal, even signals from the same firearm type are expected to be different for different environmental conditions. The most beneficial characteristic of the PHAT pre-filtering is that, as (Chen et al., 2006) state, because it normalizes the GCC function by cross-spectrum of the pair of signals, neglecting noise components, PHAT weighting and GCC algorithm together yield a weighted cross spectrum that is free from the effects of individual signal characteristics. This can be mathematically predicted by substituting the frequency weighting of Equation (27) into Equation (24) such that the resultant cross correlation output is dependent on τ but not on the two array signals. For the problem of gunshot localization on helicopters, this means that effects of different firearm types and environmental conditions can be reduced by using PHAT weighting prior to GCC algorithm, if noise components at each individual channel are successfully handled.

PHAT weighting is implemented by selecting the pre-filters of the GCC as

$$\psi_g(f) = \frac{1}{|G_{x_1x_2}(f)|} \quad (27)$$

where $\psi_g(f)$ is the GCC general frequency weighting of Equation (25) and $G_{x_1x_2}(f)$ is the cross-correlation based power spectrum.

Figure 13 reveals the enhanced SNR performance of PHAT-GCC where SNR range of successful DOA estimation is extended down by more than 20 dB, as compared to non-weighted GCC. Moreover the -3 dB beamwidth values for almost all SNR range are enhanced, too, by which PHAT-GCC promises better reliability.

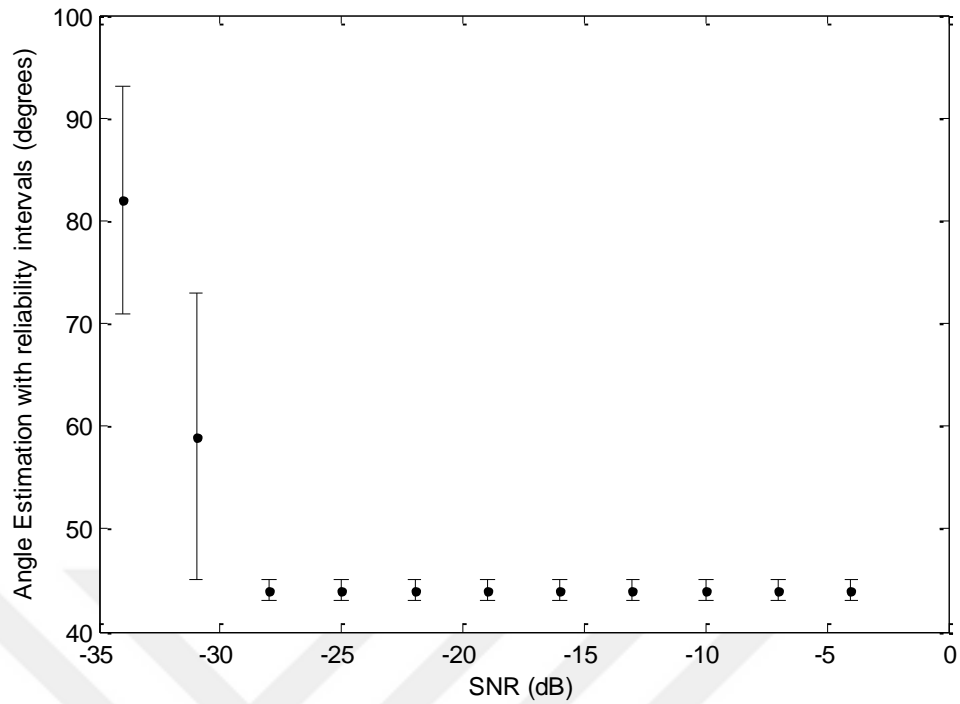


Figure 13 Combined DOA output of the whole microphone array with PHAT-weighted GCC. Target angle is 45° with microphone spacing = 0.1 m, number of microphones = 4, sampling frequency $F_s = 44100$ Hz. No Spectral Subtraction is applied.

Finally combining the both pre-processing methods of Spectral Subtraction and PHAT-weighting together with post processing for combining DOA outputs of all microphone pairs, successful DOA estimation with narrow -3 dB beamwidth were achieved for SNR values as low as -31 dB, as given by *Figure 14*.

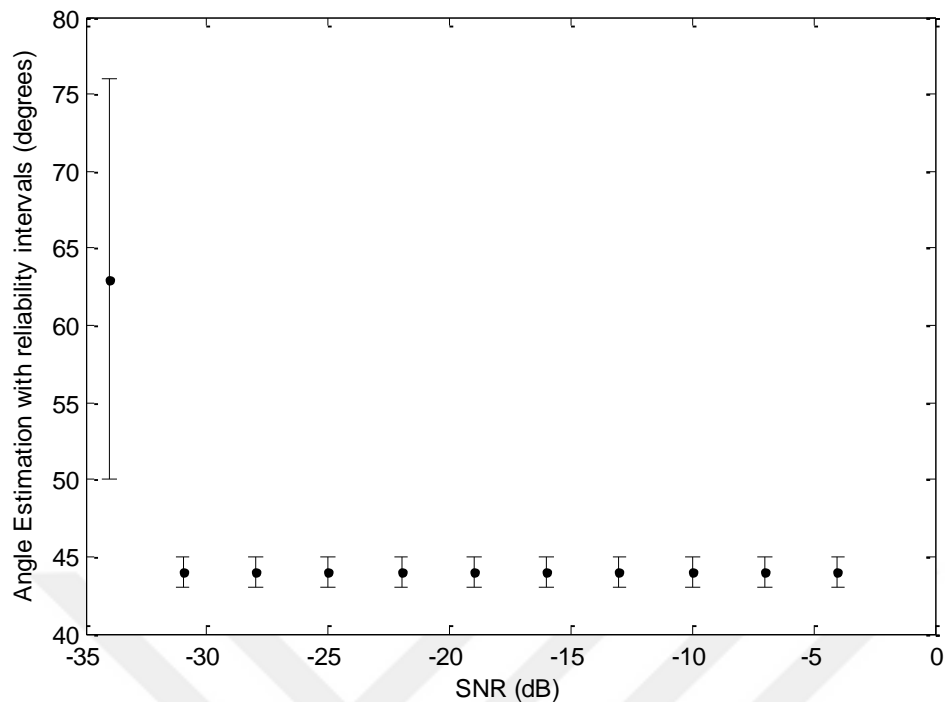


Figure 14 Combined DOA output of the whole microphone array for GCC. Target angle is 45° with microphone spacing = 0.1 m, number of microphones = 4, sampling frequency $F_s = 44100$ Hz. Both Spectral Subtraction and PHAT-weighting applied as pre-processing.

It is obvious from *Figure 14* that with application of PHAT-weighting together with spectral subtraction at pre-processing phase and taking the advantage of multiple microphone pairs at the post-processing phase, GCC offers superior performance as compared to other proposed methods in terms of both SNR and -3 dB beamwidth performance.

Finally, it should be noted that although pre-processing proposals of this study for GCC did not include a pre-filtering as opposed to the other two ASL methods, a real life implementation would require a small cut-off high pass filtering so as to eliminate possible DC components at microphone array output.

3.5 Multiple Signal Classification

3.5.1 Theory of Operation

Among the high resolution spectral estimation based localizers, Multiple Signal Classification (MUSIC) algorithm was proposed by (Schmidt, 1986) for determining the parameters of wavefronts arriving at an array of receivers. Offering a generic methodology for the examination of multiple signals, neither the implementation is restricted to the domain of sound processing, nor does the parameter of interest have to be direction of arrival. Indeed, (Schmidt, 1986) lists possible estimations as

number of signals, direction of arrival, polarizations, strength of noise/inference and cross correlations among the directional waveforms.

The method is based on computing a spatio-spectral correlation matrix and decomposing it to signal and noise components. That way vectors corresponding to (possibly multiple) sound sources as well as those that correspond to noise components are determined. Then, the vector, which can be expressed as a function of direction of arrival, is steered for different incidence angles so as to find the direction that result in minimum Euclidian distance with the noise components. Depending on the assumption that the signals of interest are uncorrelated with the noise components, minimum Euclidian distance corresponds to orthogonality between signal space and noise space.

For a better illustration of the algorithm, let there be M microphones on a microphone array and L samples arriving at each microphone in the time interval of interest. Moreover, let there be K distinct signals in the sound field that are to be localized. Input to the MUSIC algorithm, \mathbf{X} , is an $M \times L$ matrix representing the samples at all microphones. The algorithm first calculates $\mathbf{R} = \mathbf{X}^* \mathbf{X}$, namely the covariance matrix of dimensions $M \times M$, where \mathbf{X}^* is the conjugate transpose of \mathbf{X} . This square matrix has M eigenvalues, K of which correspond to the signals of interest while the remaining $M - K$ correspond to noise components. Therefore \mathbf{S}_N can be defined as the noise subspace matrix of dimension $M \times (M - K)$, whose columns correspond to noise eigenvectors. Finally considering the orthogonality between the signals and the uncorrelated noise subspace, a vector \mathbf{r} of \mathbf{R} that belongs to signal subspace should minimize the Euclidian distance to the noise subspace, which can be calculated as

$$d^2 = \mathbf{r}^* \mathbf{S}_N \mathbf{S}_N^* \mathbf{r}. \quad (28)$$

As (Günel and Hacıhabiboğlu, 2011) state, the vector \mathbf{r} can be varied as a function of angle of incidence, θ , so as to cover all directions and θ that yields the minimum distance can be determined.

3.5.2 Pre-processing and Post-Processing

The primary limitation of the MUSIC algorithm is its narrowband implementation. That is, the algorithm applies STFT on narrow frequency bins of known center frequencies, ω_{ci} , for the i^{th} frequency bin. Although the resulting resolution of the frequency observed at the output data representation can be used as an advantage, the number/width of the frequency bins as well as the window size for the calculations should be carefully selected.

Considering an L -samples window from a real-valued signal at a sampling rate F_s , taking the Fourier transform produces L complex coefficients. Only half of these coefficients are useful, the last $L/2$ being the complex conjugate of the first $L/2$, since this is a real valued signal. These $L/2$ coefficients represent the frequencies in

the range of $(0, F_s/2)$ (the Nyquist frequency) and two consecutive coefficients are spaced apart by F_s/L Hz.

To increase this frequency resolution, the frequency spacing of the coefficients needs to be reduced. Of the two variables F_s and L , decreasing F_s (and keeping L constant) will cause the window size to increase since there are now fewer samples per unit time. The other alternative is to increase L , which again means increasing the window size. So any attempt to increase the frequency resolution causes a larger window size and therefore a reduction in time resolution—and vice versa.

For illustration purposes, taking $L = 44100$ for a sound signal sampled at $F_s = 44100$ Hz, we have $F_s/L = 1$ Hz frequency resolution which is very precise; however, this also means $L/F_s = 1$ that is a window size that corresponds to 1 second. This resolution in time is not convenient considering real-time operation. Moreover, typical gunshot durations should also be considered while determining the required time resolution.

So as to decide on the appropriate intervals of time resolution in accordance with real-life requirements of a gunshot implementation, problem geometry of a basic gunshot scenario was investigated similar to the approach taken in a study by (R. C. Maher, 2006) who compared the modeling of the gunshot sound field with the actual field measurements.

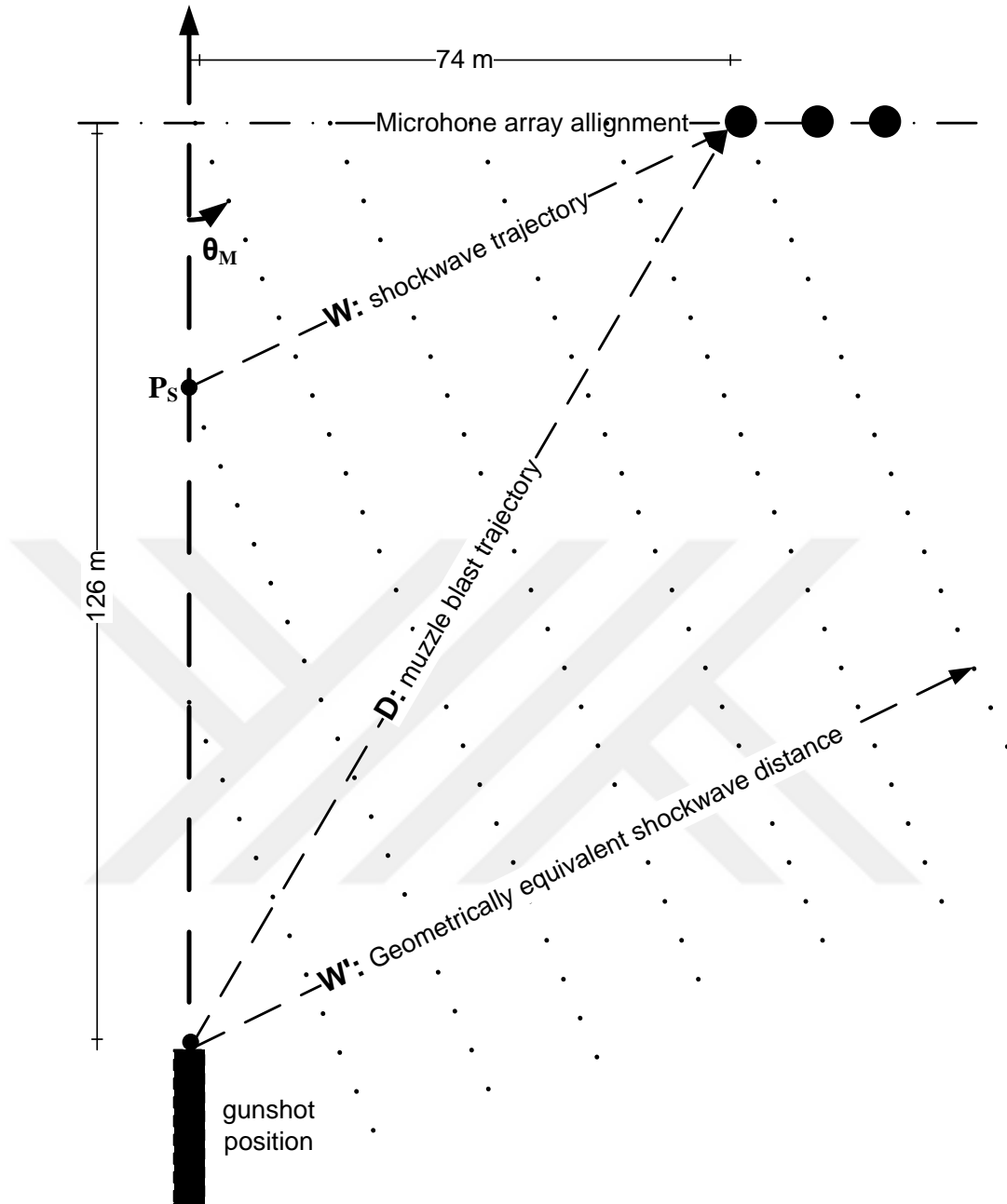


Figure 15. Gunshot sound field geometry illustration

Figure 15 illustrates such an example of gunshot sound field geometry, including both the muzzle blast and the shockwave components. Sound waves of muzzle blast follow the direct path of distance $D = 146$ m, so as to reach the first microphone of the array. The supersonic projectile, on the other hand causes a shockwave component that originated at position, P_S , the position of which depends on the Mach angle of the projectile, θ_M . This angle is dependent on the speed of the projectile and the speed of sound, calculated using Equation (2) and Equation (3).

Substituting the typical projectile speed of a Winchester 308 rifle, as 831 m/sec, θ_M can be calculated as 23° .

W represents the distance between the originating point of shockwave component and the microphones. Time delay until this shockwave reaches the microphone is the shockwave propagation time added onto the time it takes the projectile to reach at point P_S. W' is the geometrically equivalent distance, when propagation with speed of sound is considered. Taking into consideration this sound field geometry and with the speed of sound as 330 m/sec, *Table 5* was constructed, revealing the propagation distances of interest and the corresponding travel times.

Table 5. Theoretical illustration of sound field distances and travel times

Path	Distance (m)	Travel time (msec)
Bullet: muzzle to P _S	95	114.2
Shockwave: Path-W	87	246
Shockwave: Path-W'	108.2	360
Muzzle Blast: Path-D	147	448

Example values given in *Table 5* can be used as follows to determine the minimum window size, L, so that the muzzle blast and the shockwave components are not encountered together in the same window.

The time difference between the arrival of muzzle blast and shockwave is 448 – 360 = 88 msec. which corresponds to

$$\frac{88}{1000} * 44100 / 2 = 1940$$

samples, where F_S is taken as 44100 and division by 2 is included considering a 50% overlapping of windows.

Now that a framework for predicting the coupling between problem geometry and window size is constructed, it can be used to determine the low-limit for the STFT window size. Considering typical real life requirements as given in 1.2 Real-life Requirements and Scenarios, the minimum gunshot distance can be taken as 40 meters, Applying the same calculations as *Table 5*, a 26.4 msec time difference between the arrivals of muzzle blast sound and shockwave. That induces a minimum window size limit of

$$\frac{26.4}{1000} * 44100 / 2 = 582$$

samples and corresponding to an FFT frequency resolution of

$$\frac{F_S}{L} = \frac{44100}{582} = 75$$

in Hz, which is sufficient for the purposes of this study. Corresponding time resolution yields

$$\frac{L}{F_S} = \frac{582}{44100} = 0.0132$$

in seconds, which also is appropriate considering that typical gunshot signature takes 3-4 msec (R. C. Maher, 2006).

It should be noted that gunshot distances of up to 1500-2000 meters are possible with long range firearms (such as snipers). However, application of a similar approach would yield a window size that corresponds to a processing time in the affinity of 1 second, which clearly contradicts with the real-time operation. Therefore such an implementation would have to deploy means of handling both muzzle blast and shockwave in the same window. Such an attempt would have to aim identification and classification of gunshots, which is not in the scope of this study.

Once limitations on window size and frequency resolution of STFT are determined, MUSIC algorithm can be applied for the whole range of frequencies as determined by sampling frequency and the Nyquist criterion. Implementation of MUSIC with no additional post-processing results in the output given by *Figure 16*.

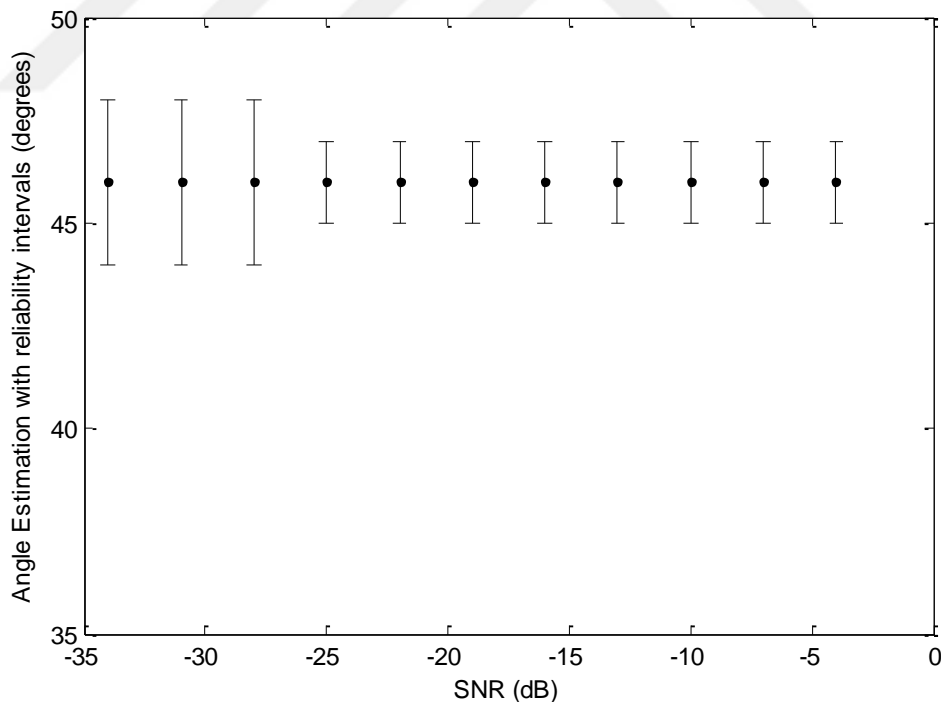


Figure 16 MUSIC with no additional post-processing. Target angle is 45° with microphone spacing = 0.1 m, number of microphones = 4. STFT size is 1024, all 512 frequency bins are used.

Although direction of arrival seems to be obtained successfully, visualizing outputs corresponding to different SNRs individually, it can be observed in *Figure 17* that spatial aliasing occurred in this calculation.

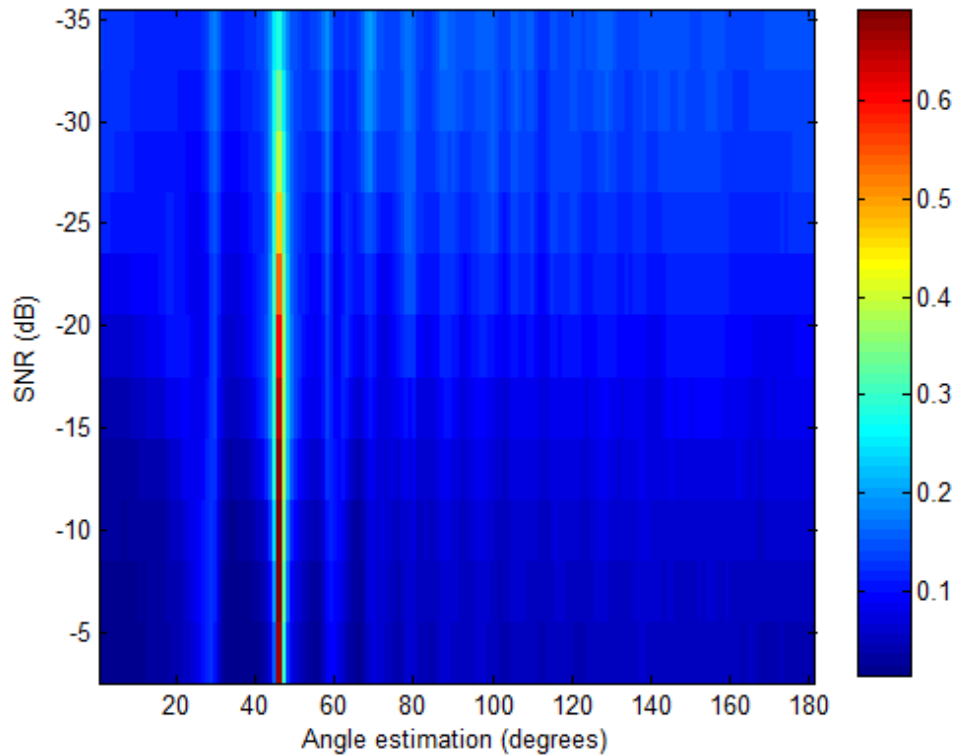


Figure 17 Spatial aliasing observed at the output of MUSIC algorithm for a source at 45°. Spatial aliasing was observed for all SNR values in the range of [-34,-4]dB with microphone spacing, $S = 0.1$ m sampling frequency, $FS = 44100$, Target angle = 45°, number of microphones = 4, STFT size = 1024.

As another illustration, *Figure 18* reveals the outputs produced by all frequency bins. It is observed that most of the frequencies have detected wrong angles together with the expected output of 45° . The high frequency limit so as not to suffer from spatial aliasing is 1750 Hz for the microphone spacing of 0.1 m as calculated by Equation (10). Observe that uneven lines at localization output are observed at frequencies above this frequency limit, clearly illustrating the effects of spatial aliasing. Therefore, frequency bins above this limit should be excluded from the final localization output calculation.

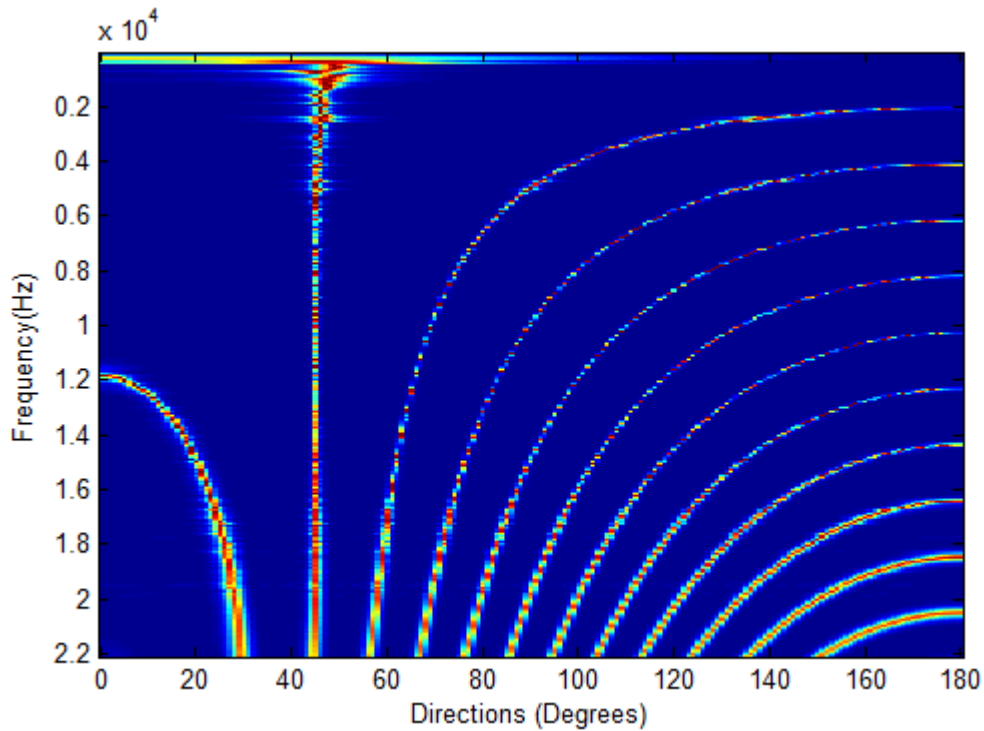


Figure 18 Spatial aliasing at different frequency bins of MUSIC output for a source at 45° . The high-limit on the frequency so as not to have spatial aliasing is 1750 Hz for microphone spacing. Microphone spacing, $S = 0.1$ m, number of microphones, $M = 4$, STFT size = 1024.

Apart from that of spatial aliasing, additional limitations on frequency bandwidth should be applied, specific to the problem of gunshot localization on helicopters. That is the low frequency noise-dominant components and high frequency components deteriorated by spatial aliasing should not be used, as suggested by this study for the Beamforming algorithm in 3.3.2 Pre-processing and Post-Processing. An important difference among these two algorithms is that, this adjustment in frequency range can be applied as post-processing for the MUSIC algorithm as opposed to re-processing of Beamforming. This way a superior frequency resolution can be observed at the output of the MUSIC algorithm without degrading localization performance, which was not possible with Beamforming algorithm. Since MUSIC algorithm's DTFT-based direction of arrival calculation of a specific frequency bin is independent of other frequency bins, the direction of arrival output of aforementioned low-frequency and high-frequency components can be excluded

from the final localization results. Accounting for both spatial aliasing limitation of 1750 Hz and helicopter noise related limitations below 400 Hz as described in 3.3.2 Pre-processing and Post-Processing of Beamforming algorithm yields a more realistic representation of localization output as given in *Figure 19*.

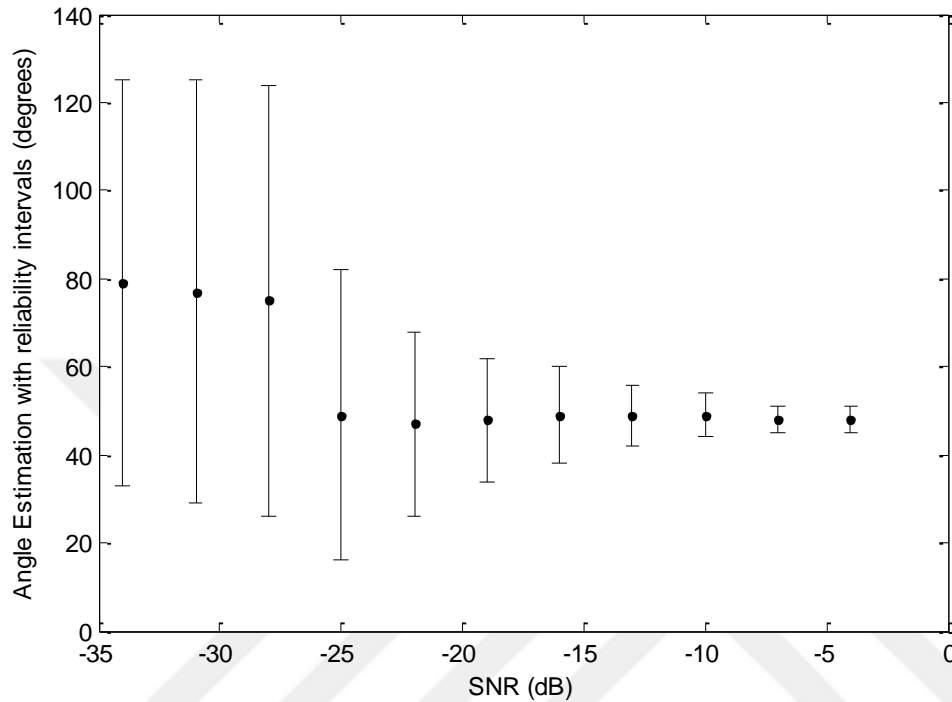


Figure 19 Output of MUSIC with post-processing for a source at 45° . Frequency bins below 400 Hz are omitted because of dominant helicopter noise components. Frequencies above 1750 Hz are omitted because of spatial aliasing limitation. STFT size = 102,4 microphone spacing, $S = 0.1$ m, number of microphones, $M = 4$.

While offering an enhanced frequency resolution while applying post-processing methods, STFT usage of MUSIC algorithm restricts usage of pre-processing methods that alter frequency characteristics. Spectral subtraction, as applied to other two methods, is one such example. As opposed to Beamforming and GCC, spectral subtraction cannot be applied before MUSIC algorithm since it changes frequency domain characteristics while MUSIC is a narrowband frequency domain algorithm. Still, SNR range of MUSIC algorithm followed by the suggested post-processing is extended to as low as -25 dB so that application of spectral subtraction was not deemed necessary, either.

CHAPTER 4

SIMULATION OF FACTORS THAT AFFECT LOCALIZATION ON HELICOPTERS

As given in Section 1.3 Implementation Challenges, there are various factors that affect gunshot localization on helicopters when outdoor wave propagation characteristics are considered. Any array based ASL implementation has to investigate signal processing parameters such as array-related parameters and algorithm-specific signal processing parameters. Apart from these, an outdoor implementation should consider factors related to wave propagation, too, as listed in *Figure 6*. *Figure 20* illustrates the parameters, all of which should be simulated in a controlled manner so as to obtain each one's specific effect on the DOA estimation.

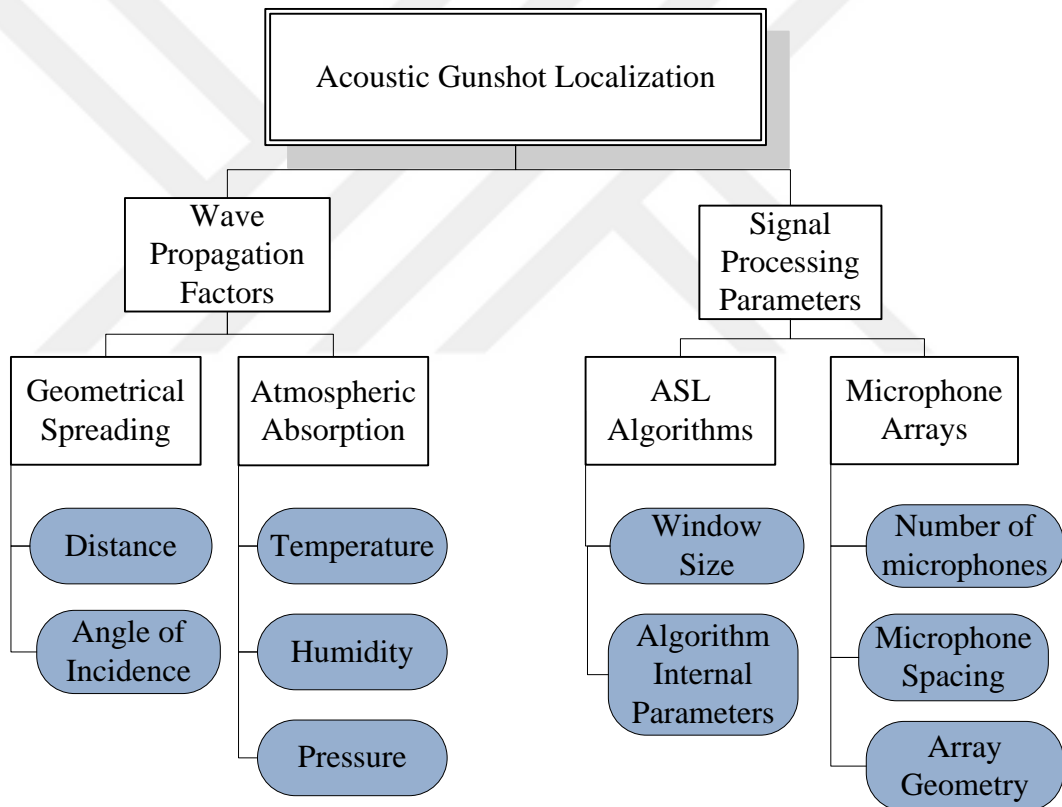


Figure 20 Parameters simulated for their effects on gunshot localization

Effects of changes in these parameters were obtained using the same simulation environment and input dataset given in Chapter 3. However, considering dimensionality of the above-given parameters, instead of exhaustive manipulations, the results were presented by forming test cases in a way that maximizes the differential effects of each parameter. Each section of this chapter illustrates DOA estimation of three different methods proposed by this study by manipulating following parameters:

- Microphone spacing, S
- Number of microphones, M
- Source to microphone array distance, D
- Angle of incidence, θ
- STFT size
- Temperature, humidity and pressure

Initial simulations revealed that the effects of air absorption related factors (temperature, humidity and pressure) were much smaller than that of spherical spreading losses, as previous studies in the literature predict. For the range of source to microphone array distance values of this study, the losses due to temperature, humidity and pressure were observed to be less than 10 dB while spherical spreading loss values of as high as 50 dB were encountered. Therefore, the effects of the air absorption related factors (temperature, humidity and pressure) were given integrated with other parameters so that their effects can be visualized in a differential manner. For all figures of this chapter, red data lines represent results of the same simulation when effects of air absorption parameters (temperature, humidity and pressure) are included. Moreover, some of the results include effects of proposed pre-processing or post-processing, too, in cases where their benefit or limitations are well-highlighted.

4.1 Microphone Spacing

The effect of microphone spacing was simulated first so that the optimal microphone spacing for all three methods could be obtained and used while simulating other parameters. The range for microphone spacing was set as 1.5 cm to 23 cm. The limitation on microphone spacing is due to spatial aliasing as explained in Section 2.3.2.2 Microphone Arrays.

For a target angle of 45° at 200 meters, *Figure 21* gives DOA estimation output of Beamforming pre-filtered for helicopter noise dominant low frequencies. Although the beamformer could locate the target angle correctly for the entire range, change in -3 dB beamwidth of the main lobe illustrates the effect of microphone spacing on the DOA estimation. Inclusion of air absorption parameters further increases the beamwidth with no loss of estimation peak.

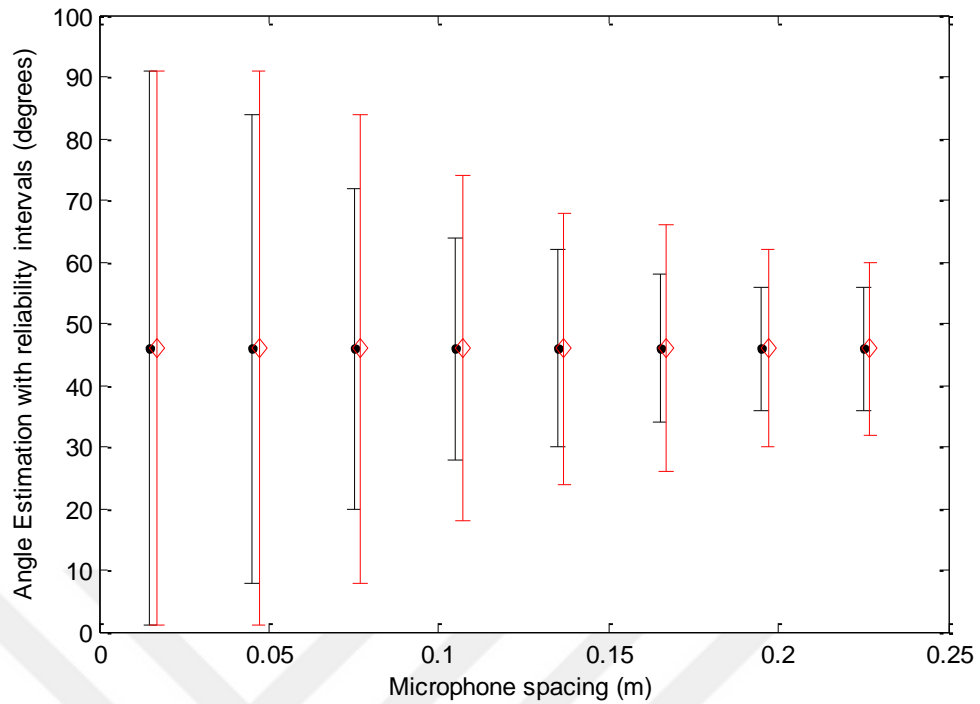


Figure 21 Beamforming with no Spectral Subtraction applied. Effects of microphone spacing with and without including air absorption. $\theta=45^\circ$, $D=200m$, $F_s=44100$, $M=4$

Application of spectral subtraction yields the output shown in Figure 22, which did not significantly improve -3 dB beamwidth performances. However, the advantages of spectral subtraction could be better illustrated for larger source-to-sensor distances as given in Section 4.3 Source to Microphone Array Distance.

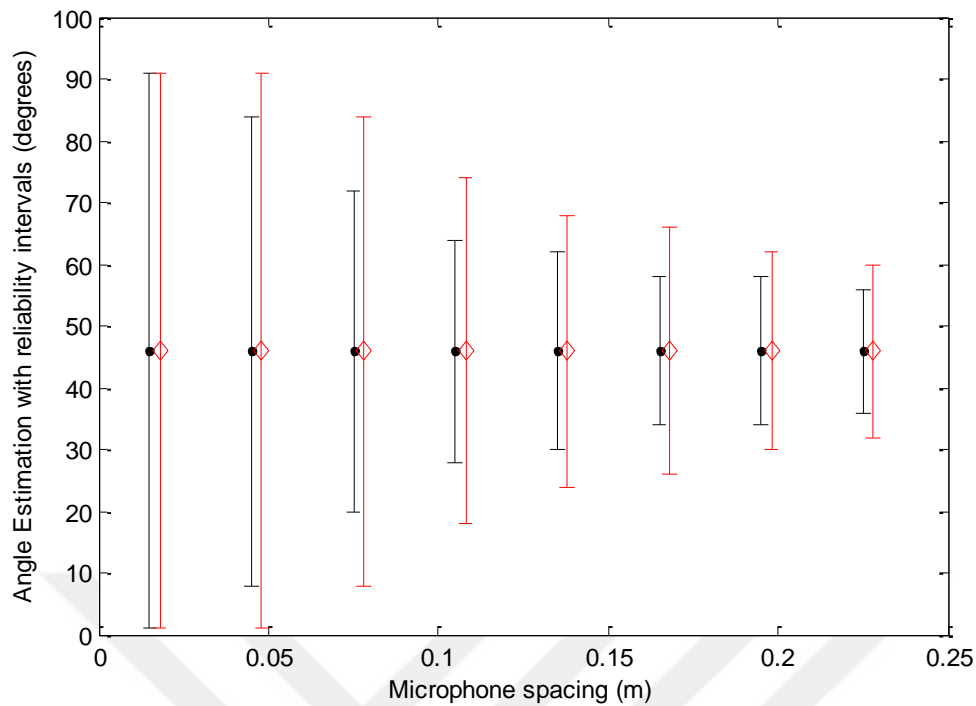


Figure 22 Beamforming with Spectral Subtraction. Effects of microphone spacing with and without including air absorption. $\theta=45^\circ$, $D=200m$, $F_s=44100$, $M=4$

As compared to Beamforming, GCC-based method was observed to be more sensitive to microphone spacing as given by Figure 23. Figure 24 reveals a slight improvement by PHAT-weighting, as well as robustness with air absorption factors. It should be noted, however, that microphone spacing below 0.05 m resulted in loss of correct estimation peak of 45 degrees.

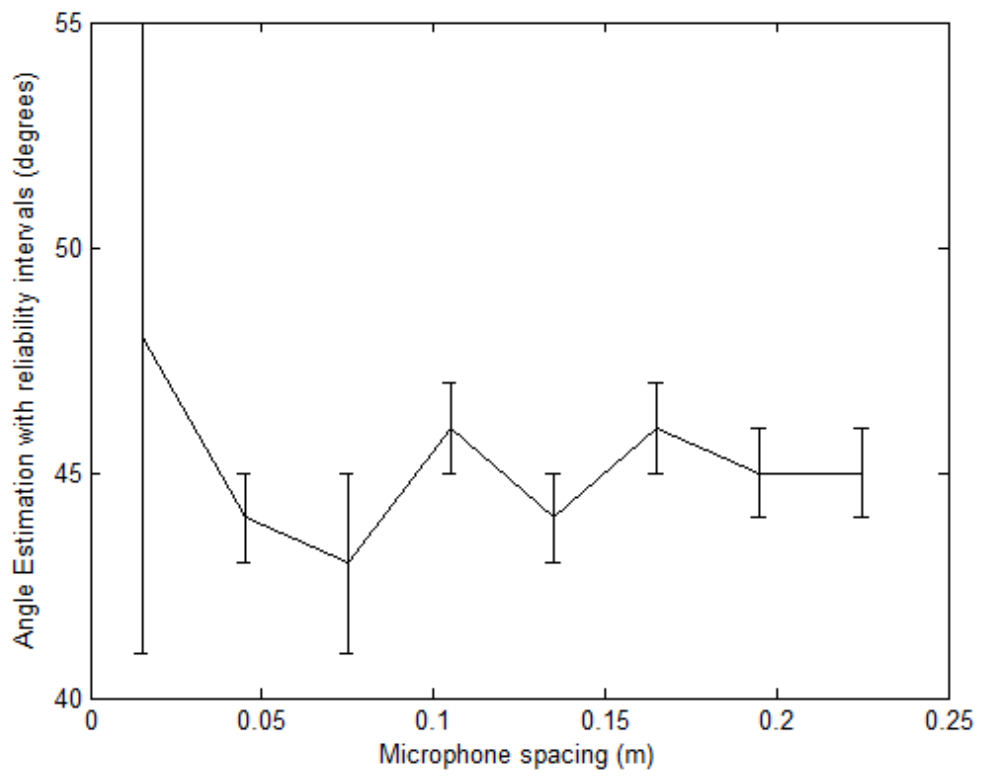


Figure 23 GCC without PHAT-weighting. Effects of microphone spacing with $\theta=45^\circ$, $D=200m$, $F_s=44100$, $M=4$

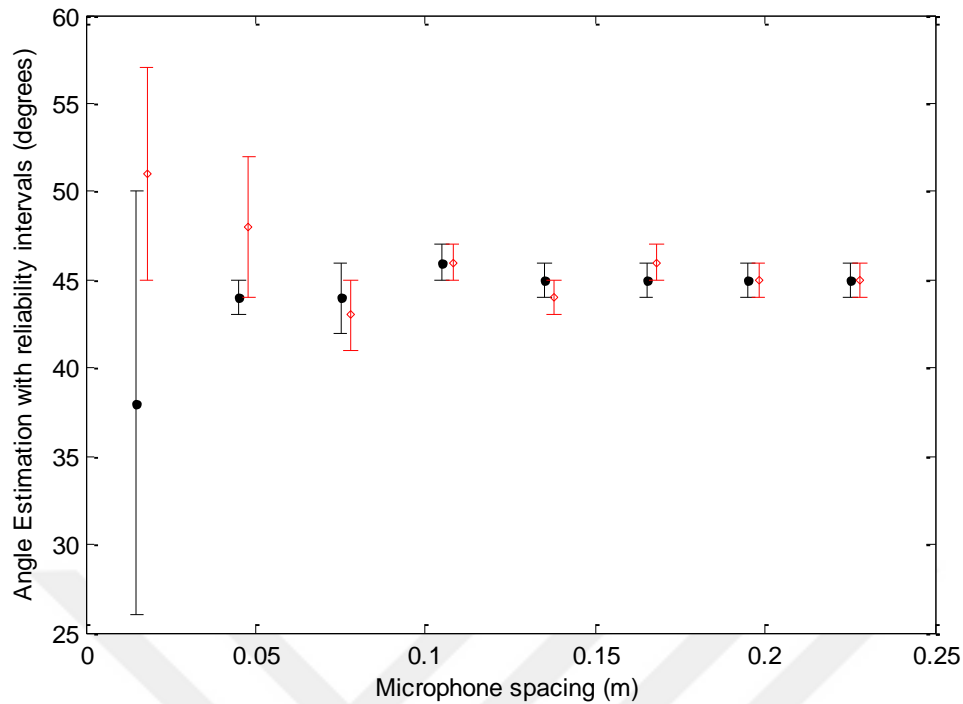


Figure 24 GCC with PHAT-weighting. Effects of microphone spacing with and without including air absorption. $\theta=45^\circ, D=200m, F_s=44100, M=4$

Spectral subtraction, as was with beamforming, did not yield significant improvement on DOA estimation for target-to-sensor distance of 200 m as given by Figure 25. However, it should be noted that both PHAT-weighting and spectral subtraction were proposed for their enhancements for low SNR cases. Therefore, insignificant improvement on DOA estimation peak and -3 dB beamwidth should be expected while manipulating microphone spacing.

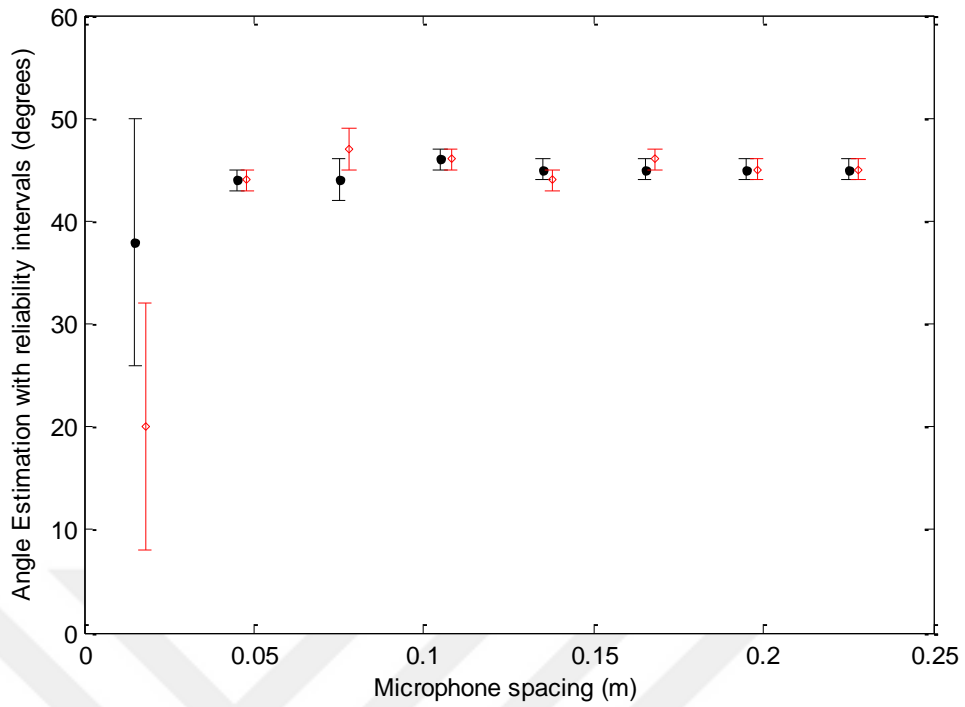


Figure 25 GCC with both PHAT-weighting and Spectral Subtraction. Effects of microphone spacing with and without including air absorption. $\theta=45^\circ$, $D=200m$, $F_s=44100$, $M=4$

Using the same microphone spacing range for MUSIC algorithm, Figure 26 reveals an increasing -3 dB beamwidth performance with increasing microphone spacing. Therefore, a further increase in microphone spacing was simulated.

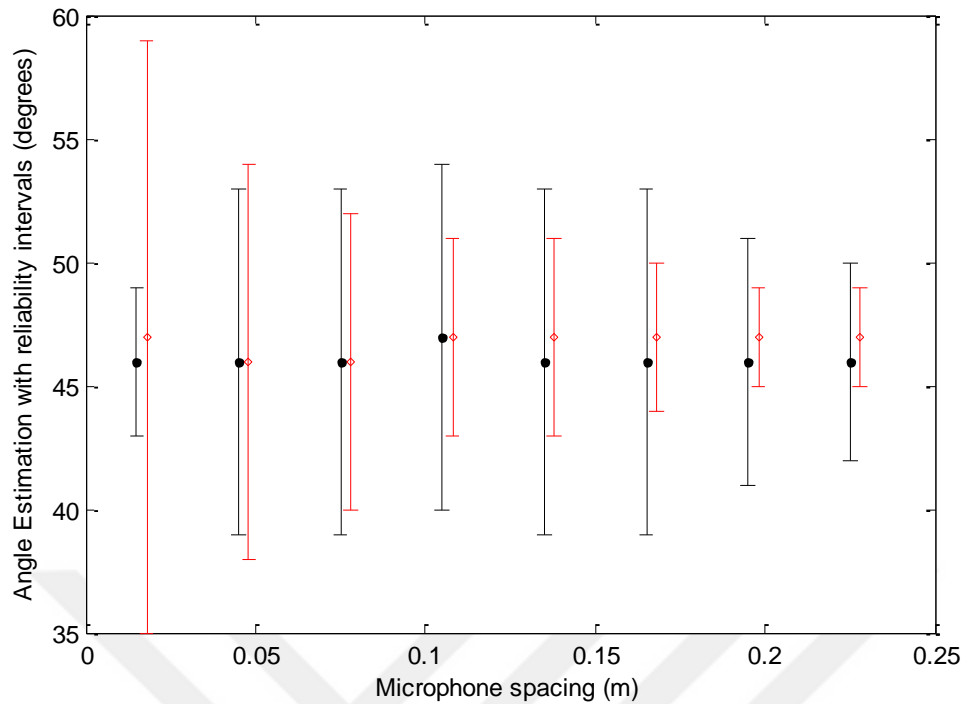


Figure 26 MUSIC with post-processing that selects frequency bins of interest. Effects of microphone spacing with and without including air absorption. $\theta=45^\circ$, $D=200\text{m}$, $F_s=44100$, $M=4$, FFT size=1024

In this regard, the simulation was repeated for microphone spacing values above 0.25 m by disabling the proposed post-processing that eliminated frequency bins that result in spatial aliasing, at the output of MUSIC. As Figure 27 illustrates, successful DOA estimation was observed for microphone spacing values as large as 0.7 m, since the post-processing phase selects peak of the estimated angles. For these simulations, the DOA estimation peak had a higher amplitude than those of aliasing components. As a result, although peaks that result from spatial aliasing cannot be observed on this illustration, microphone spacing values above the frequency limit of spatial aliasing should not be used, considering worse SNR scenarios as well as other real life conditions.

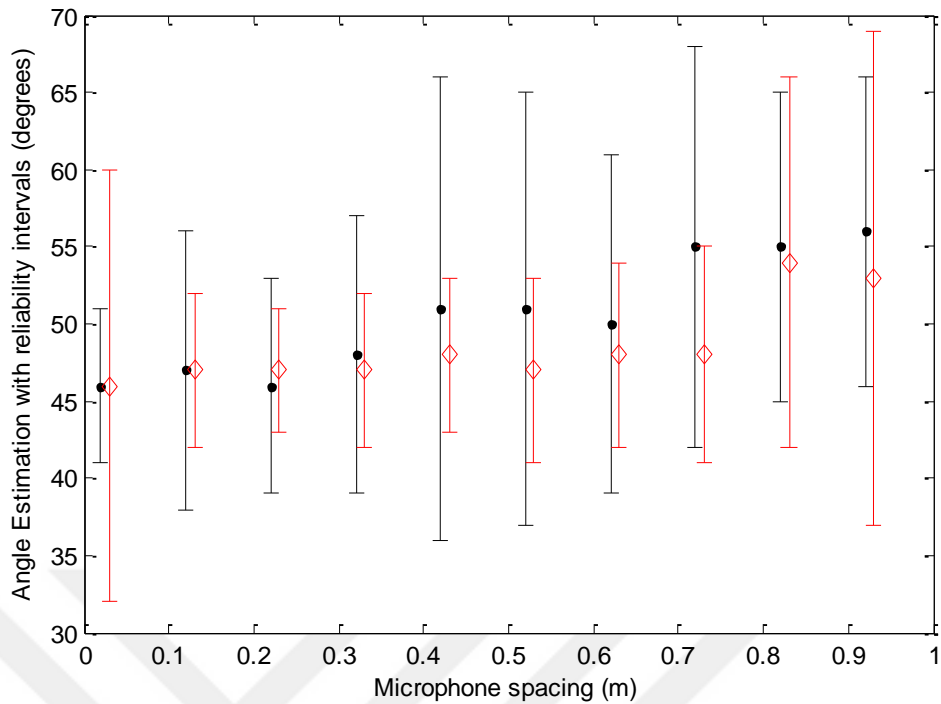


Figure 27 MUSIC with no post-processing. Effects of microphone spacing with and without including air absorption. $\theta=45^\circ$, $D=200m$, $F_s=44100$, $M=4$, STFT size=1024

4.2 Number of Microphones

Effects of number of microphones in the array were simulated by using sixteen different portions of a helicopter sound recording together with a gunshot sound signal. Cross-correlation of the sixteen helicopter samples were investigated so that the uncorrelated noise assumption was valid.

Figure 28 illustrates the DOA estimation of Beamforming with the proposed preprocessing methods. As expected, the -3 dB beamwidth performance of Beamforming based method was significantly enhanced by increasing the number of microphones. However, it should be noted that results without preprocessing were much similar as given in Figure 29. This could be due to the fact that, source to microphone distance of 400 m is not large enough to observe loss of localization peak for Beamforming, although the enhancement on beamwidth performance is well-observed.

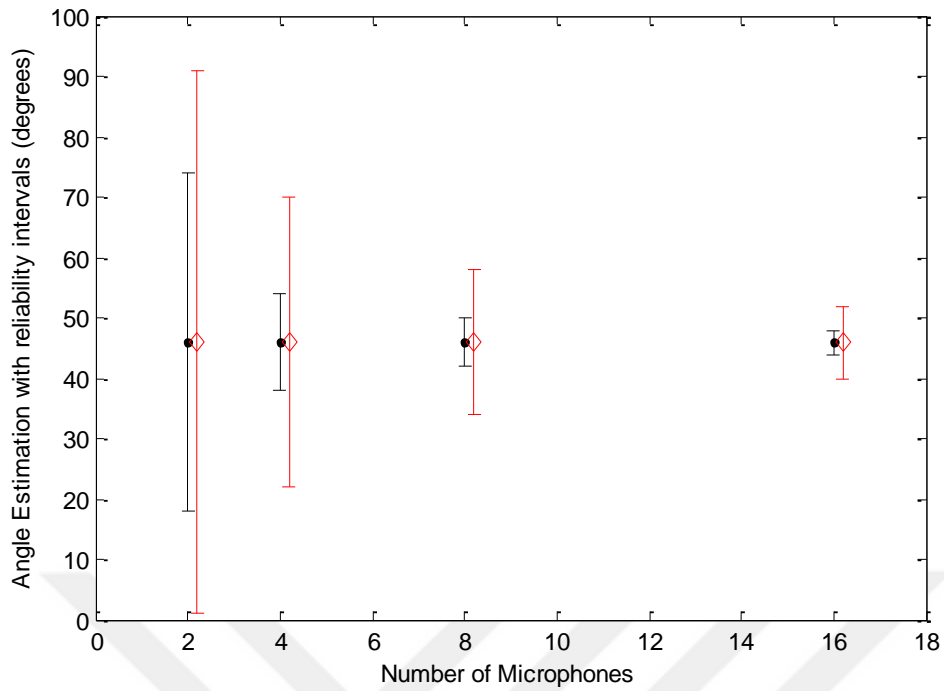


Figure 28 Beamforming with suggested pre-processing. Effects of number of microphones with and without including air absorption. $\theta=45^\circ$, $D=400m$, $F_s=44100$, $S=0.15m$.

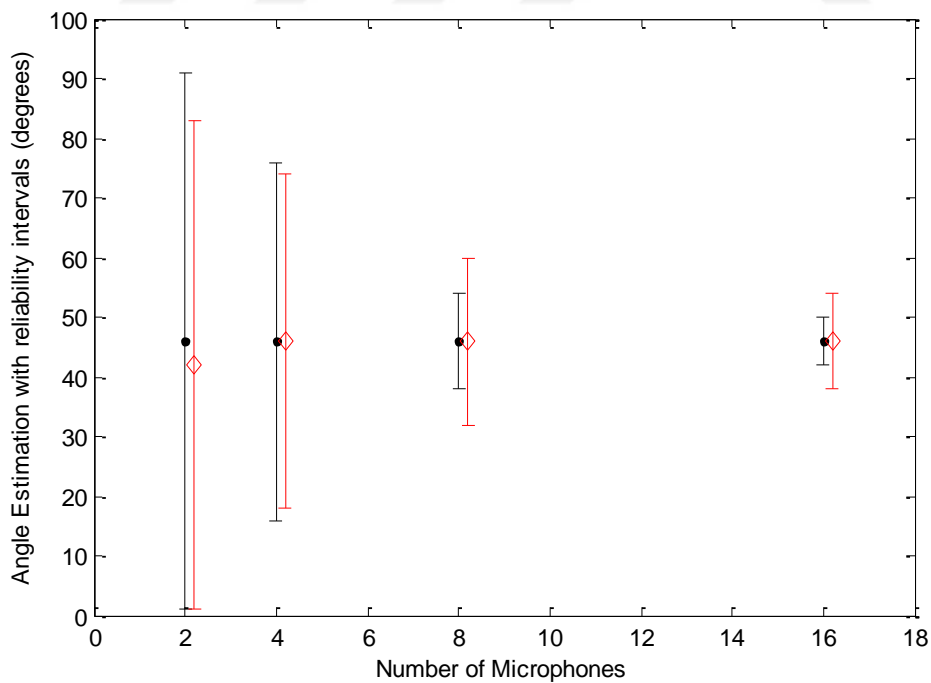


Figure 29 Beamforming without suggested pre-processing. Effects of number of microphones with and without including air absorption. $\theta=45^\circ$, $D=400m$, $F_s=44100$, $S=0.15m$.

Figure 30 gives the results of microphone spacing simulation with and without the proposed pre-processing and post-processing. Although the atmospheric absorption was not included, beamformer could not localize the target angle of 45 degrees for the 8-microphones case. This is most likely because of some helicopter noise component that should be pre-filtered. The application of both pre-filtering and spectral subtraction removes this distortion as given in Figure 31. Moreover, although it was significant with two microphones, the effects of environmental absorption, too, could be handled by the proposed pre-processing.

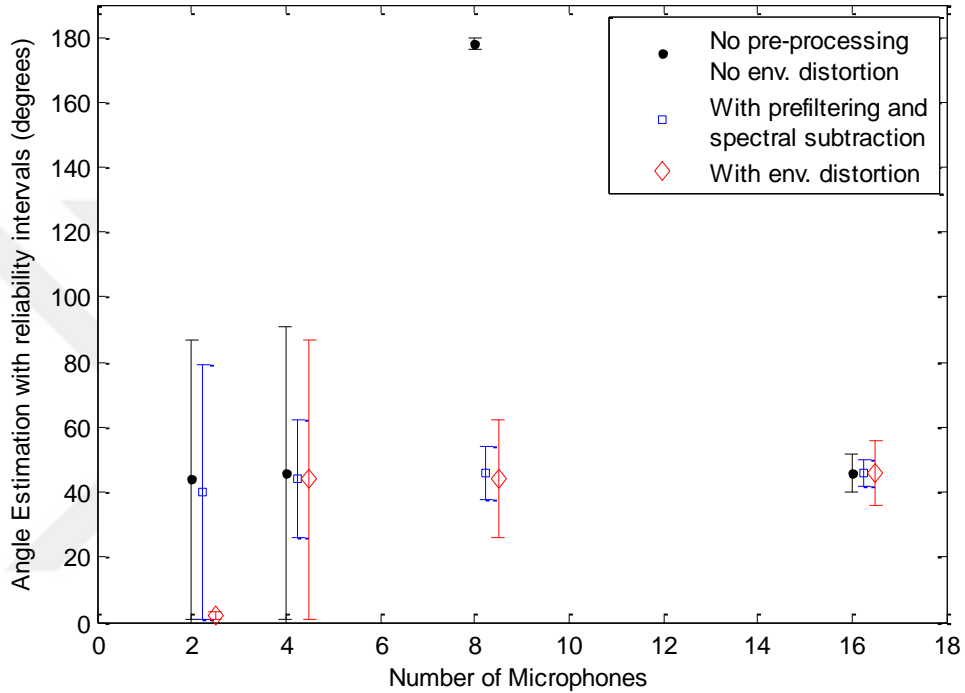


Figure 30 Beamformer with and without suggested pre-processing comparison for a larger source to microphone array distance, $\theta=45^\circ$, $D=800m$, $F_s=44100$, $S=0.15m$.

As given by Figure 31, the performance of PHAT-weighted GCC was observed to be less dependent on the number of microphones except for the case with only two microphones. The rapid increase in performance with even four microphones could be due to the fact that, the proposed post-processing phase makes use of all microphone pairs so that even with four microphones outputs of all six PHAT-GCC calculations were used. Moreover, the microphone spacing of 0.15 m and source-to-microphone distance of 400 meters were used which were optimal values for PHAT-GCC, while four microphones may not be sufficient with other microphone spacing values as illustrated by Figure 32. Moreover, an interesting result is that, despite being accurate when simulating with optimal parameters, the performance was significantly reduced by the effects of environmental absorption especially for large source to microphone array distances, as illustrated by Figure 33.

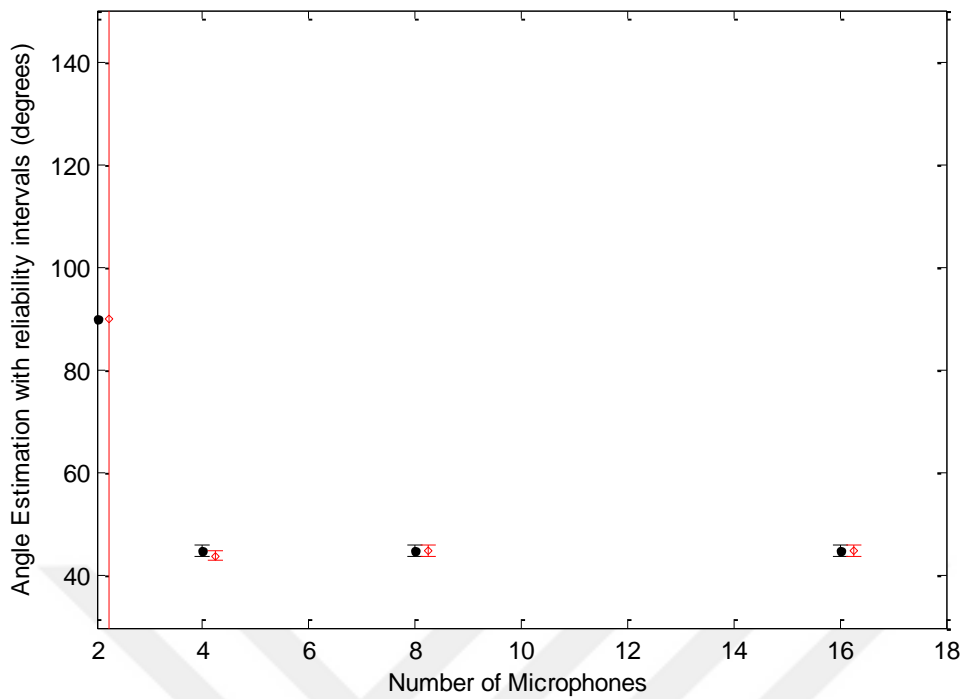


Figure 31 GCC with only PHAT-weighting. Effects of number of microphones with and without including air absorption. $\theta=45^\circ$, $D=400m$, $F_s=44100$, $S=0.15m$

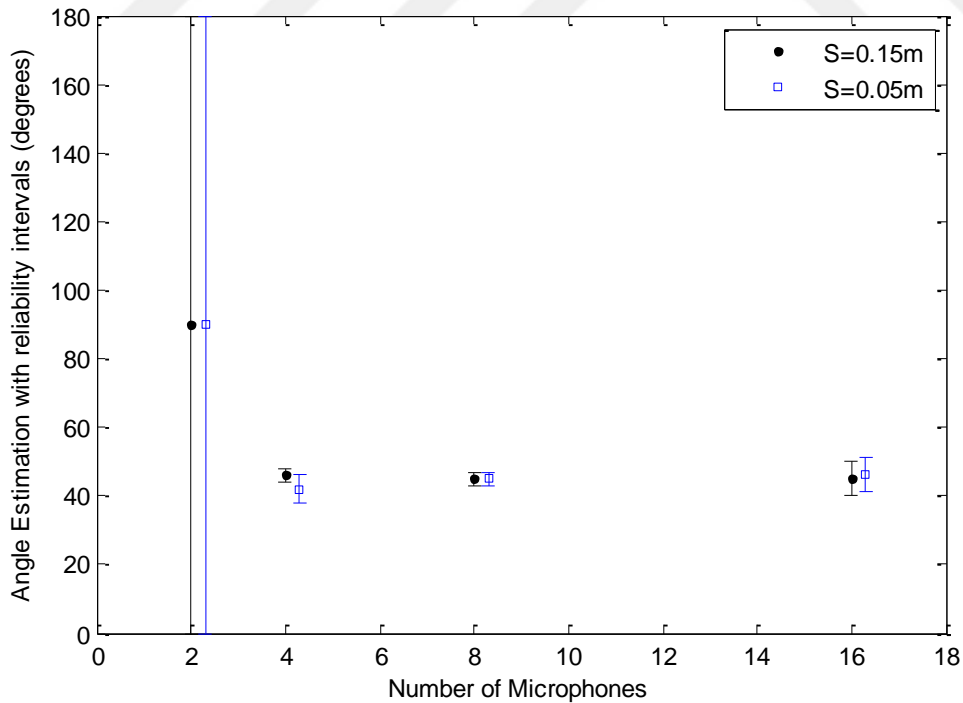


Figure 32 GCC with only PHAT-weighting with two different microphone spacing values, $\theta=45^\circ$, $D=400m$, $F_s=44100$

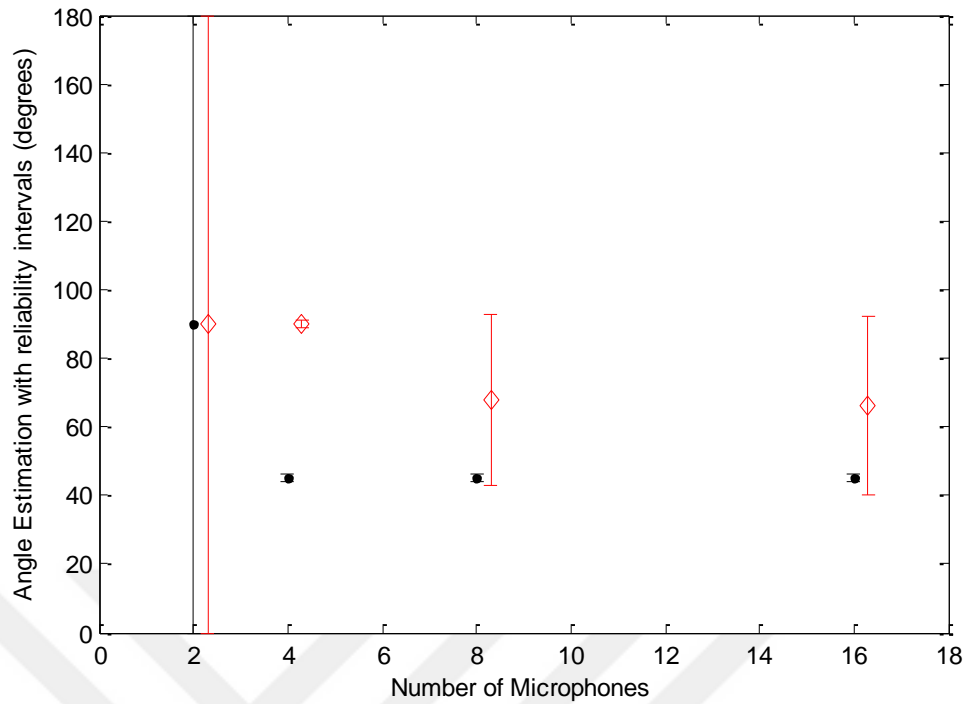


Figure 33 GCC with PHAT-weighting. Effects of number of microphones with and without including air absorption. $\theta=45^\circ$, $D=800m$, $F_s=44100$, $S=0.15m$

Simulations of MUSIC algorithm reveal better robustness with atmospheric absorption once all sixteen microphones are deployed. However, the DOA estimation peak error of 2 degrees should be noted in Figure 34. Figure 35 visualizes an attempt to decrease this error by disabling the frequency bins selection at the post-processing stage. However, as with the microphone spacing case, frequency bins above the spatial aliasing limitation should not be used.

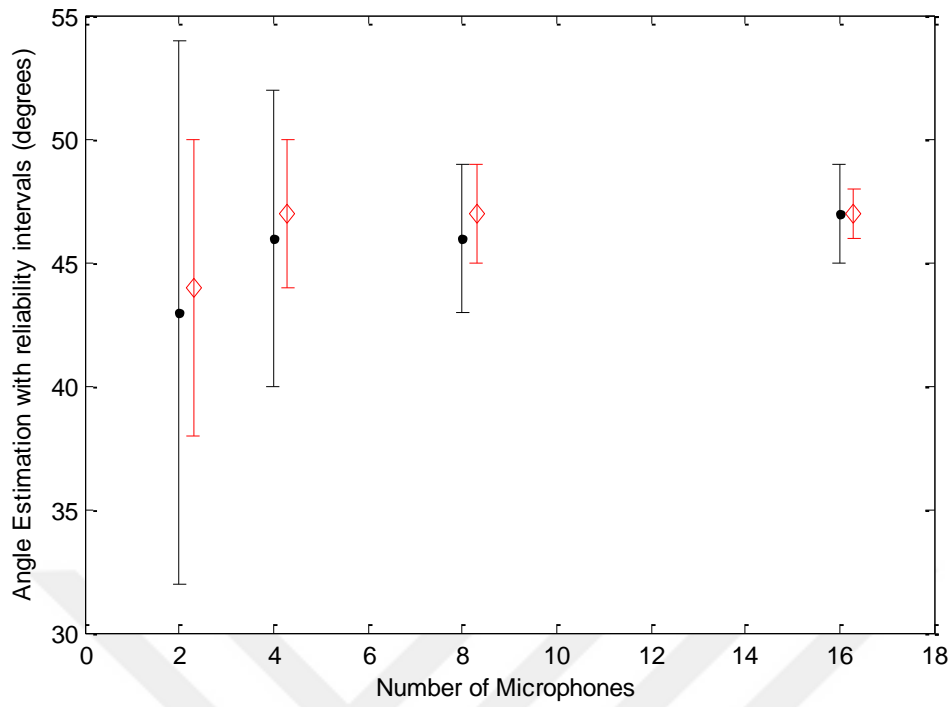


Figure 34 MUSIC with post-processing that selects output frequency bins. Effects of number of microphones with and without including air absorption. $\theta=45^\circ$, $D=300m$, $F_s=44100$, $M=4$, STFT size=4096, $S=0.15$

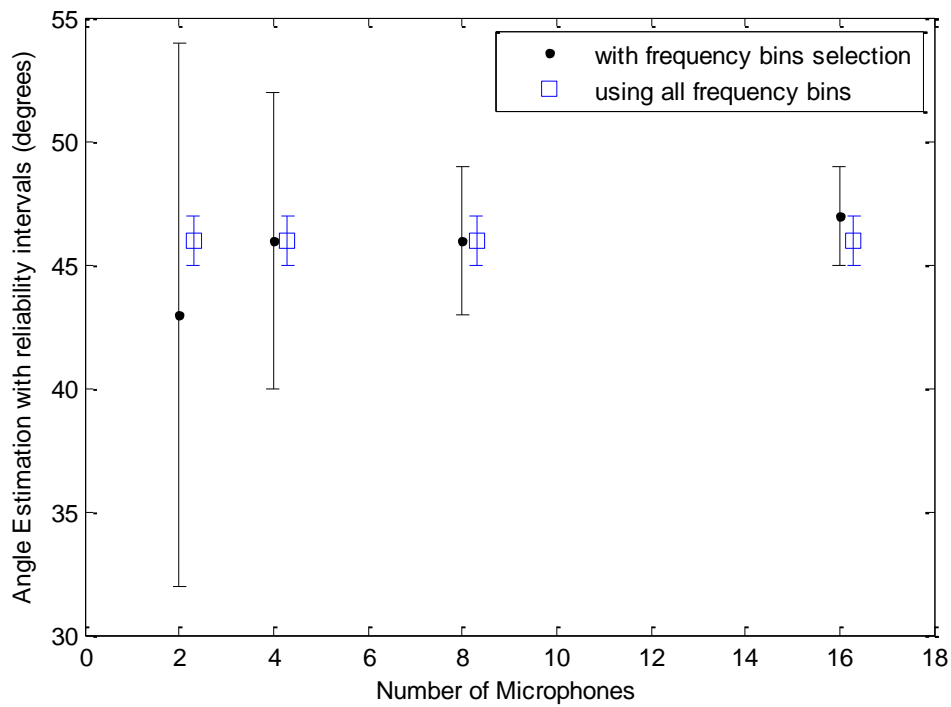


Figure 35 MUSIC, effect of proposed post-processing that selects frequency bins of interest, $\theta=45^\circ$, $D=300m$, $F_s=44100$, $M=4$, FFT size=4096

4.3 Source to Microphone Array Distance

Resulting from spherical spreading of sound signals, the major contributor to loss of gunshot SPL is source to microphone distance. Moreover, atmospheric absorption on signals increases with increasing traveling distance in the air. Although the amount of this absorption is much less than that of spherical spreading, atmospheric absorption is dependent on the frequency so that the destruction on the signal of interest is different for different frequency bands. As given in Section 1.2 Real-life Requirements and Scenarios, gunshot to helicopter distances of most realistic scenarios cover the ranges below 500 meters; however, some long range firearms pose significant threats to the crew, and especially to the pilot. This type of attacks increases the range of interest as high as 1500 to 2000 meters.

In this regard, a wide range of source-to-microphone distances were simulated in the scope of this study. Table 6 lists the simulated distances together with corresponding SNR levels calculated for 30°C temperature, 70% relative humidity and 1atm atmospheric pressure. The effects of reduced SNR as well as increased air absorption were successfully observed for most of the simulation scenarios. It should be noted, however, that long distance scenarios are, by their nature, expected to result in additional signal distortion because of upwind/downwind conditions, meteorological conditions as well as wind and temperature gradients, as explained in Section 2.2 Wave Propagation Characteristics, which were not simulated in the scope of this study.

Table 6 SNR levels corresponding to different source to microphone array distances

Source to microphone array distance	Corresponding SNR
100 meters	15.6 dB
200 meters	8.9 dB
400 meters	1.9 dB
800 meters	-5.2 dB
1600 meters	-12.7 dB

To begin with, Figure 36 reveals a significant widening of -3 dB beamwidth as the distance increases from 100 m to 1600 m. Moreover, it can be seen that the application of suggested pre-filtering together with spectral subtraction could increase the beamwidth performance.

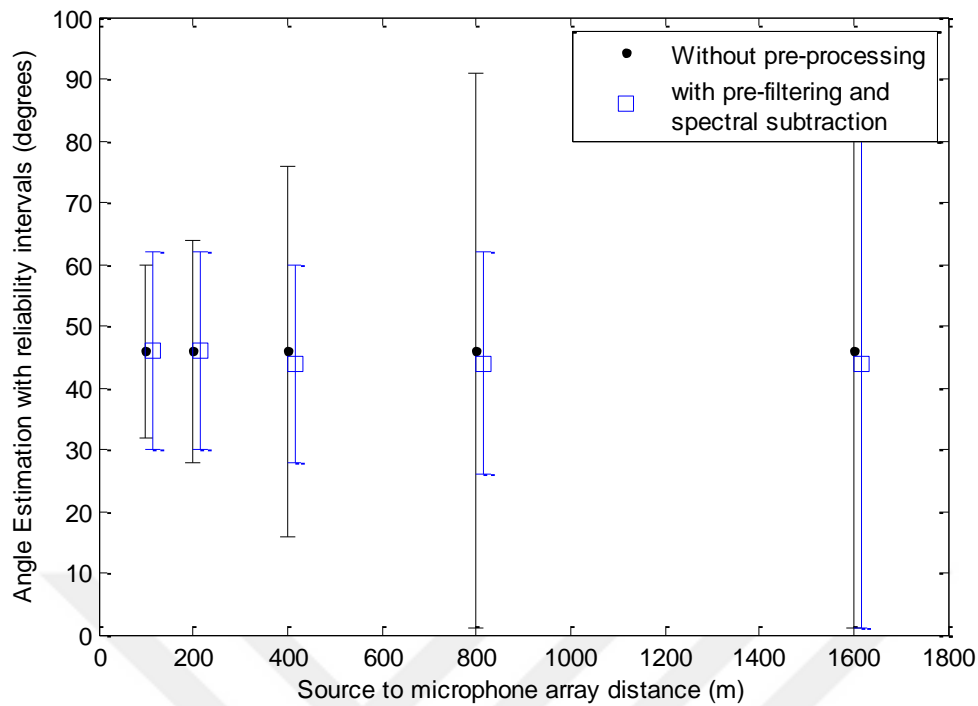


Figure 36 Effects of proposed pre-processing for Beamforming, $\theta=45^\circ$, $F_s=44100$, $M=4$, $S=0.15$ m

Having illustrated the benefits of pre-processing, the effects of air absorption can be seen in Figure 37 where only the pre-filtering of dominant low frequency components of helicopter noise was applied. It can be observed that, resulting from the air absorption the beamwidth increased as much as 100 degrees. However, the beamwidth performance could be enhanced by including spectral subtraction as given by Figure 38. Results of Figure 38 are important for Beamforming based method since they illustrate both the necessity and promising robustness of the proposed pre-processing methods.

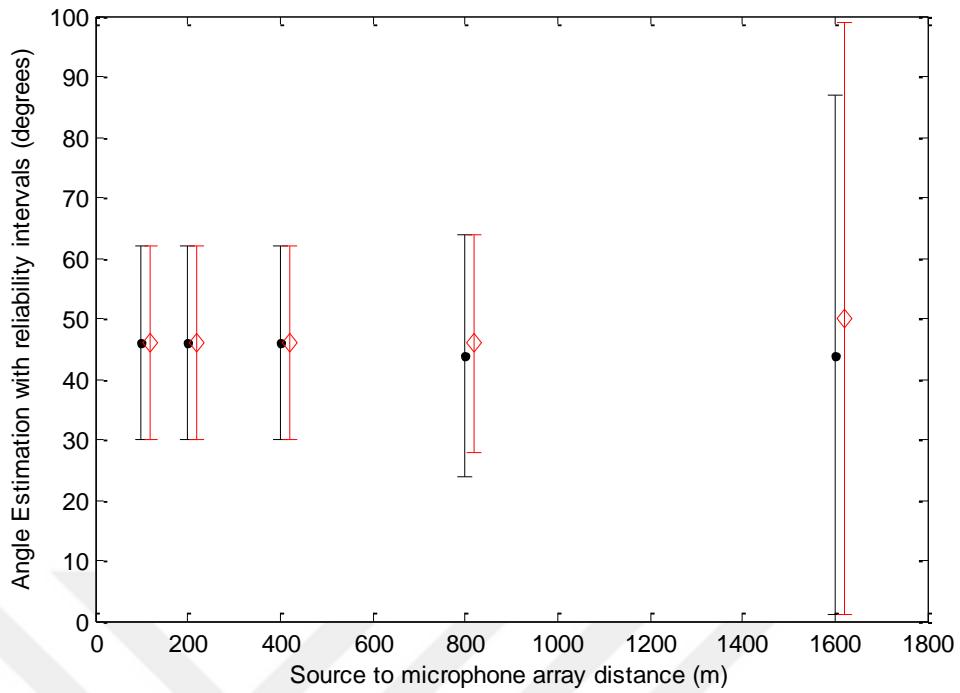


Figure 37 Beamforming with proposed pre-filtering. Effects of source to microphone array distance with and without including air absorption. $\theta=45^\circ$, $F_s=44100$, $M=4$, $S=0.15$ m

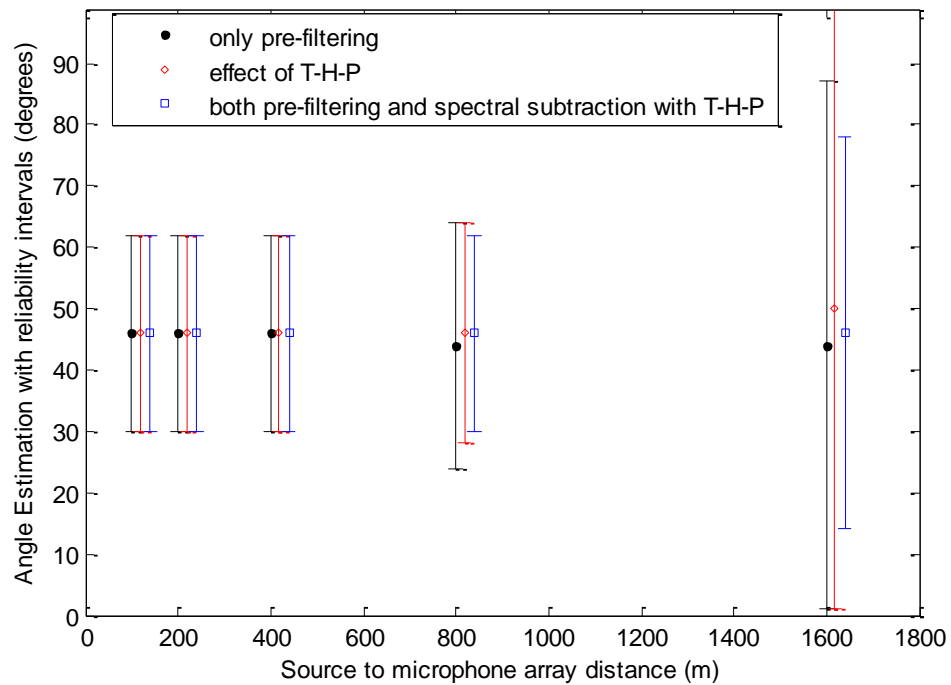


Figure 38 Beamforming with both spectral subtraction and pre-filtering applied. For both cases, effects of source to microphone array distance with and without air absorption are illustrated with $\theta=45^\circ$, $F_s=44100$, $M=4$, $S=0.15$ m

Source to microphone array distance simulations for GCC based method have yielded more interesting results. As illustrated with simulations concerning the microphone spacing and number of microphones, GCC had superior beamwidth performance as compared to other two methods; however, its performance is greatly reduced with increasing source to microphone array distances, when effects of temperature, humidity and pressure are included, as given by Figure 39.

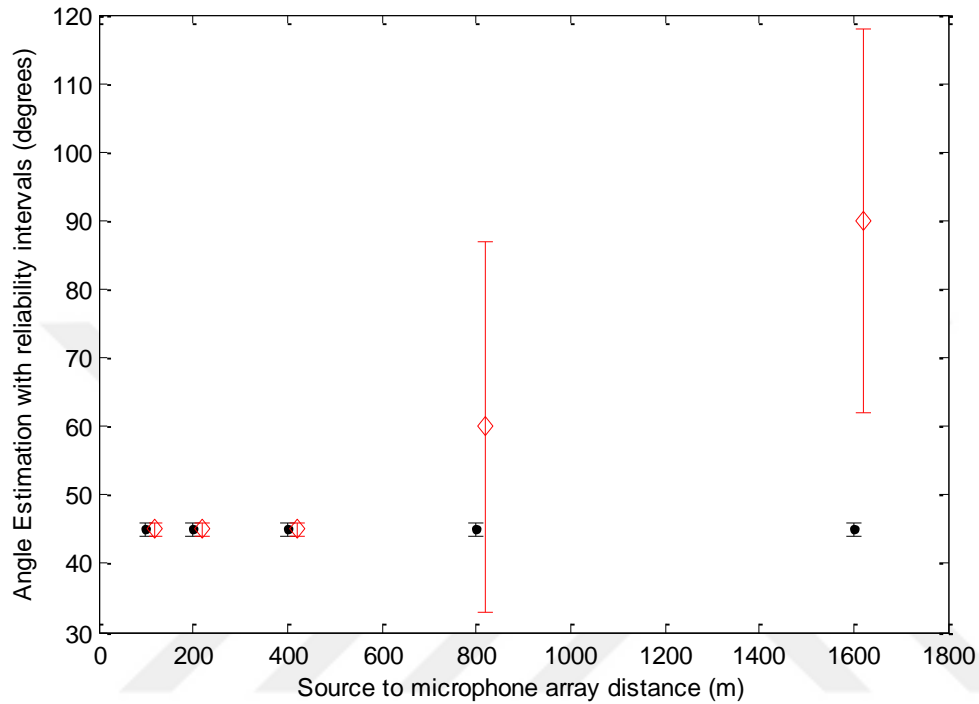


Figure 39 PHAT-GCC without spectral subtraction. Effects of source to microphone array distance with and without including air absorption. $\theta=45^\circ$, $F_s=44100$, $M=4$, $S=0.2\text{ m}$

Considering its pair-wise operation, the simulation were repeated with the number of microphones, M , increased to 8, so that the post-processing could use the outputs of 28 cross correlations instead of 6. As can be observed on Figure 40, although the error at estimation peak was reduced, PHAT-weighted GCC still could not localize the target at 45 degrees even with 8 microphones.

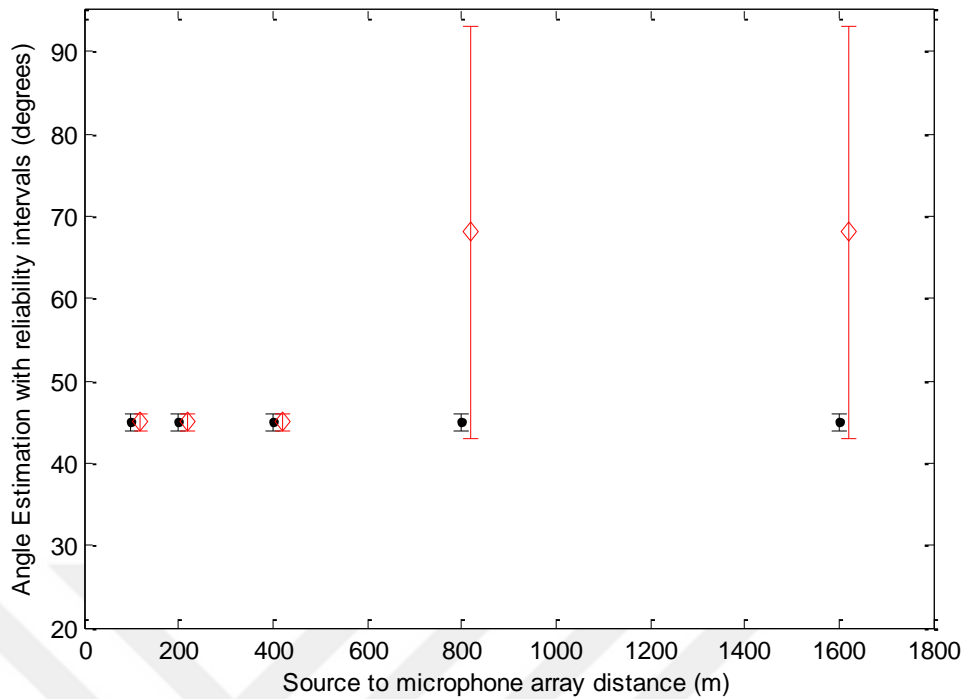


Figure 40 PHAT-GCC without spectral subtraction for an increased number of microphones. Effects of source to microphone array distance with and without including air absorption. $\theta=45^\circ$, $F_s=44100$, $M=8$, $S=0.2$ m

Finally, in order to remove the significant errors for the 800 m and 1600 m cases, the proposed spectral subtraction was applied at the pre-processing stage. Despite a slight improvement of performance, GCC could not localize the target angle of 45 degrees even when both PHAT-weighting and spectral subtraction were applied together. As given by Figure 41, this result is important for GCC, concerning its usage for outdoor environments and long ranges.

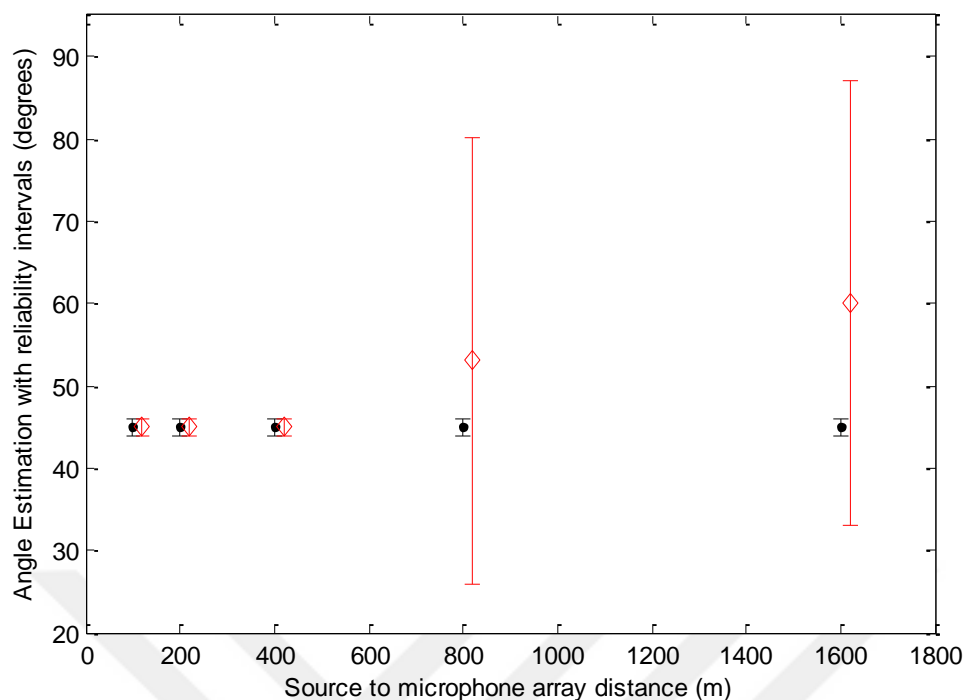


Figure 41 PHAT-GCC with spectral subtraction with an increased number of microphones. Effects of source to microphone array distance with and without including air absorption. $\theta=45^\circ$, $F_s=44100$, $M=8$, $S=0.2$ m

Results of MUSIC based method with respect to source to microphone array distance are interesting, too. Firstly, as given by Figure 42, this method's outputs appear to be less dependent on the source distance. The errors in DOA estimation did not exceed 5 degrees even for 1500 m, with post-processing applied and effects of temperature, humidity and pressure not present. Moreover, even after their inclusion, post-processed MUSIC had a smooth and predictable output with respect to source to microphone distance. The narrowing of -3 dB beamwidth, however, requires additional consideration. That is, as opposed to usual prediction, beamwidth performance of MUSIC algorithm is enhanced by including the effects of temperature, humidity and pressure. That could have resulted from an unintentional benefit of the fact that higher frequencies are more absorbed in the air. That is, high (aliasing) frequencies that increase estimation beamwidth were eliminated by air absorption over the long distances of 800 m and 1600 m. Since the frequency range selection for MUSIC algorithm was performed at the post-processing phase (instead of pre-filtering as with other algorithms), changes in the frequency characteristics of the attenuated signal could be revealed such clearly. Although this hypothesis needs further examination, it is clear in any case that the benefits of superior frequency resolution at the output of MUSIC algorithm can be exploited by performing frequency range selection as post-processing.

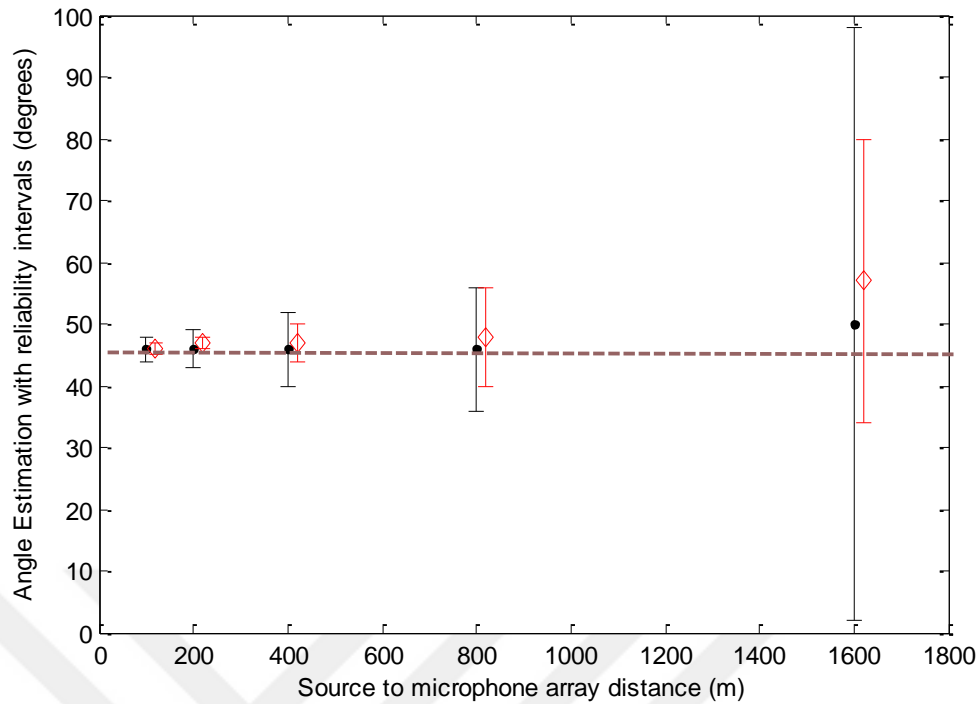


Figure 42 MUSIC with proposed post-processing. Effects of source to microphone array distance with and without including air absorption. $\theta=45^\circ$, $F_s=44100$, $M=4$, $S=0.2$ m, STFT size=4096

4.4 Angle of Incidence

Despite the target incidence angle was predetermined and fixed at 45 degrees while manipulating other parameters, it is geometrically obvious that the performances of all algorithms are expected to be dependent on the incidence angle. Therefore, the DOA estimation outputs of the three methods were simulated by applying different angles that cover the whole angular range of the array. It should be noted that this range is restricted to a half-circle since the simulated array is linear-one-dimensional. In other words, the array output is symmetric with 180 degrees.

As expected, all three methods result in smaller DOA estimation errors around 90 degrees as given by Figure 43, Figure 44 and Figure 45. This is due to the cosine term while converting time difference between channels to angle information; since the cosine function has a more rapid change around 90 degrees. On the contrary, the change of the output of the cosine function with respect to the input angle is so slow around 0 and 180 degrees that, DOA estimation performances are reduced.

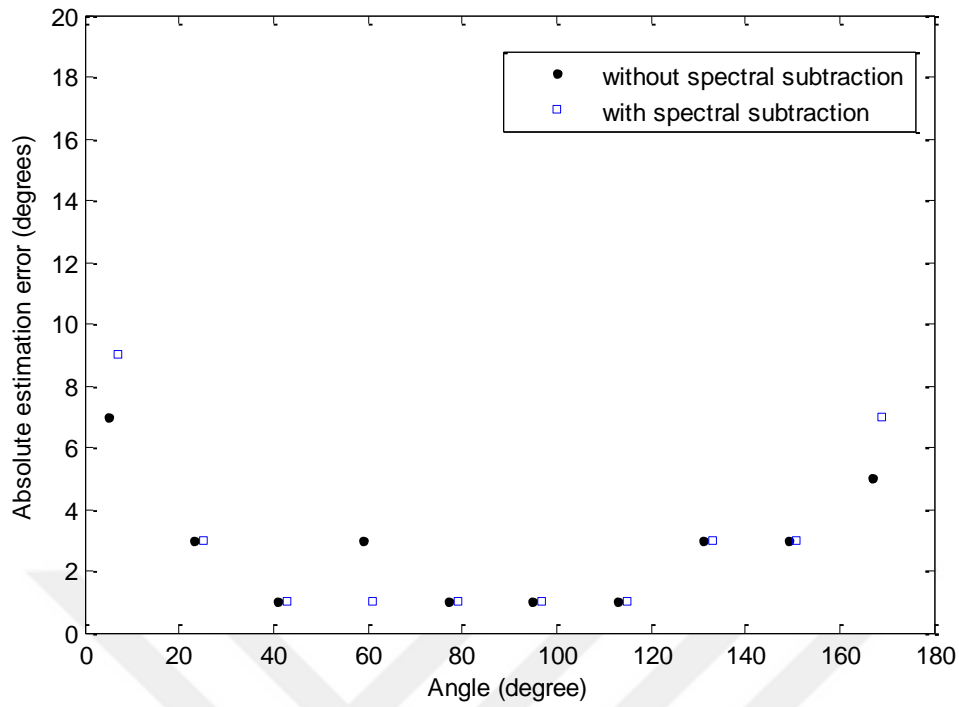


Figure 43 Beamforming with and without spectral subtraction, performance with respect to source angle. $F_s=44100$, $M=4$, $S=0.2$ m, $D=300$ m. Proposed pre-filters are applied.

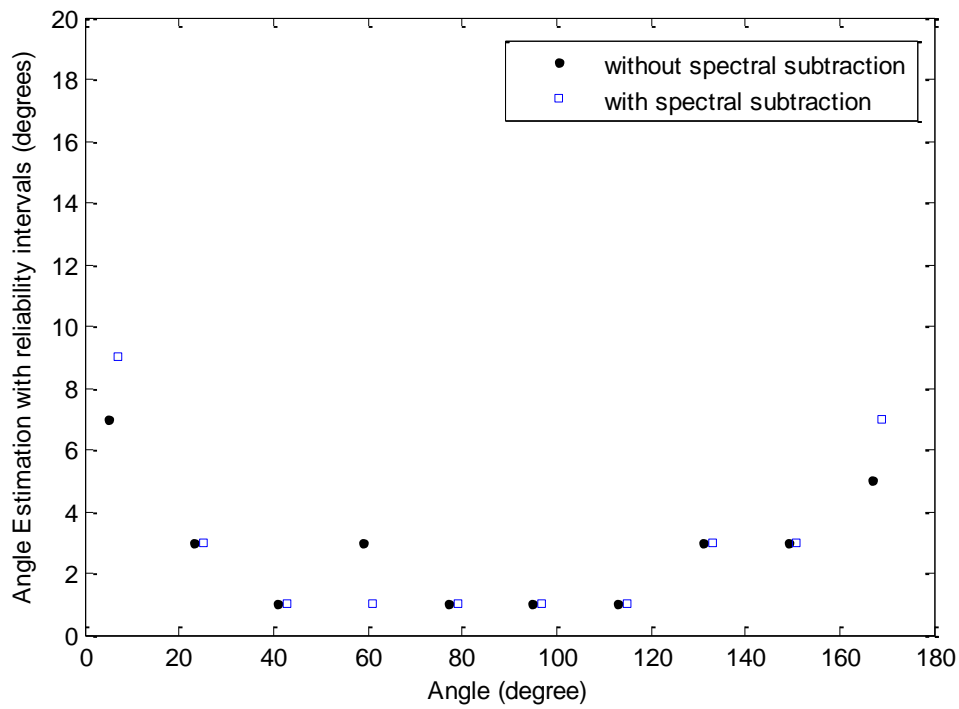


Figure 44 PHAT-GCC with and without spectral subtraction, performance with respect to source angle. $F_s=44100$, $M=4$, $S=0.2$ m, $D=300$ m.

Both Beamforming and GCC outputs reveal unexpected DOA errors around 60 degrees. Since the error was observed on no other angles, it was predicted to be caused by some directional helicopter noise component; therefore, both tests were repeated with spectral subtraction. As predicted, errors around 60 degrees were eliminated after the spectral subtraction's reduction of noise as Figure 43 and Figure 44 reveal.

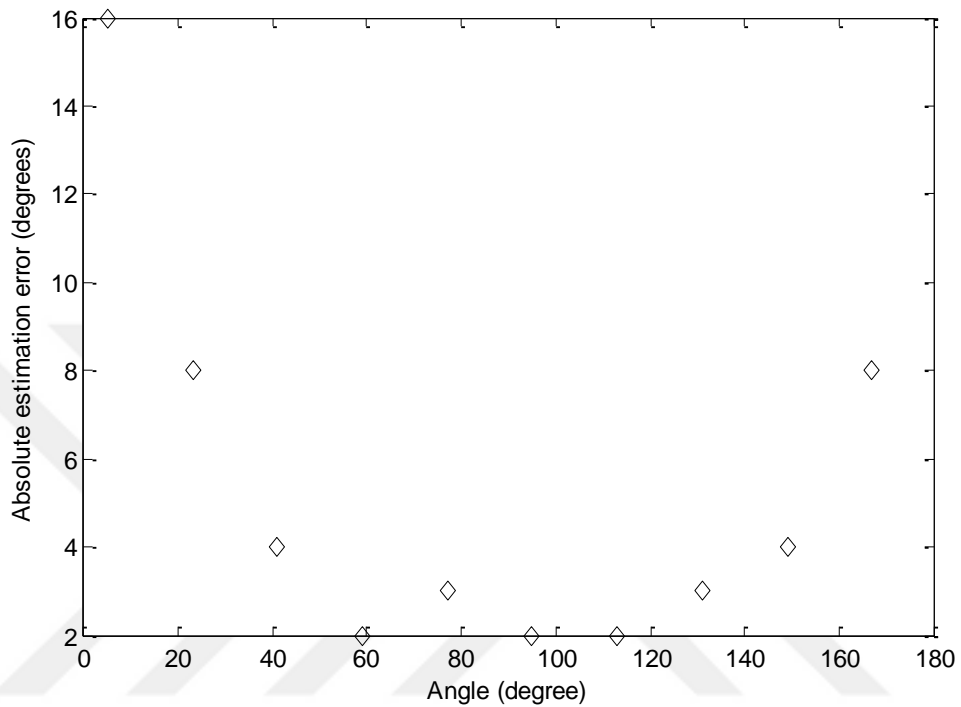


Figure 45 MUSIC with post-processing that selects frequency bins of interest, performance with respect to source angle. $F_s=44100$, $S=0.2$ m, $D=300$ m, $M=4$, STFT size = 4096

By comparing the performances of the three methods given by Figure 43, Figure 44 and Figure 45, it can be said that the estimation errors of the MUSIC algorithm were larger than those of Beamformer and GCC based methods. Indeed, DOA estimation error of MUSIC-based method around 0 degrees requires specific consideration. *Figure 46* illustrates the results of the same simulation with the number of microphones increased to 8 and 16. In this way, the DOA estimation errors could be reduced to similar values with that of Beamformer and GCC-based methods.

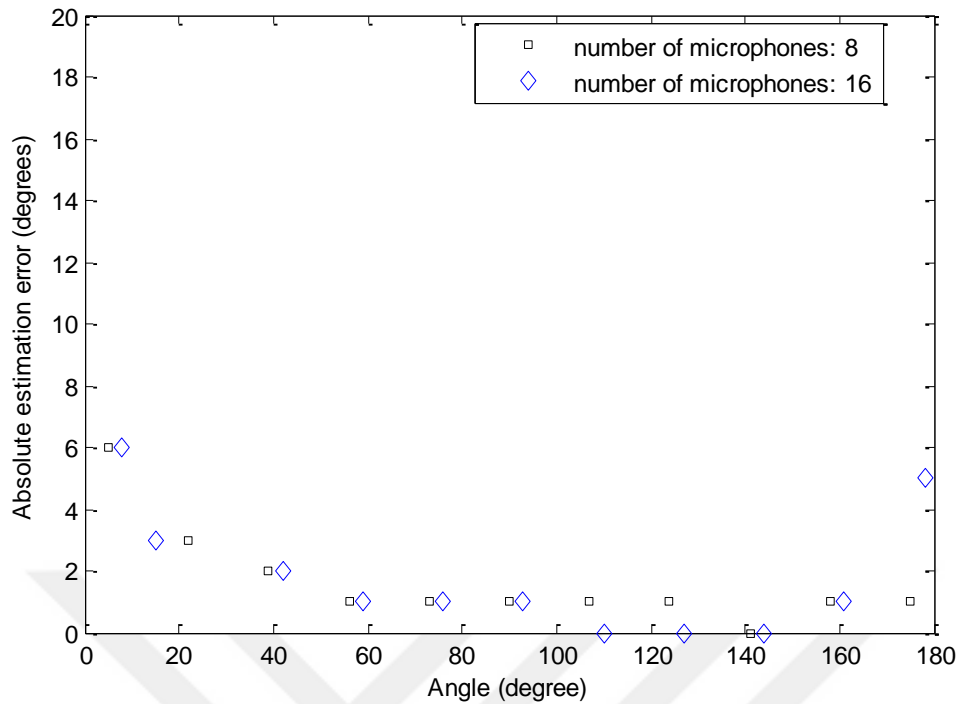


Figure 46 MUSIC with post-processing that selects frequency bins of interest for an increased number of microphones, performance with respect to source angle.
 $F_s=44100$, $S=0.2$ m, $D=300$ m, STFT size = 4096

4.5 STFT Size

As explained in Section 3.5 Multiple Signal Classification, MUSIC algorithm employs Short Time Fourier Transform (STFT) with narrowband frequency bins and operates repeatedly on each of these bins. Therefore, the selected STFT size determines the frequency resolution at the MUSIC output. Considering the complex sound field characteristics of the problem domain with various frequency components as well as the proposed frequency bin selection at the post-processing stage, the size of the STFT is an important parameter for the MUSIC-based localization method.

The procedure for determining the range of the STFT size was explained in Section 3.5 Multiple Signal Classification. To summarize, the low limit was set for a reasonable frequency resolution, while the high limit results from the real-time performance, and thus the window size, requirements. The effects of manipulating STFT size in the range of 512 to 4096 are given in Figure 47, integrated with a microphone spacing simulation. Results reveal an obvious increase in DOA estimation performance with increasing STFT size (and an enhanced frequency resolution therein).

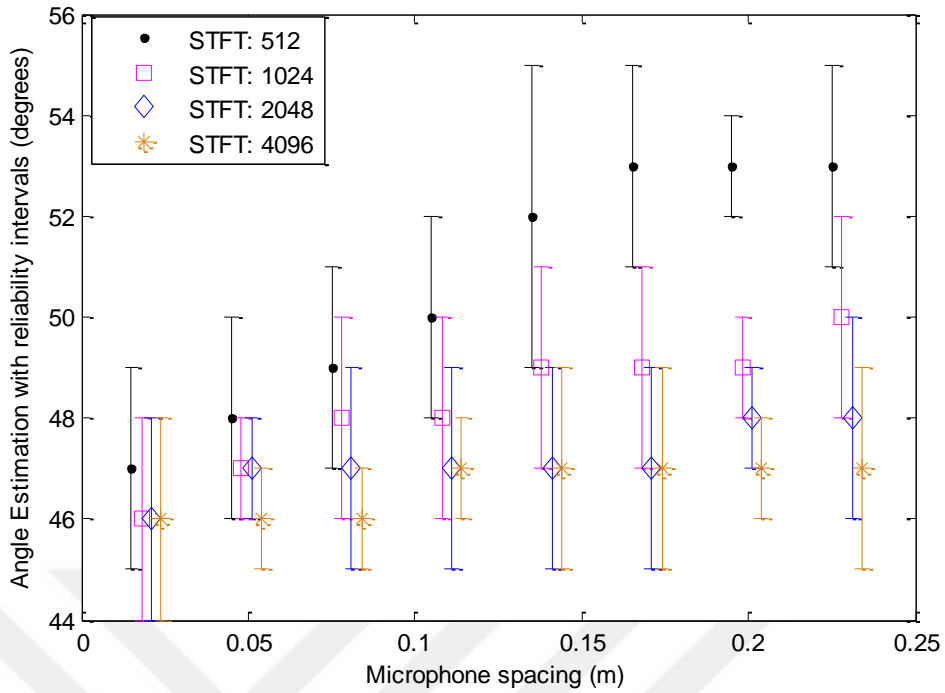


Figure 47 MUSIC with post-processing that selects frequency bins of interest. Change in DOA estimation output for different STFT sizes. $\theta=45^\circ$, $D=200m$, $F_s=44100$, $M=4$

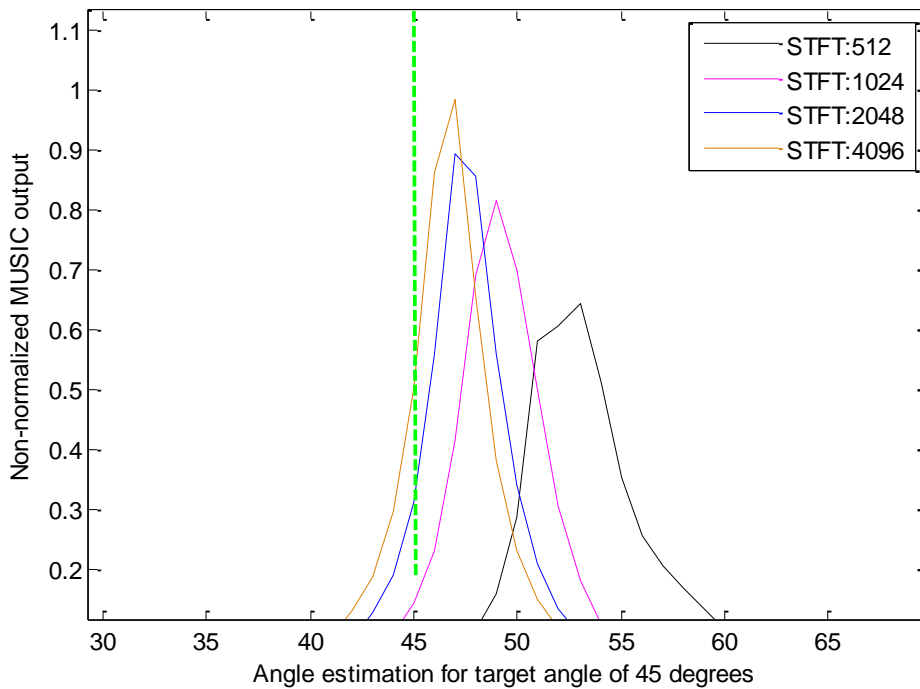


Figure 48 MUSIC with post-processing that selects frequency bins of interest. Change in DOA estimation output for different STFT sizes. $S=0.15$ m, $\theta=45^\circ$, $D=200m$, $F_s=44100$, $M=4$

Figure 48 gives another illustration of the same effect where the DOA estimation (calculated with the proposed selection of the frequency bins) benefits from increasing the STFT size in terms of both estimation peak error and peak magnitude. However, due to the fact that the MUSIC algorithm operates on all frequency bins exhaustively, this enhancement is accompanied by a significant processing cost which was eminently observable during simulations.

This is a significant conclusion on the STFT size for the MUSIC algorithm, since it illustrates the trade-off between the localization accuracy and the performance requirements. As an example, choosing the STFT size of 8192 samples for a further enhanced localization accuracy would increase the window size and limit the maximum number of calculations per second to approximately 5, assuming a 50% overlapping window.

4.6 Discussion of Results

Having obtained the results for all three localization methods with respect to different parameters, a generic comparison was available. Firstly, beamforming based method appears to be less vulnerable to almost all parameters when the estimation peak is concerned. Beamwidth of the estimation, however, is significantly affected by changing parameters with theoretically expected trends. However, benefits of the proposed preprocessing, which are pre-filtering of both helicopter and aliasing frequencies and spectral subtraction, were not as obvious as expected until the effects of the air absorption were included.

GCC with the proposed pre-processing of PHAT-weighting and spectral subtraction, as well as the post-processing that makes use of all microphone pairs, has yielded the best -3 dB beamwidth performance as compared to other two methods. However, the performance was significantly reduced over long source to microphone array ranges by the effects of air absorption simulated for 30°C temperature and 80% relative humidity.

Finally, the MUSIC-based method was observed to be more robust to air absorption and long ranges, but accompanied with slightly larger errors in DOA estimation peak for most of the simulation parameters. In other words, MUSIC-based method could provide a wider range of operating conditions for an implementation that favors reliability over accuracy.

CHAPTER 5

CONCLUSIONS

In this study, we aimed to address the problem of onboard gunshot localization such that ground based attacks targeted at helicopters could be localized. An investigation of real-life scenarios and mission conditions were performed that reveals both the criticality and characteristics of such attacks on helicopters.

There are many studies in the literature that address the subjects of gunshot localization, helicopter sound characteristics, simulation of outdoor sound propagation or acoustic source localization in general. These studies have shown that acoustic source localization algorithms could be deployed with the purpose of localizing gunshot threats. Moreover, both previous studies and international standards have described means for predicting sound propagation characteristics in outdoor environments. In order to address the problem of array based acoustic gunshot localization on helicopters, this study inherently included a combination of these subjects.

Three widely known source localization algorithms, namely Beamforming, Generalized Cross Correlation and Multiple Signal Classification, were deployed, while proposing domain-specific pre-processing and post-processing methods for each of them. Moreover, a simulation environment was developed, which is capable of manipulating both the algorithm related parameters and the outdoor wave propagation related factors. SNR range expectancy from such an application was determined considering both real life conditions and signal processing limitations. In this way, both the applicability of the proposed processing methods and the factors that affect gunshot localization on helicopters were investigated.

Simulation results revealed that gunshot localization on helicopters could be possible by applying pre-processing and post-processing methods that handle the effects of the helicopter sound characteristics and environmental factors. A thorough examination of the results has revealed that Beamforming-based localization method could yield reasonable performance with the significant enhancement offered by spectral subtraction. For GCC, PATH-weighting at the pre-processing stage and usage of all microphone pairs at the post-processing stage were proposed, by which the method yielded the most accurate outputs as compared to other two methods. However, GCC-based method suffered greatly when effects of air absorption over long ranges were included. Lastly, a selection of output frequency bins was proposed for the MUSIC algorithm, which offered robustness with air absorption and did not suffer significantly for large source to microphone array distances. Error at the DOA estimation peak, however, was larger for this method, concluding that MUSIC with proposed post-processing would be convenient for implementations that favor long range reliability over accuracy.

It should be noted that, considering the large number of parameters and extreme real life conditions of the problem domain, all of the factors were not simulated in the scope of this study. Some of the factors possess nonlinearities and require non-

diffuse sound field considerations. These factors can be listed as effects of helicopter-specific aerodynamics, turbulence, and the temperature and wind gradients in air as well as meteorological events and are expected to have hardly predictable difficulties in a real-life implementation. This might have resulted in an optimistic shift in SNR levels of the wave propagation related simulations. Moreover, multi-channel microphone array inputs were formed by replication of a single channel by applying geometrical and wave propagation related calculations. That eliminates possible effects of inter-microphone discrepancies and self-noise which might be different for each microphone in the array. In that sense, this study does not take into account sensor noise and calibration issues related to the microphones. Besides, although simulations of this study depend on a diffusive sound field assumption, a real-life implementation should consider that both sound travel times and amount of signal attenuation could vary considerably among different points in the atmosphere.

Considering above-given limitations, directions for further studies were determined. First of all, extension of the simulation framework so as to cover the effects of correlated wind noise would be beneficial for more realistic SNR scenarios. Moreover, simulation of multi-dimensional microphone arrays could be easily achieved, which might improve robustness with both the helicopter noise and the environmental factors. Since the simulation environment is developed and operative, further tests with different input sound samples would be beneficial considering that there are numerous sound recording libraries that are commercially available.

Finally, a real-life implementation of the array based solution is considered as a future study that would use parameter values as determined by simulations of this study during the field tests and sound recordings. That way, various microphone locations on the helicopter could be selected for not only obtaining smaller noise SPL but also application of different SNR enhancement solutions. One such future solution could be obtaining sound recordings from locations selected at major helicopter noise contributors so as to predict the noise contribution at microphone array position by deploying Wiener filtering.

REFERENCES

- Ahmed, T., Uppal, M., & Muhammad, A. (2013). Improving efficiency and reliability of gunshot detection systems. *Acoustics, Speech and ...*, 513–517.
<http://doi.org/10.1109/ICASSP.2013.6637700>
- Allen, J. B., & Berkley, D. A. (1979). Image Method for Efficiently Simulating Small Room Acoustics. *Journal of the Acoustical Society of America*, 65(4), 943–950.
- American Institute of Physics. (1995). American National Standard for the Calculation of the Absorption of Sound by the Atmosphere ANSI S1.26-1995.
- Aravindakshan, B., Aravind, A. S., & Vyawahare, M. K. (2002). Analysis of on-ground and in-flight sound levels produced by Chetak and Pratap helicopters. *Aerospace Medicine*, 51–61.
- Arntzen, M., Rizzi, S. A., Visser, H. ., & Simons, D. G. (2012). A framework for simulation of aircraft flyover noise through a non-standard atmosphere. *18th AIAA/CEAS Aeroacoustics Conference (33rd AIAA Aeroacoustics Conference)*, 1–17.
<http://doi.org/10.2514/1.C032049>
- Bandi, A. K., Rizkalla, M., & Salama, P. (2012). A novel approach for the detection of gunshot events using sound source localization techniques. *2012 IEEE 55th International Midwest Symposium on Circuits and Systems (MWSCAS)*, 494–497.
<http://doi.org/10.1109/MWSCAS.2012.6292065>
- Barabell, a. (1983). Improving the resolution performance of eigenstructure-based direction-finding algorithms. *ICASSP '83. IEEE International Conference on Acoustics, Speech, and Signal Processing*, 8, 8–11. <http://doi.org/10.1109/ICASSP.1983.1172124>
- Beck, S. D., Nakasone, H., & Marr, K. W. (2011). An introduction to forensic gunshot acoustics. *The Journal of the Acoustical Society of America*, 130(4), 2519.
<http://doi.org/10.1121/1.3655043>
- Benesty, J. (2001). Spatial Correlation and Time Delay Estimation.
- Benesty, J., Chen, J., & Huang, Y. (2008). *Microphone Array Signal Processing*. Springer.
- Boll, S. (1979). Suppression of acoustic noise in speech using spectral subtraction. *IEEE Transactions on Acoustics, Speech and Signal Processing*, 27(2), 113–120.
<http://doi.org/10.1109/TASSP.1979.1163209>
- Boré, G., & Peus, S. (1999). Microphones Methods of Operation and Type Exemplation and Type Examples.
- Bronuzia, F., Monaib, L., & Patruccob, M. (2012). Correct and Effective Characterization of Fire-arms Noise: a Basic Aspect to Provide Reliable Input Data for the Reduction of Emitted Noise from Shooting Ranges in Urbanized Area. *Chemical Engineering*, 26, 507–512. Retrieved from <http://www.aidic.it/cet/12/26/085.pdf>
- Chacón-Rodríguez, A., Julián, P., Castro, L., Alvarado, P., & Hernández, N. (2011). Evaluation of gunshot detection algorithms. *IEEE Transactions on Circuits and Systems I: Regular Papers*, 58(2), 363–373. <http://doi.org/10.1109/TCSI.2010.2072052>

- Chen, J., Benesty, J., & Huang, Y. (2006). Time delay estimation in room acoustic environments: An overview. *Eurasip Journal on Applied Signal Processing*, 2006(i), 1–19. <http://doi.org/10.1155/ASP/2006/26503>
- Chung, K. (2012). Comparisons of spectral characteristics of wind noise between omnidirectional and directional microphones. *The Journal of the Acoustical Society of America*, 131(6), 4508–17. <http://doi.org/10.1121/1.3699216>
- Duckworth, G. L., Gilbert, G. C., & Barger, J. E. (1996). Acoustic Counter-Sniper System. In *Command Control, Communications, and Intelligent Systems for Law Enforcement* (p. Vol. 2938).
- Eunkuk, S., Seungmin, L., & Soogab, L. (2010). Helicopter Noise Propagation Characteristics in the Refracting Atmospheric Conditions.pdf. In *20th International Congress on Acoustics*. Sydney.
- Fertig, L., Young, R., & Nance, D. (2012). Hybrid Cramer-Rao Lower Bound for Sniper Localization via a Helicopter-Based Acoustic Array : v (Tz Pin J, 862–866.
- Freire, I. L., & Apolinario, J. A. (2011). DoA of gunshot signals in a spatial microphone array: Performance of the interpolated Generalized Cross-Correlation method. *Argentine School of Micro-Nanoelectronics Technology and Applications (EAMTA), 2011*, 1–6.
- Gazer, S., & Grenier, Y. (1995). Criteria for positioning of sensors for a microphone array. *IEEE Transactions on Speech and Audio Processing*, 3(4), 294–303. <http://doi.org/10.1109/89.397094>
- Gerosa, L., Valenzise, G., Tagliasacchi, M., Antonacci, F., & Sarti, A. (2007). Scream And Gunshot Detection In Noisy Environments. *European Signal Processing Conference, (Eusipco)*, 1216–1220.
- Günel, B., & Hacıhabiboğlu, H. (2011). Sound SOURCE Localization: Conventional Methods and Intensity Vector Direction Exploitation. In *Machine Audition: Principles, Algorithms and Systems* (pp. 126–161).
- Harris, C. M. (1966). Absorption of sound in air versus humidity and temperature. *The Journal of the Acoustical Society of America*, 40(1), 11–17. <http://doi.org/10.1121/1.1910031>
- Hero, A., & Schwartz, S. (1984). Alternatives to the Generalized Cross Correlator for Time Delay Estimation.
- International Organization for Standardization. (2007). Acoustics - Attenuation of sound during propagation outdoors - Part 2: General Method of Calculation.
- JanakiRam, R. D., Sim, B. W., Kitaplioglu, C., & Straub, F. K. (2009). Blade-Vortex Interaction Noise Characteristics of a Full-Scale Active Flap Rotor. *American Helicopter Society 65th Annual Forum*. Retrieved from <http://oai.dtic.mil/oai/oai?verb=getRecord&metadataPrefix=html&identifier=ADA529297>
- Khan, S., Divakaran, A., & Sawhney, H. S. (2009). Weapon identification using hierarchical classification of acoustic signatures. *Proceedings of SPIE - The International Society for Optical Engineering*, 7305, 1–5. <http://doi.org/10.1117/12.818375>

- Knapp, C. H., & Carter, G. C. (1976). The Generalized Correlation Method for Estimation of Time Delay. *Ieee Transactions on Acoustics, Speech and Signal Processing, ASSP-24(4)*, 320–327. <http://doi.org/10.1109/TASSP.1976.1162830>
- Lago, T., L., J., Sven, H., & P.-a. (1997). Analysis of helicopter sound for the development of a new generation active headset. *Proceedings of the International Modal Analysis Conference - IMAC, 2*, 1708–1714. Retrieved from <http://www.scopus.com/inward/record.url?eid=2-s2.0-0031332134&partnerID=40&md5=04522aab0448f648cd5dccba59e7c2bb>
- Lentz, T., Schröder, D., Vorländer, M., & Assenmacher, I. (2007). Virtual Reality System with Integrated Sound Field Simulation and Reproduction. *EURASIP Journal on Advances in Signal Processing, 2007(1)*, 070540. <http://doi.org/10.1155/2007/70540>
- Maher, R. (2007). Acoustical characterization of gunshots. *Signal Processing Applications for Public Security ...*, (April), 109–113. Retrieved from http://ieeexplore.ieee.org/xpls/abs_all.jsp?arnumber=4218954
- Maher, R. C. (2006). Modeling and Signal Processing of Acoustic Gunshot Recordings. *Services and Security*, 257–261. <http://doi.org/10.1109/DSPWS.2006.265386>
- Maher, R. C., & Shaw, S. R. (2008). Deciphering gunshot recordings. *AES 33rd International Conference*, 1–8.
- Oraizi, H., & Fallahpour, M. (2008). Nonuniformly Spaced Linear Array Design for the Specified BeamWidth/Sidelobe Level or Specified Directivity/Sidelobe Level with Coupling Considerations, *4*, 185–209.
- Pertilä, P. E., Tuomo W Pirinena, A. J. V., & Korhonen, T. S. (2003). Comparison of three post-processing methods for acoustic localization. *Proceedings of SPIE Unattended Ground Sensor Technologies and Applications V, 5090(April)*, 9–17.
- Piercy, J. E., Embleton, T. F. W., & Sutherland, L. C. (1986). Review of Noise Propagation in the Atmosphere. In A. Lara Saenz & R. W. B. Stephens (Eds.), *Noise Pollution* (pp. 95–132). John Wiley & Sons Ltd.
- Pourmohammad, A., & Ahadi, S. (2012). Real Time High Accuracy 3-D PHAT-Based Sound Source Localization Using a Simple 4-Microphone Arrangement. *IEEE Systems Journal, 6(3)*, 455–468. <http://doi.org/10.1109/JSYST.2011.2176766>
- Rabinkin, D. V. (1997). Optimum microphone placement for array sound capture. *The Journal of the Acoustical Society of America, 101(5)*, 3114. <http://doi.org/10.1121/1.418950>
- Ramos, A. L. L., Holm, S., Gudvangen, S., & Otterlei, R. (2011). Delay-and-sum beamforming for direction of arrival estimation applied to gunshot acoustics. *Proc. SPIE, 8019*, 80190U–80190U–9. <http://doi.org/10.1117/12.886833>
- Ramos, A. L. L., Holm, S., Gudvangen, S., & Otterlei, R. (2013). A Spectral Subtraction Based Algorithm for Real-time Noise Cancellation with Application to Gunshot Acoustics. *International Journal of Electronics and Telecommunications, 59(1)*, 93–98. <http://doi.org/10.2478/eletel-2013-0011>
- Rizzi, S. A., & Sullivan, B. M. (1996). Aircraft Community Noise Impact Model.

- Rizzi, S. A., & Sullivan, B. M. (2003). A Three-Dimensional Virtual Simulator for Aircraft Flyover Presentation. *International Conference on Auditory Display (ICAD)*, Boston, MA, (July), 87–90.
- Rizzi, S. A., Sullivan, B. M., & Aumann, A. R. (2008). Recent Developments in Aircraft Flyover Noise Simulation at NASA Langley Research Center. *NATO/AVT TG 158 Specialists' Meeting on Environmental Noise Issues Associated with Gas Turbine Powered Military Vehicles*, 17–1 to 17–14. Retrieved from http://www.ausim3d.com/pdf/CNoTE_2008.pdf
- Robinson, F. (Hughes H. (1973). *Component Noise Variables of a Light Observation Helicopter NASA-CR-114761*. Culver City, California.
- Roy, R., & Kailath, T. (1989). ESPRIT - Estimation of Signal Parameters via Rotational Invariance Techniques. *IEEE Transactions on Acoustics, Speech, and Signal Processing*, 37(7), 984–995. <http://doi.org/10.1109/29.32276>
- Sadler, B. M., Sadler, L. C., & Pham, T. (1997). Optimal and Robust Shockwave Detection and Estimation, (7), 1889–1892.
- Sallai, J., Volgyesi, P., Pence, K., & Ledeczki, A. (2013). Fusing Distributed Muzzle Blast and Shockwave Detections. *14th International Conference on Information Fusion*, 1–8. Retrieved from papers3://publication/uuid/86D3C415-8ED7-43D3-8234-460B8038A273
- Satué-villar, A., & Fernández-rubio, J. (2005). Environment simulator for audio signals. *13th European Signal Processing Conference*.
- Schmidt, R. (1986). Multiple emitter location and signal parameter estimation. *IEEE Transactions on Antennas and Propagation*, 34(3), 276–280. <http://doi.org/10.1109/TAP.1986.1143830>
- Schmitz, F. H., Greenwood, E., Sickenberger, R. D., Gopalan, G., Sim, B. W., Conner, D., ... Decker, W. A. (2007). Measurement and Characterization of Helicopter Noise in Steady-State and Maneuvering Flight. In *American Helicopter Society Annual Forum*. Virginia Beach, VA.
- Shanan, S. S., & Pomalaza-Raez, C. A. (1989). The Use Of Nonuniform Element Spacing In Array Processing Algorithms. *International Geoscience and Remote Sensing Symposium (IGARSS)*. <http://doi.org/10.1109/IGARSS.1989.575979>
- Sujatha, J. (2010). *Vibration and Acoustics: Measurement and Signal Analysis*. Tata McGraw Hill.
- Thom, A., & Duraisamy, K. (2010). High-Resolution Simulation of Parallel Blade-Vortex Interactions. *AIAA Journal*, 48(10), 2313–2324. <http://doi.org/10.2514/1.J050381>
- True, H. C., & Rickley, E. J. (1977). *Noise Characteristics of Eight Helicopters FAA-RD-77-94*. Springfield, Virginia.
- Valenzise, G., Gerosa, L., Tagliasacchi, M., Antonacci, F., & Sarti, A. (2007). Scream and gunshot detection and localization for audio-surveillance systems. *2007 IEEE Conference on Advanced Video and Signal Based Surveillance*, 21–26. <http://doi.org/10.1109/AVSS.2007.4425280>

- Wagner, R. A. (n.d.). *Noise Levels of Operational Helicopters of the OH-6 Type Designed to Meet the LOH Mission NASA-CR-114760*. Culver City, California.
- Walker, K. T., & Hedlin, M. A. H. (2009). A Review of Wind Noise Reduction Methodologies. In *No Infrasound Monitoring for Atmospheric Studies* (pp. 141–182). <http://doi.org/10.1007/978-1-4020-9508-5>
- Ward, D. B., Kennedy, R. A., & Williamson, R. C. (2001). Constant Directivity Beamforming. In *Microphone Arrays: Signal Processing Techniques and Applications* (pp. 3–16). Springer.
- Zhang, R. G., & Kanapathipillai, S. (2008). A study of wind induced noise in microphones. In *Acoustics 2008* (pp. 24–27). Geelong, Victoria, Australia.
- Zhang, Y., & Abdulla, W. (2005). A comparative study of time-delay estimation techniques using microphone arrays. *Department of ...*, (619), 1–57. Retrieved from <http://www.mendeley.com/research/comparative-study-timedelay-estimation-techniques-using-microphone-arrays/>
http://homepages.engineering.auckland.ac.nz/~wabd002/Technical Reports/Technical Report 619_Yushi.pdf